

STUDIES OF THE ACTION OF  
IONISING RADIATION  
ON AQUEOUS SOLUTIONS

Thesis

Submitted by

JOHN WILKINSON

A.R.C.S., B.Sc.(London)

For the Degree of  
Doctor of Philosophy

University of Edinburgh

November, 1952.



### ACKNOWLEDGMENTS

The author wishes to express his gratitude to Dr. N. Miller for his unstinted advice and continued interest in this work, to Mr. L.O. Brown and Dr. H.A. Dewhurst for many helpful discussions and to the Department of Scientific and Industrial Research for a maintenance grant.

## CONTENTS

	Page
I. INTRODUCTION . . . . .	1
1. General . . . . .	1
2. The radiation chemistry of the ferrous system . . . . .	7
3. The objects of the present work	15
II. GENERAL EXPERIMENTAL TECHNIQUE .	18
1. Preparation of purified water .	18
2. Cleaning of glassware . . .	18
3. Analytical Methods . . .	18
4. Irradiation procedure . . .	21
5. The deaeration of aqueous solutions . . . . .	22
III. THE CHEMICAL EFFECTS OF $\alpha$ -RADIATION ON AQUEOUS FERROUS SULPHATE .	32
1. Introduction . . . . .	32
2. General experimental technique	33
3. Preliminary irradiation experiments . . . . .	44
4. Physical measurements . . .	66
(1) Introduction . . . . .	66
(2) The ionisation chamber .	71
(3) Measurements using the ionisation chamber .	76
(4) Discussion . . . . .	82

## CONTENTS (Contd).

	Page
5. Chemical dosimetry . . .	84
(1) Introduction . . .	84
(2) Irradiations in air-filled cells . . .	85
(3) Irradiations made in cells where contact between the solution and the gaseous phase was effectively eliminated . . .	91
(4) Irradiations made in cells swept with inert gases .	99
(5) Summary of the results .	105
(6) Possible sources of error	107
(7) Ferrous sulphate as a chemical dosimeter for mixed radiation . . .	111
(8) Discussion of the results	114
Appendices I, II and III.	
6. The mechanism of the chemical effects produced in aqueous solutions by $\alpha$ -particles .	118
(1) Introduction . . .	118
(2) Experimental and results	122
(3) Discussion . . .	142
IV. THE CHEMICAL EFFECTS OF $\gamma$ -RAYS ON AQUEOUS SOLUTIONS . . .	147
1. The benzene system	
(1) Introduction	147



CONTENTS (Contd).

	Page
(2) Spectrophotometric studies . . .	148
(3) Conclusions . . .	156
2. The nitrite-nitrate system .	157
(1) Introduction . . .	157
(2) Spectrophotometric estimation of the nitrite ion	159
(3) Studies in $\gamma$ -irradiated solutions . . .	170
Summary . . .	-
References . . .	-

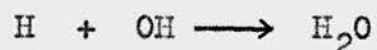
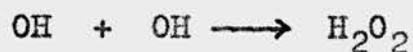
## I. INTRODUCTION.

### 1. General.

During recent years much interest has been shown in the field of radiation chemistry and particularly in the study of the chemical effects of ionising radiations on aqueous solutions. The experiments of several groups working in the early part of the century have been summarised in the book by Lind<sup>1</sup>. The large number of more recent publications has been comprehensively reviewed<sup>2-5</sup> and no attempt will be made here to present a complete survey of the literature.

In solutions, we can distinguish two modes of action of ionising radiation on the solute: (i) direct and (ii) indirect. Direct action may be defined as the "change brought about when radiation is absorbed by the solute," and indirect action as "the change induced in the solute due to the radiation absorbed in the solvent." In aqueous solutions, the indirect action may take place either by the transference of energy to the solute from excited or ionised water molecules or, more likely, by the production during the passage of the radiation of chemically active free radicals which diffuse away

from the tracks of the particles and ultimately react with the solute. The suggestion by Weiss<sup>6</sup> that an important result of the absorption of high energy radiations in water is the formation of hydrogen atoms and hydroxyl radicals, has received wide acceptance. The further suggestion that, in the case of solutions which are in equilibrium with air and therefore contain an appreciable amount of dissolved oxygen, the hydrogen atoms react with oxygen molecules to give the radical  $\text{HO}_2$ , has also gained much support. The distribution of radicals throughout the solution depends on the type of incident radiation. For  $\alpha$ -particles, low energy protons and very low energy electrons, the radicals are formed in close proximity along the densely ionised tracks of the particles and may react with each other.



In the case of X- and  $\gamma$ -rays where the ionisation is due to ejected photoelectrons or Compton electrons, the ion density along the tracks is relatively low, and most of the radicals produced diffuse away and become uniformly distributed throughout the solution.

In the absence of a solute recombination takes place



and in pure water little decomposition occurs.

Almost anything dissolved in the water has the effect of increasing the amount of decomposition which can be obtained on irradiation. The radiation-induced reactions occurring in aqueous solution may be summarised as follows:-

1. Oxidation of inorganic substances, e.g. ferrous ion (this will be reviewed in a later section), nitrite ion<sup>7,8</sup>, and selenite, arsenite and ferrocyanide ions<sup>9</sup>.
2. Reduction of inorganic substances, e.g. ceric ion<sup>10,11</sup>, dichromate ion<sup>12</sup>, persulphate ion<sup>13</sup>, and nitrate ion<sup>14</sup>.
3. Decomposition of organic substances, e.g. production of phenol from benzene (this will be described in a later section), deactivation of enzymes<sup>15</sup>, and the decomposition of acids and alcohols<sup>16</sup>.
4. Polymerisation reactions. E.g. acrylonitrile<sup>2,17</sup>.

The oxidation of inorganic ions by hydroxyl radicals or their reduction by hydrogen atoms explains most of the inorganic reactions which have been studied. In oxidation reactions, hydroxyl radicals are removed

and the hydrogen atoms which accumulate in the solution combine (in the absence of dissolved oxygen) to give hydrogen gas, which is evolved. Similarly, reductions occur by the removal of hydrogen atoms, and the hydroxyl radicals in solution combine with subsequent evolution of oxygen. The oxidation of organic compounds is accompanied by evolution of hydrogen.

To determine the efficiency of a radiation in inducing a chemical reaction, it is necessary to measure the rate of energy absorption in the system. This can be easily calculated for internal  $\alpha$  - and  $\beta$  -sources where the radioactive material is dissolved in the solution to be irradiated. For external sources, the energy input is usually estimated by ionisation methods, although calorimetric methods have been used<sup>18</sup>. These methods are attended by considerable experimental difficulty especially for X- and  $\gamma$ -rays. By making use of a chemical reaction in which the amount of radiation-induced chemical change is directly proportional to the amount of energy absorbed by the system, many of the difficulties of dosimetry may be avoided. The correlations between chemical changes and energy input have become well established for X- and  $\gamma$ -rays

and the various systems used have been recently reviewed<sup>4,19,20</sup>. The features of an ideal chemical dosimeter are as follows:-

- (i) the reaction should be simple and the chemical change easily measured over a wide range,
- (ii) the solution should be stable and easily prepared,
- (iii) the amount of chemical change per unit of energy absorbed should be constant for all concentrations,
- (iv) the chemical change should be independent of the presence of dissolved impurities or oxygen,
- (v) the chemical change should be independent of the wavelength and dose-rate of the incident radiation.

No chemical dosimeter yet proposed satisfies all these requirements but valuable contributions have been made by Stein and Weiss<sup>21</sup> who investigated the formation of phenol in irradiated solutions of aqueous benzene and Miller<sup>22</sup> who studied the oxidation of ferrous ions in an aerated 0.8N sulphuric acid solution. The amount of chemical change was compared with the current produced in an ionisation chamber under similar irradiation conditions, and an

absolute value for the yield of ferrous ions oxidised per known energy input was determined. The ferrous system is considered, at present, to be the most important chemical dosimeter for X- and  $\gamma$ -radiation, within the dose-rate range  $1 - 10^3$  roentgens per minute. Publications relating to the radiation chemistry of the ferrous system are summarised in a later section.

A certain amount of confusion exists in the literature as to the best method of expressing the efficiency of a radiation in initiating chemical changes. It has been customary to express this as the ratio of the number of molecules M undergoing chemical change to the number N of ion pairs produced in the system. This ratio  $M/N$  is, in many cases, not of great value, as the number of ion pairs produced in the system is not experimentally known. A method of expressing yield for X- and  $\gamma$ -ray experiments is micromoles or microequivalents per litre reacting per thousand roentgens. The method most in favour to-day is to express the amount of chemical change per unit of energy absorbed, namely G, the radiation yield, as molecules per hundred electron volts. In the present work the yield of say, an X-ray-induced oxidation of ferrous ion, will be expressed as

$$G_{\text{Fe}}^{\times} \quad \text{molecules/100 e.v.}$$

2. The Radiation Chemistry of the Ferrous System.

(a) Preliminary Experiments.

The system was first studied by Fricke and Morse<sup>23</sup> with a view to developing it as a chemical dosimeter. They showed that the amount of oxidation produced on X-irradiation of  $10^{-3}M$  ferrous sulphate in 0.8N sulphuric acid solution, was a linear function of dose, was independent of wavelength from 0.204 Å to 0.765 Å and that for a given dose of X-rays was independent of ferrous ion concentration between  $4 \times 10^{-5}M$  and  $10^{-2}M$ . The ferrous ion oxidation yield in airfree solution was found to be half that in aerated solution. On prolonged irradiation of aerated solutions it was found that at a certain critical dose the ferrous ion oxidation yield decreased by a factor of two but still remained a linear function of dose. This break in the curve was attributed to complete removal of the dissolved oxygen. A radiation equilibrium was also observed at about 94% oxidation indicating that ferric ions were reduced by X-rays. Fricke and Hart<sup>24</sup> made a more detailed study of the system involving analysis of the evolved gas which, from an airfree solution, was found to be hydrogen in an amount equal to



approximately half the number of ferrous ions oxidised. No hydrogen was evolved from aerated solutions and it was shown that four ferrous ions were oxidised for every oxygen molecule consumed. The reaction was shown to be pH dependent between pH 1 and pH 3.

Nurnberger<sup>25</sup> studied the  $\alpha$ -particle-induced oxidation of ferrous sulphate solutions and compared the ferrous ion oxidation yield with the yield of hydrogen evolved. Both internal and external sources were used and consisted of radon either dissolved in the airfree solution or sealed inside thin-walled bulbs which were immersed in the solution. The gas evolved was found to be almost 100% hydrogen and the ferrous ion oxidation was linear with dose up to 100% oxidation for the internal source but deviated slightly for the external source. The yield was independent of ferrous ion concentration between  $5 \times 10^{-4}M$  and  $5 \times 10^{-3}M$  although at greater concentrations the yield was found to increase. The yields using the internal source were found to be about half as great as those obtained with the external source. In the concentration independent region the ferrous ion oxidation yield using the external source was  $G_{Fe}^{\alpha} \approx 5$  molecules/100 e.v. (calculated from Nurnberger's figure for the ionic yield  $M/N$ )

and when the internal source was used

$G_{Fe^{2+}}^{\alpha} \approx 2.4$  molecules/100 e.v. The yields for hydrogen evolution were found to be in a similar ratio. In the concentration independent region, the ratio of the ferrous ion oxidation yield to the yield for hydrogen evolution was found to be approximately one.

Confirmation of many of the experiments on the X- and  $\gamma$ -ray oxidation of the aqueous ferrous system was provided by Liechti and his co-workers<sup>26</sup> who also showed that in a  $2 \times 10^{-3}M$  ferrous sulphate solution the oxidation yield was independent of temperature between  $4^{\circ}$  and  $54^{\circ}C$ .

(b) The Use of Ferrous Sulphate as a Chemical Dosimeter.

Data relating to the use of air saturated solutions of ferrous sulphate in 0.8N sulphuric acid as a chemical dosimeter have been recently tabulated<sup>20</sup>. Part of this table is reproduced in Table 1.

Great care was taken by Miller<sup>22</sup> to determine the relationship between the energy dissipated in the irradiated solution and the ionisation observed in an equal volume of dry air under the same

TABLE 1.

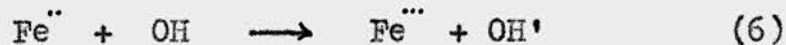
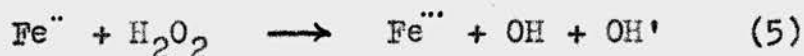
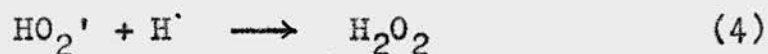
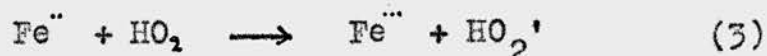
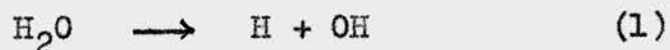
Data relating to the use of air saturated ferrous sulphate in 0.8N sulphuric acid solution as a chemical dosimeter.

G Molecules/100 e.v.	Type of Radiation	Dose rate r/min. (X- or γ-rays) r/equiv./min. (β-rays)	Mode of Energy Measurement	Observers
19.9	γ (Ra)	93.7	Ionisation	Miller <sup>22</sup>
20.0 ± 0.3	γ (Co <sup>60</sup> )	98 - 104	"	Hardwick <sup>27</sup>
15.5 ± 0.3	γ (Co <sup>60</sup> )	1,500 - 15,000	Ionisation and calorimetry	Hochanadel <sup>18</sup>
19.8 ± 0.7	X(2.25 MV)	814 - 150,000	Ionisation	Miller <sup>44</sup>
21.1 ± 1.3	X(1.2 MV)	442	"	"
20.3	X(250kV peak)	10 - 500	"	Tod and Whitcher <sup>28</sup>
19.7	X(200kV peak)	~3000	"	Rigg Stein and Weiss <sup>29</sup>
21.1 ± 0.5	β (P <sup>32</sup> )	30 - 150	4π counting and calorimetry	Hardwick <sup>30</sup>
20.2 ± 0.9	β (S <sup>35</sup> )	30 - 150	4π counting and calorimetry	"
16.0 ± 1	β (H <sup>3</sup> )	-	4π counting and ionisation	Hardwick <sup>31</sup>
15.4	β (H <sup>3</sup> )	42 - 240	gas density measurement and ionisation	Hart <sup>32</sup>

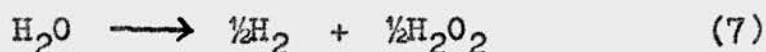
irradiation conditions. Miller's value for G has been confirmed in recent work<sup>27,29</sup> and is becoming accepted as one of the more reliable values in the literature. Hardwick<sup>33</sup> has expressed the ferrous ion oxidation yield as a function of the initial energy of the ionising electron and has shown that yield decreases with decreasing energy.

(c) Kinetics of the Radiation-Induced Oxidation  
of the Ferrous Ion.

In aerated solutions the following mechanism for the radiation-induced oxidation of the ferrous ion has been proposed<sup>34,35</sup>



Reactions (3), (5) and (6) have been studied in connection with the ferrous ion catalysed decomposition of hydrogen peroxide<sup>36</sup>. Allen<sup>5(b)</sup> has recently proposed that a further reaction should be taken into account to represent the "molecular" decomposition of water occurring in the regions of high energy density along the track of a charged particle.



In aerated solution reactions (1) - (6) take place and four ferrous ions are oxidised for every primary ionisation of a water molecule. In airfree solution, Krenz and Dewhurst<sup>35</sup> reported that the yield was one quarter that in aerated solution and proposed that this could be accounted for if reactions (2) - (5) did not take place, the yield being thus reduced by a factor of four. This factor was not in agreement with the published results of other workers shown in Table 2.

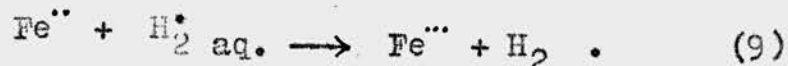
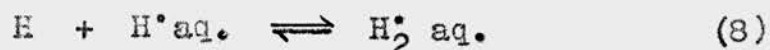
It has been recently shown<sup>29,38</sup>, however, that the ratio of the yield in aerated solution to that in airfree solution varies with the concentration of ferrous ion and approaches a value of two at high concentrations. The ratio of four obtained by Krenz and Dewhurst<sup>35</sup> was shown<sup>38</sup> to be due to the presence

TABLE 2.

Results obtained when aerated and airfree solutions of ferrous sulphate in 0.8N sulphuric acid were irradiated.

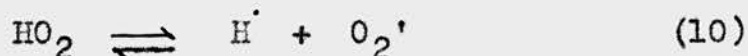
ratio of yield in aerated solution " " airfree	Type of radiation	Observers.
2.55	X	Fricke and Morse <sup>23(a)</sup>
2.59	X	Fricke and Hart <sup>24</sup>
2.58	X and $\gamma$	Shishacow <sup>37</sup>
4.0	$\gamma$	Miller <sup>22</sup>
2.86	$\gamma$	Krenz and Dewhurst <sup>35</sup>
2.52	$\beta$	Hart <sup>34</sup>
		"

of impurities in the irradiated solution. To account for the ratio of two, it has been proposed<sup>29,39</sup> that two more steps should be added to the reaction scheme outlined above, namely



In aerated solution reaction (2) predominates over reaction (3), and in airfree solution only reactions (1), (6), (8) and (9) take place.

In 0.8N sulphuric acid the ferrous ion oxidation yield is constant to 100% oxidation, but as pH increases, the initial yield gradually decreases and evidence of a back reaction appears. The dependence of yield on pH has been investigated<sup>29,38,40</sup> and the results obtained at low acidity have been qualitatively explained by the following reactions



It has been shown that at high pH the reduction of ferric ion can be inhibited by adding suitable complexing agents.

A study has been made recently<sup>41</sup> of the effects

produced when aliphatic alcohols are added to ferrous ion solutions before irradiation. The ferrous ion oxidation yield was found to increase, probably due to the formation of organic peroxides as a result of competition between the alcohol and the ferrous ions for the hydroxyl radicals. The addition of sodium chloride to the system before irradiation completely suppressed the effect of the alcohol. This was probably due to the reaction of hydroxyl radicals with chloride ions producing chlorine atoms which, in turn, preferred to oxidise ferrous ions rather than react with the alcohol.

### 3. The Objects of the Present Work.

The ionisation produced along the track of an  $\alpha$ -particle is very dense compared with that produced along the track of an electron, and when studying the biological action of radiation it is often important to compare the relative efficiencies per ionisation, of different types of radiation. In addition, it has long been established that the chemical effects produced in aqueous systems by  $\alpha$ -rays differ markedly from those produced by X- and  $\gamma$ -rays. The relative



efficiency of different types of radiation in inducing chemical changes in aqueous solution has been recently attracting attention<sup>5,33</sup>.

It was considered therefore, that owing to the lack of experimental data on the chemical effects of  $\alpha$ -radiation on aqueous solutions, a quantitative study would be of value. The large amount of published experimental work on the radiation-induced oxidation of aqueous ferrous sulphate and the general acceptance of the ferrous system as the most reliable chemical dosimeter for X- and  $\gamma$ -radiation, made it a natural choice for  $\alpha$ -ray studies. The principal object of the work presented in this thesis was to determine, as accurately as possible, the chemical yield for the  $\alpha$ -particle-induced oxidation of ferrous sulphate in 0.8N sulphuric acid solution, i.e.  $G_{Fe}^{\alpha}$ . Preliminary kinetic experiments have been made in an attempt to elucidate the mechanism by which chemical effects are produced in aqueous solutions by  $\alpha$ -particles.

Studies have also been made of the chemical effects produced by  $\gamma$ -rays on aqueous solutions, with special reference to the technique of producing air-free solutions.

The aqueous benzene system has been suggested as

a chemical dosimeter for X- and  $\gamma$ -radiation and a spectrophotometric study of this system has been made with a view to comparing it with the ferrous system.

Finally, a determination has been made of the oxidation and reduction yields of the nitrite and nitrate ions in the radiation equilibrium system



In connection with the latter study, an improved spectrophotometric method for the determination of nitrite, has been developed.

## II. GENERAL EXPERIMENTAL TECHNIQUE.

### 1. Preparation of Purified Water.

Water was distilled first in a commercial "Manesty" still, then re-distilled from alkaline potassium permanganate. The vapour was passed through about three feet of silica tubing heated to approximately  $800^{\circ}\text{C}$ , condensed and stored in a pyrex flask. The second distillation was always made immediately before preparing solutions for irradiation.

### 2. Cleaning of Glassware.

All glassware used in radiation-chemical experiments was cleaned in the following way. The glassware was allowed to stand, overnight, in chromic oxide-sulphuric acid cleaning mixture, rinsed thoroughly with distilled water and finally rinsed with purified water.

### 3. Analytical Methods.

The amount of oxidation taking place in an irradiated solution of ferrous sulphate was estimated in early experiments, by determining the amounts of ferrous ion present in solution before and after irradiation. In more recent experiments the chemical change was determined by measuring the formation

of ferric ion.

(a) Ferrous ion.

Ferrous ion was determined colorimetrically with orthophenanthroline according to the method described as follows.

To an aliquot of the iron solution in a 25 ml. graduated flask were added 1.5 ml. of a 1% aqueous solution of o-phenanthroline, 1.5 ml. of a 10% solution of ammonium acetate in 20% acetic acid and 1:1 ammonia until the solution was neutral to Congo Red. The solution was diluted to 25 ml. with distilled water. The percentage transmission of the orange-coloured complex was measured with a Unicam SP 500 spectrophotometer at a wave length of 510 m. $\mu$ . It has been shown<sup>27,42,38</sup> that Beer's Law is obeyed over a considerable range of ferrous ion concentration. The concentration of ferrous ion was calculated using a value of 11,020 for the molar extinction coefficient of the ferrous-o-phenanthroline complex. The total error in the measurement has been assessed at approximately  $\pm 1\%$ .

(b) Ferric Ion.

The amount of ferric ion in solution was determined spectrophotometrically at a wave length of 304 m. $\mu$ ., the ferric ion absorption maximum. Quartz cells were used and for percentage transmissions

between 30% and 100% the tungsten lamp with a Chance OX.7 filter was employed. Below 30% the hydrogen lamp was used. For solutions containing a large amount of ferric ion, measurements were made against blank solutions containing a known amount of ferric ion instead of the usual water blank. The molar extinction coefficient was found to change slightly with sulphuric acid concentration. Values for the molar extinction coefficients of ferric ion in sulphuric acid solutions of varying concentration were determined and the results are given in Table 3.

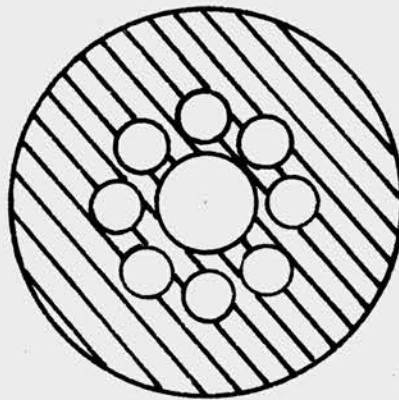
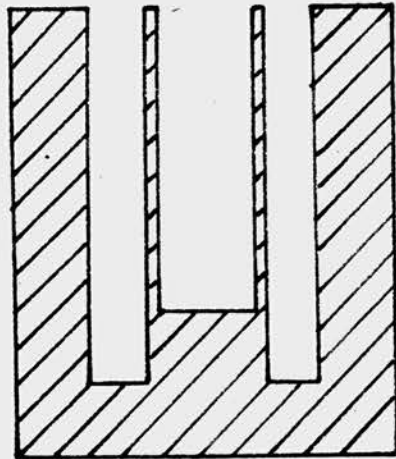
TABLE 3.

Molar extinction coefficients of ferric ion at  
304 m. $\mu$ . in sulphuric acid at  $20 \pm 1^\circ\text{C}$ .

Sulphuric Acid Concentration N	Molar Extinction Coefficient at $20 \pm 1^\circ\text{C}$
0.8	2150
0.1	2125
0.016	1990
0.01	1950
0.001	1893

The molar extinction coefficient of the ferric ion was shown<sup>38,43</sup> to increase with temperature by approximately

FIGURE 1.



$\gamma$ - IRRADIATION BLOCK

SCALE  $\approx \frac{1}{2}$  FULL SIZE

0.7% per degree C in the temperature range 18-25 degree C. A correction for temperature was therefore applied in all ferric ion determinations.

#### 4. Irradiation Procedure.

##### (a) $\gamma$ -rays.

Two sources of radioactive  $\text{Co}^{60}$  (5.3 years half-life, 1.1, 1.3 M.e.v.  $\gamma$  ) were used; one of 800 millicuries and the other of two curies activity. The irradiation vessels (one of which is shown in Figure 1) consisted of cylindrical blocks of well seasoned teak. Solutions were irradiated in pyrex glass tubes which fitted closely into holes spaced symmetrically around the central hole which contained the source. The geometry of the system was kept constant by inserting the sources in a reproducible fashion and, when a tube was removed a dummy tube filled to the same level with water, was inserted in its place. Holes and tubes were numbered and the small differences in the doses received by each tube were determined in preliminary experiments using standard ferrous sulphate solutions as a chemical dosimeter<sup>22</sup>. The amount of energy received by each tube was calculated using  $G_{\text{Fe}}^{\gamma} = 20$  molecules/100 e.v. for the ferrous ion oxidation yield, and corresponded to dose rates of about 6.6 r/min. and 12.4 r/min. for the two sources.

FIGURE 2.

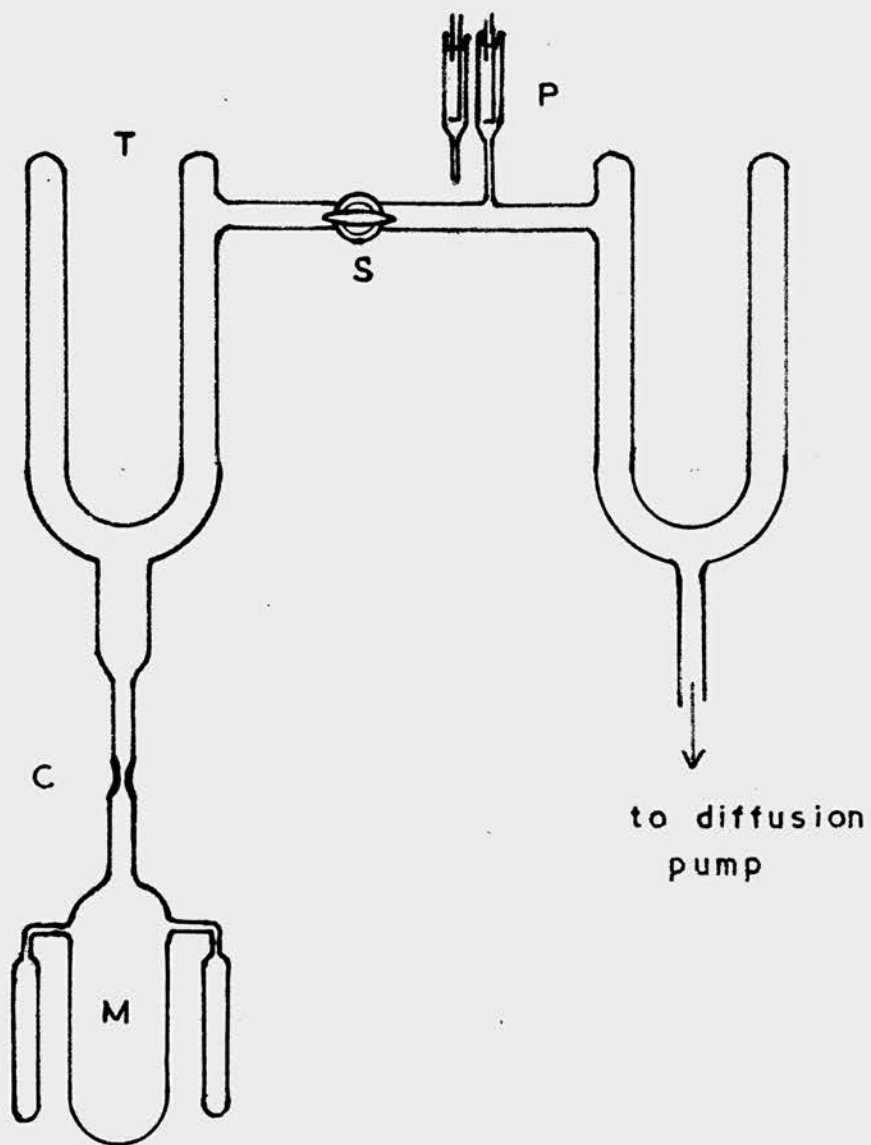
Deaeration Pumping Line "a"

- M    pyrex glass vessel of 250 ml capacity  
     fitted with 8 graduated side tubes of  
     15 ml capacity (only 2 are shown).
- C    constriction
- T    liquid air trap
- S    stopcock
- P    Pirani gauge.



FIGURE 2.

DEAERATION PUMPING LINE "a"



(b) X-rays.

50 kV peak X-rays were obtained from a Philips Metalix contact therapy tube. Solutions were irradiated in a glass bulb of approximately 15 ml. capacity mounted reproducibly on the end of the X-ray tube which was pointed vertically upwards. The rate of oxidation in an aerated ferrous sulphate solution was found to be independent of the volume of the solution between 7 ml. and 9 ml. In all irradiations the volume of the solution was therefore kept constant at 8 ml. Irradiations were usually made at a tube-current of 1.5 m.a. where the integral dose rate was estimated at approximately 540 r/min.

(5) The Deaeration of Aqueous Solutions.

(a) Preliminary Experiments.

(1) The low values of  $\sim 2.5$  obtained for the ratios of the amounts of radiation-induced oxidation in aerated ferrous sulphate solutions to those in airfree solutions (Table 2) were attributed by Krenz and Dewhurst<sup>35</sup> to incomplete removal of oxygen from the solutions. In an attempt to produce an airfree solution, a pumping line similar to that used by

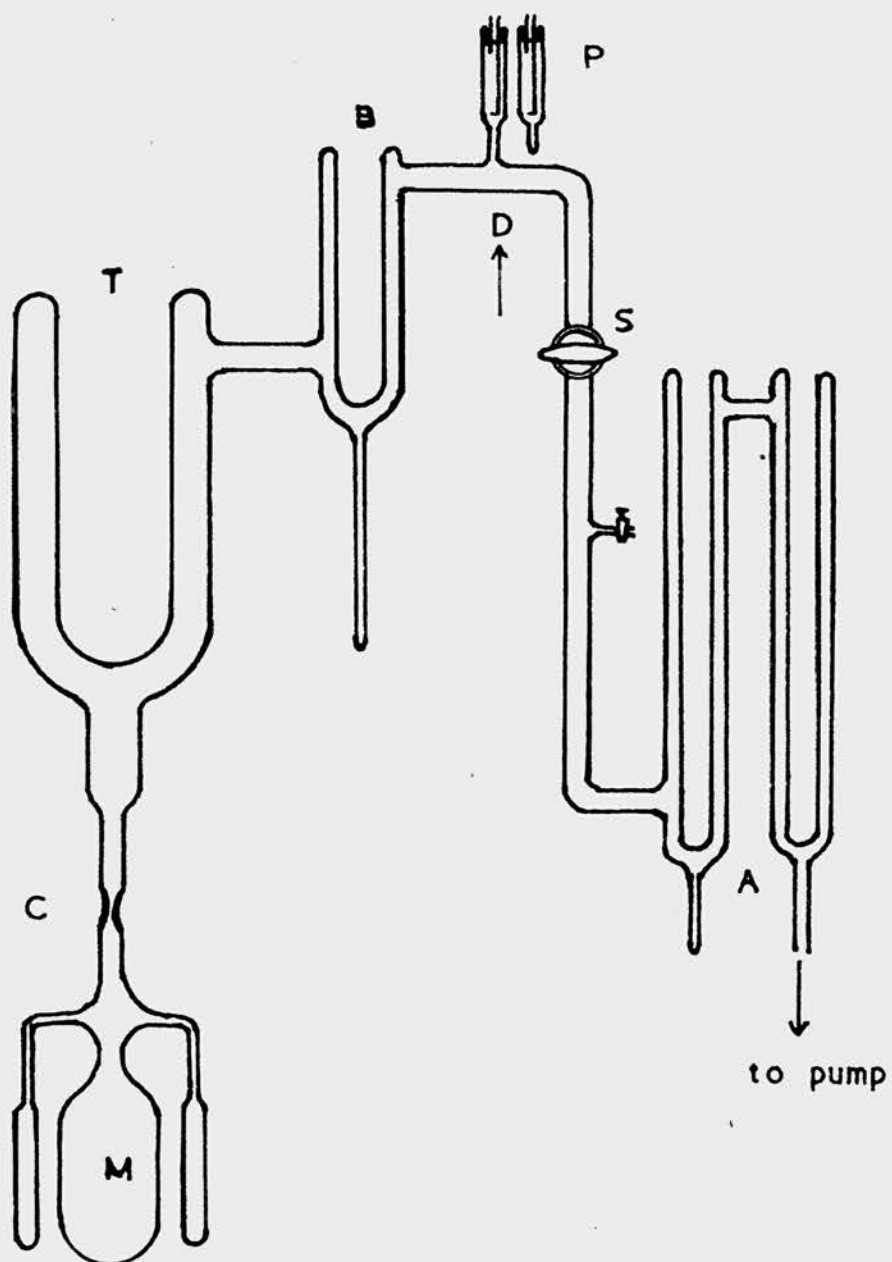
FIGURE 3.

Deaeration Pumping Line "d"

- M      pyrex glass vessel of 250 ml capacity,  
         fitted with 8 graduated side tubes of  
         15 ml capacity (only 2 are shown).
- A.B.T.    liquid air traps
- P      Pirani guage
- S      stopcock
- D      the point at which the apparatus shown  
         in Figure 4, was attached.

FIGURE 3.

DEAERATION PUMPING LINE     d



Krenz and Dewhurst was constructed (Figure 2). About 100 ml. of the solution to be deaerated were placed in the vessel M. The solution was heated in vacuo and the dissolved gases were exhausted using a high speed mercury diffusion pump backed by a Speedivac rotary oil pump. To prevent a change in the concentration of the solution due to evaporation, a liquid air trap T was installed and the ice forming on it was subsequently melted back into the deaeration vessel. The process of pumping, condensing and melting was performed several times until the Pirani gauge P indicated complete exhaustion of the dissolved gases. The vessel M was sealed off at the constriction C and after thorough mixing, the 8 tubes (only 2 are shown in Figure 2) were filled to the required level with the airfree solution, sealed off and irradiated with

$\gamma$ -rays. The irreproducible results obtained are given in Table 4.

(ii) A modified pumping line with a better trapping system was constructed (Figure 3). In this experiment, the trapping system at A consisted of only one short liquid air trap. Traps T and B were filled with a freezing-mixture of dry-ice and trichloroethylene and the process of pumping, condensing and melting was carried out as described in (a) (i). On

irradiation of the airfree ferrous sulphate solution produced, reproducible results were obtained and are given in Table 4.

(b) Standard deaeration procedure.

The mercury diffusion pump was removed from the line, the amalgam from the traps at A and the freezing-mixture in traps T and B was replaced by liquid air. The solution to be deaerated was heated gently, in vacuo, until most of the solution had been transferred, in the form of ice, to the inside of trap T. The stopcock S was closed and the ice was allowed to melt back into the deaeration vessel M, which was then sealed off at the constriction C. After thorough mixing of the airfree solution the vessel was tilted so that each side tube in turn could be filled to the 5 ml. mark and sealed off. The reproducible results obtained on  $\gamma$ -irradiation of airfree ferrous sulphate solutions, are shown in Table 4.

(c) Standard deaeration technique adopted  
for solutions containing dissolved  
radioactivity.

In order to study the effects of polonium  $\alpha$ -particles on airfree solutions of ferrous sulphate, the apparatus shown in Figure 4 was attached

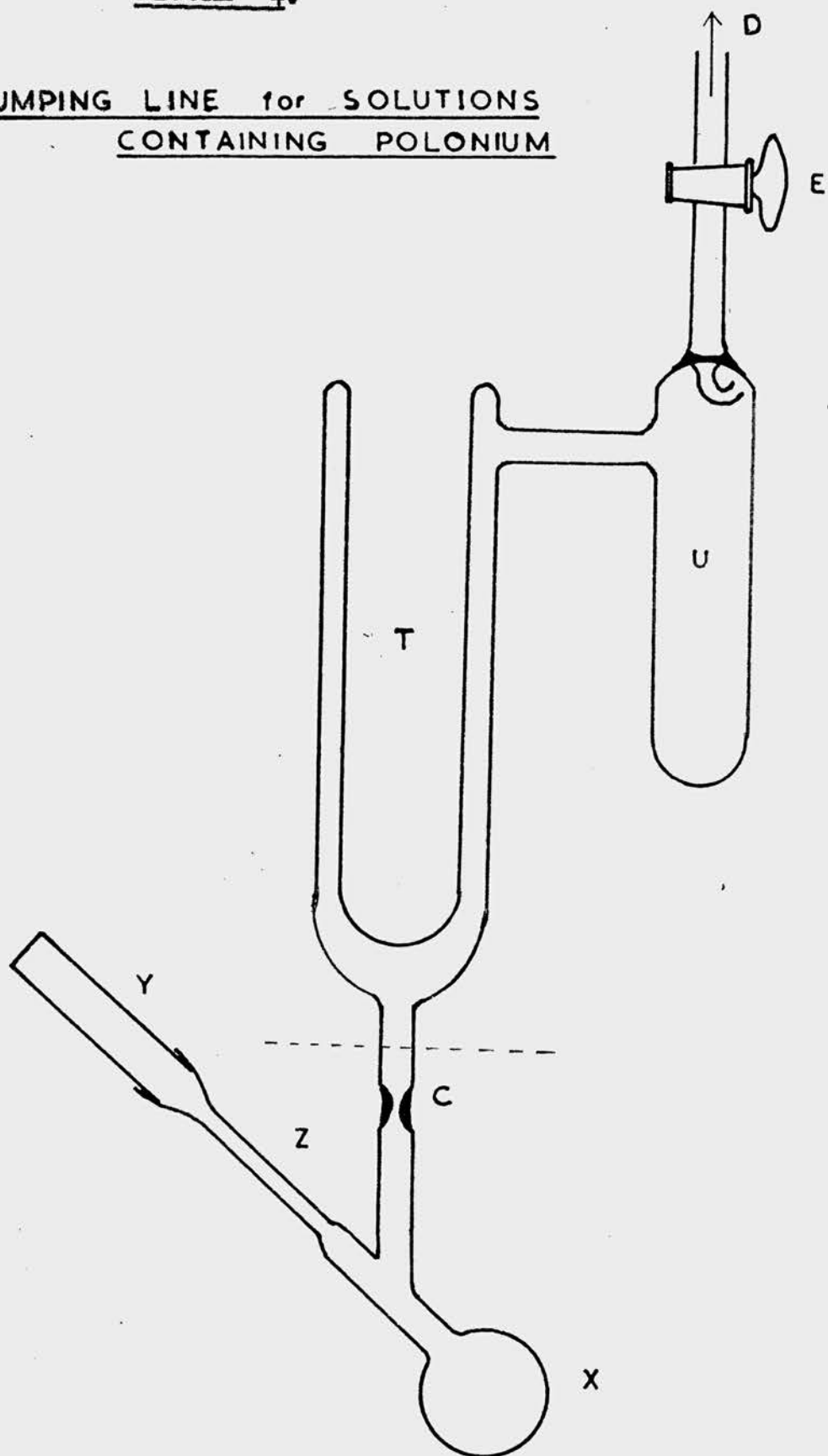
FIGURE 4.

Pumping Line for Solutions  
Containing Polonium.

- X     pyrex glass bulb of 15 ml capacity
- Z     graduated tube
- Y     1 cm quartz spectrophotometer cell
- C     constriction
- T     liquid air trap
- U     spray trap
- E     stopcock
- D     point of attachment to the pumping line "d"  
shown in Figure 3.

FIGURE 4.

PUMPING LINE for SOLUTIONS  
CONTAINING POLONIUM





to the pumping line "d" (Figure 3) at the point D. The deaeration vessel consisted of a bulb X of approximately 15 ml. capacity connected to a quartz spectrophotometer cell Y by means of a graduated tube Z. The quartz cell was sealed into the apparatus with picein wax. The pumping arrangements and deaeration procedure were the same as in section (b), described previously. This apparatus could be used to follow the course of oxidation with time of both aerated and airfree solutions of ferrous sulphate. *the section of the apparatus shown below the broken line (fig 4),* By inverting, at intervals, the formation of ferric ion could be measured with the spectrophotometer.

To check the efficiency of the apparatus and to determine whether the presence of picein wax in the deaeration vessel had any effect on the results, a series of experiments was made in which solutions of ferrous sulphate were irradiated with X-rays. Approximately 8 ml. of aerated ferrous sulphate were pipetted into the bulb X. The vessel was inverted and the amount of ferric ion originally present in the solution was determined spectrophotometrically. The exact volume of the solution was observed from the position of the meniscus in the graduated tube Z. The solution was then allowed to run back into the bulb

and the apparatus was clamped in such a way that the bulb could be mounted reproducibly on the end of the X-ray tube. The amount of ferric ion produced was measured after each 5 minute period of a total irradiation time of 40 minutes. A 5 minute irradiation at 1.5 m.a. was found to raise the temperature of the solution by approximately  $3^{\circ}\text{C}$ . As described previously the extinction coefficient of ferric ion was found to be temperature dependent. The solution was therefore brought to  $20 \pm 1^{\circ}\text{C}$  before analysis. The amount of ferric ion produced was linear with irradiation time and a value was obtained for the ferrous ion oxidation yield expressed as micromoles oxidised per minute. In a second experiment a further 8 ml. quantity of aerated solution was pipetted into the bulb and the apparatus was attached to the pumping line through a constriction C. The solution was deaerated, sealed off and the X-ray oxidation yield in airfree solution was determined in the same manner as the aerated yield described previously. The values for the ratios of the yields in aerated solutions to those in airfree solutions are given in Table 4.

To determine whether organic impurities were present in solution, due to contact with the picein, solutions which had been irradiated in airfree

solution were allowed to become air saturated, then irradiated once more. As an additional check ferrous ion solutions containing  $\sim 10^{-3}M$  sodium chloride, were irradiated in both the aerated and airfree state. The results obtained are given in Table 4.

For purposes of comparison some results obtained by Dr. H.A. Dewhurst<sup>38</sup>, of this laboratory, are included in Table 4.

(d) Discussion of the Results.

It has been realised for some time that impurities play an important part in radiation-induced reactions in aqueous solution<sup>10,16</sup>. Impurities have been shown to have a considerable effect in solutions where hydrogen peroxide builds up during irradiation<sup>5(a)</sup> and to influence the course of reactions where the concentration of hydrogen peroxide is low. The oxidation of ferrous ion by  $\gamma$ -rays was found to be accelerated on addition of organic impurities and retarded on addition of inorganic impurities<sup>45</sup>. The addition of small amounts of aliphatic alcohols<sup>41</sup> was found to increase the rate of ferrous ion oxidation.

As considerable care was taken in purifying the

TABLE 4.

Results obtained on irradiating airfree and air saturated solutions of ferrous sulphate in 0.8N sulphuric acid.

Conditions of Deaeration	Type of Radiation	Concentration of Ferrous ion M	Ratio of Yield in aerated Yield in airfree solution
(a)	$\gamma$	$5 \times 10^{-4}$	2 - 10
(i) Using the Krenz-Dewhurst apparatus	"	"	$\sim 2.7$
(ii) Small trap at A: traps T and B filled with a freezing mixture of dry ice and trichlorethylene	"	"	$\sim 2.3$
(iii) Large amalgam lined traps at A			
(b)	"	"	$\sim 2.3$
Standard deaeration procedure adopted for solutions to be irradiated with $\gamma$ -rays	"	$1.22 \times 10^{-3}$	2.26
	"	$5.3 \times 10^{-4}$	2.28
	"	$4.87 \times 10^{-4}$	2.48
	"	$4.62 \times 10^{-4}$	2.36

(c) Standard deaeration procedure adopted for solutions to be irradiated either externally with X-rays or with $\alpha$ -rays from an internal source	X " " " "	5 x 10 <sup>-3</sup> 1.79 x 10 <sup>-3</sup> 1.41 x 10 <sup>-3</sup> 10 <sup>-3</sup> M in NaCl 1.25 x 10 <sup>-3</sup>	2.0 2.33 2.34 2.31
Results obtained by Dewhurst <sup>38</sup> using a deaeration procedure similar to (b)	$\gamma$ " " " " " "	10 <sup>-2</sup> 5.2 x 10 <sup>-3</sup> 10 <sup>-3</sup> 5.1 x 10 <sup>-4</sup> 2.2 x 10 <sup>-4</sup> 10 <sup>-4</sup> 4.5 x 10 <sup>-5</sup>	2.06 2.06 2.25 2.36 2.70 3.45 4.96

water used in the experiments described previously, it was suspected that the irreproducible results obtained in (a) (i) were due to the presence of impurities introduced during deaeration. It was thought possible that volatile components from the stopcock grease or from the pump oil may have diffused back, condensed on the liquid air trap T and eventually have become dissolved in the deaerated solution. The stopcock S was therefore placed at a greater distance from the deaeration vessel and an additional trap B was installed. It was considered that when the traps B and T were filled with a dry-ice-trichloroethylene freezing mixture they would be less likely to condense impurities than when filled with liquid air. The experiments ((a)(ii)) made with this system lowered the aerated/airfree ratio to  $\sim 2.7$  and appeared to confirm this theory. Long traps lined with a copper-mercury amalgam and installed at A were found ((a)(iii)) to reduce the ratio to  $\sim 2.3$  and the theory that back diffusion of mercury vapour was responsible for the high ratios was confirmed when deaerations were made (b) employing the rotary oil pump alone. Dewhurst<sup>38</sup> has shown that the presence of stopcock grease does not affect the oxidation yield of ferrous ion either in aerated or airfree solution. It was

clear, therefore, that the results obtained in airfree solutions by Krenz and Dewhurst<sup>35</sup> were influenced by the presence of impurities introduced during the deaeration process.

In confirmation of the results of Rigg, Stein and Weiss<sup>29</sup> and Dewhurst<sup>38</sup> it was shown in experiments (b) and (c) that the ratio of the oxidation yield in aerated ferrous sulphate to that in airfree solution, varied with the ferrous ion concentration and approached a value of 2 at high concentrations.

The results obtained with the apparatus described in section (c) for use in X- and  $\alpha$ -ray irradiations, confirmed the results obtained in  $\gamma$ -ray experiments. The irradiation with X-rays of a reaerated solution which had previously been deaerated, produced the same amount of oxidation as that produced in the original aerated solution. This indicated that no impurities were present in the solution as a result of its contact with picein. This was confirmed when ferrous sulphate solutions containing sodium chloride were irradiated with X-rays. Had organic impurities been present, the ferrous ion oxidation yield would have increased and on addition of sodium chloride the yield would have been lowered. No such effects were observed.

As a result of these experiments, the methods

employed for the deaeration of solutions for  $\bar{X}$ -,  $\gamma$ -  
and  $\alpha$ -irradiations were considered to be adequate.



III.      THE CHEMICAL EFFECTS OF  $\alpha$ -RADIATION ON  
            AQUEOUS FERROUS SULPHATE.

1.      Introduction.

The problem of using ferrous sulphate as a chemical dosimeter for  $\alpha$ -radiation may be approached along two general lines.

(i) Using an internal source, when the  $\alpha$ -emitter is dissolved in the ferrous sulphate solution. The production of ferric ions may be followed by a suitable analytical technique and the energy input may be estimated by counting.

(ii) Using an external  $\alpha$ -source. The energy input is measured in an ionisation chamber.

Owing to the high cost of polonium and the difficulty of recovering it from waste solutions, it was decided to undertake the experimental programme described in this section using mainly external sources which could be used over long periods of time. For certain of the kinetic studies, however, external sources were found to be impracticable and internal sources had to be used.  $\text{Po}^{210}$  (138 days half-life, 5.3 Mev  $\alpha$ ,  $R_{\text{air}}$  3.87 cm) was selected as the emission of radiation other than  $\alpha$ -rays is negligible.

## 2. General Experimental Technique.

### (1) Preparation of Polonium Sources.

#### (a) External.

Polonium was received from the Radiochemical Research Centre, Amersham, as a solution in 0.5N nitric acid containing approximately 0.2 mg/ml lanthanum carrier. The lanthanum was precipitated as the hydroxide, thoroughly washed and dissolved in 2% trichloroacetic acid containing a trace of hydrazine (to keep the polonium in the lower valent state). The polonium was deposited electrolytically as a spot, approximately 0.75 cm. in diameter, in the centre of one face of a platinum disc 0.1 mm in thickness and 2 cm. in diameter. The edges and back of the disc were covered with a thin layer of piccin wax to prevent the polonium from depositing over the whole disc. A thin sheet of mica ( $1.43 \text{ mg/cm}^2$ , equivalent to  $\sim 1 \text{ cm.}$  of air for  $\alpha$ -particles) was then sealed on top of the deposited polonium, enclosing it completely. The strongest source used (initially  $\sim 20 \text{ m.c.}$ ) was prepared at Amersham where the mica was sealed down with cold-setting "araldite" (Messrs. Aero Products Ltd., Cambridge). Even after twelve months use, the amount of polonium leaking from a source of this kind was found to be negligible. The preparation

of the sources was carried out in a "gloved box" which enabled dangerous activities to be handled without risk of contamination. The apparatus was monitored at regular intervals using a scintillation-type  $\alpha$  bench monitor (McMichael Radio Type 1021B). The sources were found to be excellent for irradiations where they could be suspended above the solutions. Unfortunately, they were found to be impracticable for immersion in solution and for irradiations in vacuo. After a very short period of immersion, moisture was observed between the mica and the deposited polonium. This was particularly noticeable for sources where the mica was sealed down with "araldite".

(b) Internal.

Polonium was received as a solution in 0.8N sulphuric acid containing 5 mg/ml neodymium carrier. The neodymium was found to have no effect on the  $\alpha$  - induced oxidation of ferrous sulphate (this will be described in a later section). Irradiations using internal polonium sources were always made in the apparatus described previously in Section II, 5(c). The vessel was thoroughly cleaned and washed out with the solution to be irradiated. An aliquot of the polonium solution was pipetted into the bulb, using an eye-dropper, and diluted to approximately 8 ml.

with the solution to be irradiated.

(c) Polonium recovery.

Internal sources were used only for irradiations of ferrous sulphate solutions in sulphuric acid. Polonium was recovered from these solutions in the following manner. Excess ammonia was added to the solution to precipitate the ferric and neodymium hydroxides. Polonium was carried down with the precipitate. The suspension was centrifuged and the supernatant liquid was removed and discarded. The precipitate was thoroughly washed with distilled water to remove traces of ammonia, dissolved in a small quantity of 7N hydrochloric acid and the ferric chloride was extracted with ether. The polonium and the neodymium carrier were left in solution. Excess ammonia was added to precipitate neodymium hydroxide; polonium was carried down with the precipitate. The suspension was centrifuged and the supernatant liquid discarded. The precipitate was thoroughly washed with distilled water and dissolved in concentrated nitric acid. The solution was transferred to a platinum basin and boiled for several hours to remove traces of organic material. Neodymium hydroxide was precipitated once more with ammonia, centrifuged, washed, and finally dissolved in a small quantity of 0.8N

sulphuric acid. The solution was then ready for further use as a polonium source.

2. The Irradiation System for External Sources:

Figure 5.

The irradiation cell (Figure 5B) consisted of a small pyrex dish about 3.5 cm. in diameter and 1 cm. in depth. This was made by sawing off the bottom of a 30 ml pyrex beaker with a diamond wheel then grinding the rim flat. A polystyrene cap fitted closely into the top of the cell and was threaded to take the source holder (Figure 5A). It was possible to take the cell apart for cleaning purposes. Care was taken that no solution in the cell should come in contact with the cap. The polonium source on its platinum disc was waxed to a brass support with picein. The source holder was threaded to fit the irradiation cell and was equipped with two small tubes which enabled gases to be circulated between the source and the surface of the irradiated solution. When solutions were irradiated it was found that moisture condensed on the surface of the mica. This led to irreproducible results owing to the absorption of a considerable amount of  $\alpha$ -particle energy in the moisture layer.

FIGURE 5.

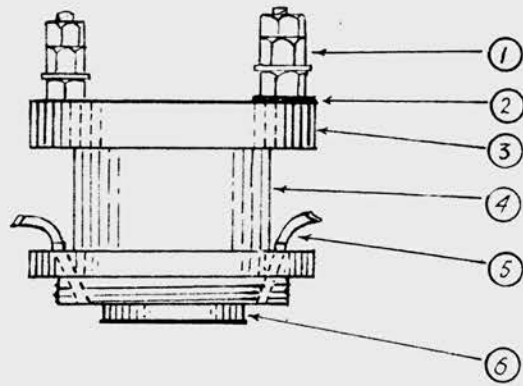
Irradiation System.

- A The source holder
  - 1 heating element terminals
  - 2 rubber pad insulator
  - 3 brass source support
  - 4 heating element
  - 5 gas inlet tube
  - 6 polonium source
- B The Irradiation cell
  - 7 polystyrene cap
  - 8 pyrex glass dish
  - 9 stirrer
- C10 The Magnet
- D The ionisation chamber head (cross section)
  - 11 gold leaf-nylon window
- E The ionisation chamber head (plan)

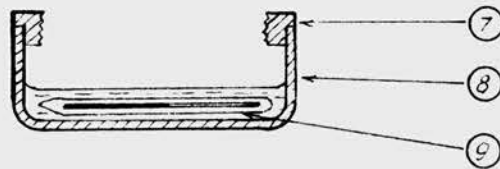
FIGURE 5.

$\alpha$  IRRADIATION SYSTEM

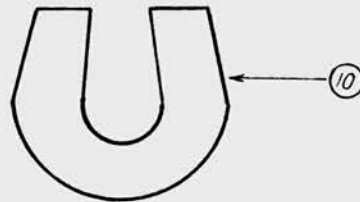
A



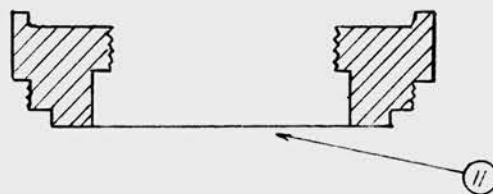
B



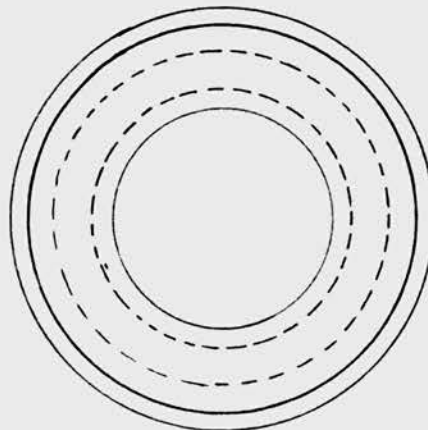
C



D



E



scale = full size

In order to prevent condensation, it was found necessary to raise the temperature of the source holder a few degrees above that of the irradiated solution.

This was done by winding a heating element of about 20 ohms resistance round the brass support. A current of about 0.1 amp. was sufficient to keep the source holder a few degrees above room temperature.

The distance between the surface of the irradiated solution and the source was measured before and after every irradiation. A glass-tipped screw, supported by a plate which bridged the top of the cell, was adjusted so that it just touched the surface of the solution. The distance between the tip of the screw and the top of the plate was measured with a micrometer gauge. The dimensions of the source holder and the plate were known and the source-surface distance could be calculated.

The volume of solution irradiated was 4 ml in every case. It was possible to vary the distance between the source and the surface of the irradiated solution by fitting the irradiation cell with interchangeable polystyrene caps of varying thickness. Most irradiations were made with the source as near to the surface of the solution as possible (approximately 2 mm). This ensured that most of the  $\alpha$ -particles



emerging from the source were absorbed in the liquid. This was checked by exposing a panchromatic plate at a distance of approximately 2 mm from the  $\alpha$ -source. The plate was developed and the diameter of the irradiated area was measured and found to be less than that of the surface of the irradiated solution. A Kodak NT4 nuclear emulsion plate was also exposed at the same distance. The plate was developed and the irradiated area was examined with a microscope for other radiation such as protons produced, possibly, by  $\alpha$ -irradiation of moisture absorbed on the mica covering the source. None was observed.

For the purposes of analysis, the solution which had been irradiated was transferred quantitatively to a 5 ml graduated flask using an eye-dropper. For example, after the irradiation of ferrous sulphate in 0.8N sulphuric acid, the solution was transferred to the flask and the cell was washed out with small quantities of 0.8N sulphuric acid. The washings were transferred to the flask and the solution was diluted to 5 ml with 0.8N sulphuric acid. The solution was analysed for ferric ion as described in a previous section. It was found necessary to remove the whole of an irradiated solution for analysis in order to eliminate errors due to evaporation which was considerable for a long irradiation where a gas was passed

through the cell.

Certain experiments required that the solution should be stirred during the irradiation. This was done by sealing a short iron rod inside a glass tube which was then placed in the irradiation cell. The solution could be stirred by rotating a magnet below the cell. The magnet was rotated by a 50-cycle A.C. induction motor and by varying the reduction gearing system, speeds up to two revolutions per second could be obtained. This was the maximum stirring speed which could be used without splashing solution on to the source or altering the source-solution distance by causing vortex formation.

Every irradiation was accompanied by a control experiment in which the exact irradiation conditions were reproduced. A dummy source was threaded into a cell which had the same geometry as the irradiation cell. The chemical change which took place in a solution in the control cell was measured after a period of time equal to that for the irradiation.

(3) Discussion of the General Experimental Technique.

The  $\alpha$ -particle sources used by previous workers<sup>1, 25, 46</sup> for the irradiation of aqueous solutions were of two main types:-

1. Internal sources in which radon or polonium was dissolved in the solution to be irradiated.
2. External sources such as thin glass bulbs filled with radon, or metal foils on which polonium had been deposited electrolytically. The bulb or foil was then immersed in the solution.

Both these types of sources have serious disadvantages. About 5% of the total energy output from a radon source is due to  $\beta$ -particles from the radon decay-products. Many chemical reactions are induced more efficiently by  $\beta$ -rays than by  $\alpha$ -rays. An example of this is the deactivation of carboxypeptidase by X- and  $\alpha$ -radiation<sup>47</sup>. The  $\alpha$ -ray ionic yield was found to be only one-twentieth of the X-ray ionic yield (500 kV X-rays were shown to be comparable in their chemical action to the  $\beta$ -rays from RaB and RaC, the decay products of radon). When radon is used as an  $\alpha$ -source a correction must therefore be made for the effects produced by the  $\beta$ -particles. This entails

knowledge of the additivity of the effects produced by the  $\alpha$ - and  $\beta$ -rays acting simultaneously. Many experimental difficulties are encountered when using radon. These include the distribution of radon between the gaseous and liquid phases and the adsorption of activity on the surface of the irradiation vessel. When radon is sealed inside thin-walled  $\alpha$ -bulbs, a considerable amount of the  $\alpha$ -particle energy is absorbed in the glass.

The use of uncovered polonium sources is not to be recommended purely from considerations of contamination and health-hazard. Polonium tends to spread activity owing to the phenomenon of aggregate recoil. Attempts have been made to overcome this difficulty by covering the deposited polonium with shellac or a thin layer of gold. These were unsuccessful as the covering material soon disintegrated under the intense  $\alpha$ -particle bombardment. Difficulties are sometimes experienced when polonium is used as an internal source. It has been alleged that dissolved activities may have a chemical effect on the solution irrespective of the effects produced by the radiation. For example polonium has been shown to catalyse the decomposition of hydrogen peroxide.<sup>48</sup> Reactions of this type were not considered likely to affect the results

obtained on irradiation of ferrous sulphate solutions with an internal polonium source, on account of the rapid reaction between ferrous ions and hydrogen peroxide.

The external polonium source described in the previous section (2(i)(a)) did not possess any of the disadvantages outlined above but, owing to its inability to stand up to immersion in solution or to vacuum conditions, the source was suspended above the solution. Great experimental difficulty was encountered owing to the presence of a gaseous phase between the source and the solution. The methods by which these difficulties were overcome will be discussed in a later section.

A certain amount of  $\alpha$ -particle energy was lost due to absorption in the mica which covered the polonium. The thickness of the mica corresponded to approximately 1 cm of air so that polonium  $\alpha$ -particles (range = 3.87 cm in air) which emerged normal to the surface of the source would have a range, in air, of approximately 2.87 cm. Particles leaving the platinum disc at angles greater than approximately  $75^\circ$  to the normal would be totally absorbed by the mica.

$\alpha$ -particles of all ranges up to approximately 2.87 cm in air, were emitted from the surface of the mica

which covered the polonium.

The important part played by impurities in radiation-induced chemical reactions, has been stressed in previous sections. Preliminary experiments were made in which ferrous sulphate solutions contained in irradiation cells constructed entirely from polystyrene, were irradiated with polonium  $\alpha$ -particles. The ferrous ion oxidation yields observed were completely irreproducible. This was attributed to the presence of impurities introduced during the irradiation, probably as a result of organic matter from the polystyrene cell becoming dissolved in the solution. Irradiations were therefore made in glass-polystyrene cells where the solution was not allowed to touch the polystyrene cap. Reproducible results were obtained.

Polonium  $\alpha$ -particles penetrate an 0.8N sulphuric acid solution to an approximate depth of 0.002 cm (calculated from Lea<sup>49</sup>). With very strong sources it is conceivable that owing to the great density of ionisation products in the surface layer, stirring would be necessary to prevent depletion of ferrous ions in this layer. Experiments which will be described in a later section showed that except for solutions in which the concentration of ferrous

ions was low, stirring had no effect on the oxidation yield.

### 3. Preliminary Irradiation Experiments.

#### (1) Irradiation of Ferrous Sulphate Solutions in Air Filled Cells.

Five 4 ml. portions of ferrous sulphate in 0.8N sulphuric acid solution were pipetted into identical irradiation cells. Five weak ( $<0.5$  mc) polonium sources of varying strength were threaded into the cells. The source-solution distance in each cell was approximately 6.0 mm. The space between the source and the solution was filled with air. Each solution was stirred at a rate of approximately two revolutions per second. The amount of ferric ion produced by each source was found to be a linear function of irradiation time. The initial concentration of the ferrous ion in the solutions irradiated, was varied. The rate of ferrous ion oxidation at each concentration was obtained from the slope of the ferric ion production/irradiation time curve. The rate of ferrous ion oxidation was expressed as a function of the initial ferrous ion concentration. The curves obtained with the five sources are given in Figure 6, the number above each curve denoting the source used.

FIGURE 6.

Ferrous Ion Oxidation Yield as a Function  
of Initial Ferrous Ion Concentration.

Irradiations made on stirred solutions of  
ferrous sulphate in 0.8N Sulphuric acid.

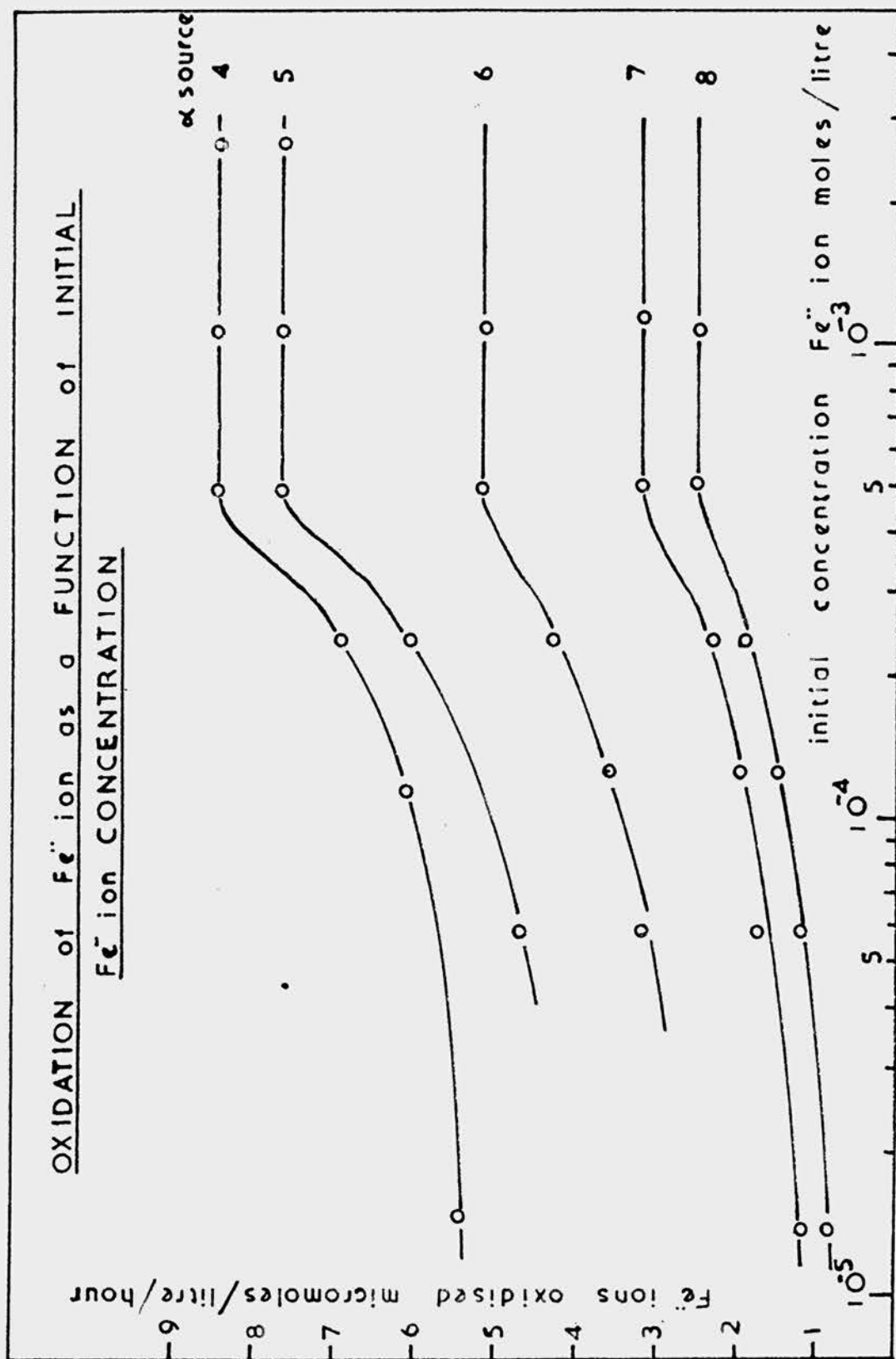
Irradiations made in air-filled cells.

Sources of strength  $< 0.5$  mc.

Source-solution distance 6 mm.



FIGURE 6.



For initial ferrous ion concentrations greater than  $5 \times 10^{-4}M$ , the rate of oxidation was found to be independent of ferrous ion concentration. This was an extension of the concentration independent region observed by Nurnberger<sup>25</sup>. For initial ferrous ion concentrations less than  $5 \times 10^{-4}M$ , the rate of oxidation decreased slowly as the initial ferrous ion concentration was decreased. The significance of this fall-off will be discussed later in this section.

The results obtained in an air-filled cell are of no great value in view of the importance of the gaseous phase which will be discussed later in this section.

(2) The Effects Produced on Irradiation of the  
Gaseous Phase above a Ferrous Sulphate  
Solution.

Dee and Richards<sup>50</sup> have recently suggested that the bulk of the chemical effect of  $\alpha$ -particles on aqueous solutions is due to the secondary effects of quantum emission arising from the primary ionisations. If light produced by  $\alpha$ -irradiation of liquids was capable of producing a chemical effect, it was thought possible that the light emitted on  $\alpha$ -irradiation of gases might have the same effect.

The glass base of an irradiation cell was fitted with a polystyrene cap of such dimensions that a source could be placed at a distance of approximately 4 cm from the surface of a ferrous sulphate solution in the cell. The solution was thus outside the maximum range of the  $\alpha$ -particles. Irradiations were made on different gases and the chemical effects which occurred in the ferrous sulphate solution, were observed. The irradiations made were as follows:-

- (a) Air filling the space between the source and the solution.
- (b) A slow current of air passing through the cell.
- (c) " " " " nitrogen " " "
- (d) " " " " carbon dioxide passing through the cell.

The results of these experiments are given in Table 5.

A small amount of ferrous ion oxidation was detected in an air-filled cell. This was, however, found to decrease when slow currents of gases were passed through the cell. These experiments seemed to indicate that some oxidising substance was produced on irradiation of air and was subsequently absorbed in the solution with the result that ferrous ions were oxidised. Sweeping out the irradiation cell with air had little effect although when nitrogen and

TABLE 5

The Effect of  $\alpha$ -Rays on the Gaseous Phase above a Ferrous Sulphate Solution.

Conditions in the irradiation cell	Source-Solution Distance mm	Irradiation time hours	Amount of Ferric Ions produced $\mu$ M	Ferrous ion oxidation yield $\mu$ M/l/hour
(a) Air filled cell	40	19.62	9.7	0.494
" " "	"	19.65	9.55	0.486
(b) Current of air through the cell	"	20.17	10.9	0.541
" " "	"	38.8	13.6	0.351
(c) Current of nitrogen through the cell	"	41.42	8.85	0.214
(d) Current of carbon dioxide through the cell	"	42.82	6.21	0.145
Air filled cell	6.0			~ 8.0

carbon dioxide were used, the ferrous ion oxidation yield was appreciably lowered. The significance of these results will be enlarged upon later in this section.

(3) The Chemical Effects of Light Produced by  
 $\alpha$ -rays.

The result of the previously described experiment was not conclusive as to the possibility of chemical effects being produced in solutions by light emitted on irradiation of the gaseous phase. An attempt was made, therefore, to detect the light by other methods.

Several pieces of clear quartz, approximately 4 cm square, were examined for light transmission down to 2000 Å with the spectrophotometer. One piece 3.52 mm in thickness was of fused quartz. The others, 2.94 mm in thickness were of highly polished crystalline quartz. The results obtained are given in Table 6. The crystalline quartz was found to have better light-transmitting properties than the fused variety and was therefore selected for use in the following experiments.

TABLE 6.

Wave length Å	Percentage Transmission	
	Fused Quartz	Crystalline Quartz
3000	83.7	90.0
2500	72.0	88.0
2000	37.5	73.0

Dee and Richards<sup>50</sup> performed an experiment in which a chemical effect was observed in a solution, allegedly due to the light produced by  $\alpha$ -irradiation of a thin film of water supported above the solution by a quartz slide. An attempt was made to confirm these results.

The glass base of an irradiation cell was filled to the brim with approximately  $10^{-3}M$  ferrous sulphate in 0.8N sulphuric acid solution. A piece of crystalline quartz was placed on top of the cell so that the solution overflowed and air was completely excluded from the cell. A polonium source was clamped approximately 1 mm above the quartz and the solution was irradiated for twenty hours. Analysis showed that no chemical effect had taken place in the solution. The experiment was repeated with a thin film of liquid

covering the upper surface of the quartz. Dilute sulphuric acid was used as it was found impossible to maintain a thin film of water during the irradiation period, owing to evaporation. Again, no chemical change was observed.

These results are in direct contradiction to those obtained by Dee and Richards. An attempt was made, therefore, to detect the light by physical means.

The polonium source was clamped approximately 4 cm above a panchromatic plate, covered on the emulsion side with yellow vaseline. The panchromatic plate is light sensitive down to 2000 Å. This sensitivity is increased by the vaseline which, under ultra-violet light produces a fluorescence and renders the plate light sensitive down to 1800 Å. The plate was exposed for fifteen minutes. The vaseline was removed with amyl acetate and the plate was developed. No light was detected.

The experiment was repeated with a piece of crystalline quartz, whose upper surface was covered with a thin film of dilute sulphuric acid, interposed between the source and the plate which were approximately 1 cm apart. The plate was exposed for thirty minutes and again no light was detected.

These experiments indicated that if any light was

produced in the air or in the thin layer of liquid, it had wavelength less than 1800 Å.

The comprehensive experiments reported by Miller<sup>51</sup> confirmed that no chemical change occurred in solutions irradiated according to the method of Dee and Richards. Furthermore, in an extensive physical study it was shown that, contrary to the experiments of Dee and Richards, the amount of light of wavelength greater than 1800 Å emitted by irradiated water was not appreciable and the possibility of it producing a chemical effect, negligible. In view of this work it was considered safe to neglect completely the possibility of a chemical effect due to secondary light emission.

#### (4) The Effect of Varying the Gaseous Phase in the Irradiation Cell.

The importance of the gaseous phase over an irradiated solution has been indicated in the experiments described previously in section (2). These experiments were repeated with the 20 m.c. source a distance of 6.91 mm above the approximately  $10^{-3}M$  ferrous sulphate solution. Irradiations were made first in an air filled cell. The amounts of ferrous ion oxidised were expressed as a function of the





FIGURE 7.

The Dependence of the Ferrous Ion  
Oxidation on the Gaseous Phase.

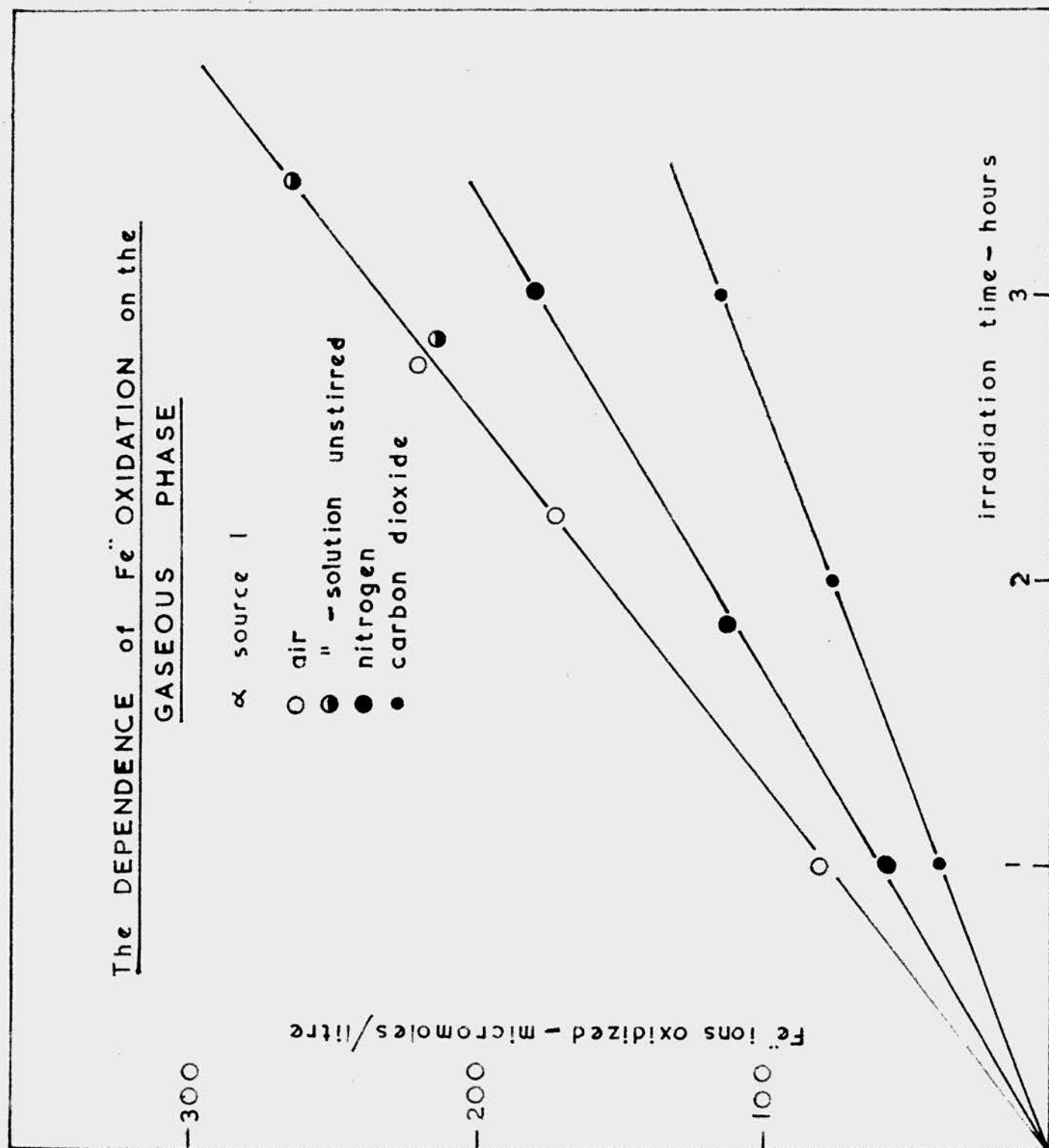
Oxidation of the ferrous ion as a function of  
irradiation time.

A solution of  $\sim 10^{-3}$  M ferrous sulphate in  
0.8N sulphuric acid.

Source-solution distance 6.91 mm.

Strength of source  $\sim 13$  mc.

FIGURE 7.



irradiation time (Figure 7). The ferrous ion oxidation/irradiation time curve was repeated with a slow current of commercial nitrogen passing through the irradiation cell, then with commercial carbon dioxide. The amount of ferric ion produced in each experiment was found to be a linear function of irradiation time (Figure 7). The ferrous ion oxidation yield was found to be constant whether irradiations were made on stirred or unstirred solutions. The effects produced by stirring solutions under irradiation will be discussed later in this section. The ferrous ion oxidation yield was markedly reduced when currents of nitrogen or carbon dioxide were passed through the cell during irradiation. These reductions were of too great a magnitude to be attributed to variations in the  $\alpha$ -particle stopping-power of the gases. It was apparent that some oxidising agent had been produced in the air as a result of  $\alpha$ -irradiation, and had been subsequently absorbed in the ferrous sulphate. The effect of passing a current of an inert gas through the cell would be to lower the concentration of the oxidising agent and consequently decrease the ferrous ion oxidation yield. After the irradiation of a solution in an air filled cell was completed, the source was removed. It was found possible to detect,

by smell, the presence of ozone in the cell.

The formation of ozone by  $\alpha$ -irradiation of oxygen was studied by Lind and Bardwell<sup>52</sup> and a calculation of the yield from the  $M/N$  value quoted by these workers gave  $G_{O_3}^{\alpha} = 6.1$  to  $7.6$  molecules/100 ev. It will be described in a later section how, by observing the ferrous ion oxidation yields at different source-solution distances in the air filled irradiation cell, it was possible to calculate an approximate value for  $G_{O_3}^{\alpha}$ . The value obtained was close to that quoted by Lind and Bardwell. It was concluded therefore that the high value of the ferrous ion oxidation yield observed in air, compared with that in nitrogen and in carbon dioxide, was due to the  $\alpha$ -induced formation of ozone and its subsequent absorption in the solution.

Weininger and Adler<sup>53</sup> showed that nitrogen dioxide was produced in air under  $\alpha$ -particle irradiation from a polonium source. The commercial nitrogen used in the experiments described previously was not purified and the presence of oxygen as an impurity or the incomplete sweeping out of air from the irradiation cell would lead, possibly, to the formation of nitrogen dioxide. The absorption of nitrogen dioxide by the irradiated ferrous sulphate solutions may

account for the greater ferrous ion oxidation yield observed in a nitrogen-swept cell than in one swept with carbon dioxide. Lind and Bardwell<sup>54</sup> showed that carbon dioxide was unaffected by  $\alpha$ -irradiation. The use of nitrogen was therefore discontinued.

(5) Possible Effects Produced in Solution by Gases  
Passed Through the Irradiation Cell.

Two difficulties may arise as a result of gases passed over irradiated aerated solutions.

- (a) The gas may dissolve in solution and produce a chemical effect on irradiation,
- (b) The surface layer of the solution may become depleted in dissolved oxygen.

Garrison<sup>55</sup> and his co-workers studied the chemical effects produced on  $\alpha$ -irradiation of ferrous sulphate solutions saturated with carbon dioxide. Molar solutions of ferrous sulphate in 0.1N sulphuric acid were saturated with carbon dioxide and irradiated with 45 Mev helium ions from a cyclotron. The yield for carbon dioxide decomposition was shown to be extremely small compared with that for ferrous ion oxidation. Chemical effects owing to dissolved carbon dioxide in the irradiated solution were therefore assumed to be negligible. Any decrease in the ferrous ion

oxidation yield observed in cells through which carbon dioxide had been passed, could therefore be attributed to the solution having become deaerated. That little effect was produced in a ferrous sulphate solution as a result of carbon dioxide passed through the irradiation cell, was demonstrated by the experiment described as follows:-

A dummy source holder was fitted into an irradiation cell which contained an aerated ferrous sulphate solution. The cell was clamped so that it could be mounted reproducibly on the end of the X-ray tube. Irradiations were made first on aerated ferrous sulphate solutions in air filled cells. The amounts of oxidation were observed after 5 minute periods of irradiation with 50 kV peak X-rays at 1.5 m.a. The oxidation yields, in  $\mu\text{M}/\text{minute}$ , are given in Table 7. A slow current of carbon dioxide was passed through the cell for periods of time equal to those normally used in  $\alpha$ -irradiations. The ferrous sulphate solution in the cell was irradiated with the carbon dioxide still passing over its surface. The ferrous ion oxidation yields observed on irradiation of solutions over which carbon dioxide had been passed for varying periods of time, are given in Table 7.

TABLE 7.

The X-ray Induced Oxidation of Ferrous Sulphate Solutions in  
Cells through which Carbon Dioxide was Passed.

Irradiation Conditions	Period of passing CO <sub>2</sub> before irradi- ation of the solution-hours	Ferrous ion oxidat- ion yield $\mu\text{M}/\text{min.}$
Air filled cell	-	9.58
"	-	9.89
"	-	9.83
"	-	<u>9.77</u>
		Mean = <u>9.77</u> , $\sigma = 0.02$
Carbon dioxide passed		
through the cell	1.08	10.05
"	1.23	9.49
"	3.50	10.07
"	5.17	9.24
"	6.83	<u>9.58</u>
		Mean = <u>9.69</u> , $\sigma = 0.16$

The results indicated that no significant deaeration had occurred as a result of carbon dioxide passed through the irradiation cell. The chemical effects produced in a ferrous sulphate solution irradiated from below with X-rays, are not necessarily the same as those produced by  $\alpha$ -particles from a source above the solution. The results indicated that the solution as a whole had not been appreciably deaerated but gave no indication whether deaeration had occurred in the surface layer of the solution. Since the  $\alpha$ -particles are absorbed in this layer any de-aeration would have a pronounced effect on the ferrous ion oxidation yield (the effects of  $\alpha$ -particles on airfree solutions of ferrous sulphate will be discussed fully in a later section). The ferrous ion oxidation/irradiation time curves for  $10^{-3}M$  solutions of ferrous sulphate irradiated with a 20 m.c. polonium source in cells through which carbon dioxide was passed, were linear, even for irradiations of 16 hours duration. Had any solution been deaerated by the continuous stream of gas passing through the cell, the rate of oxidation would have decreased and the ferrous ion oxidation/irradiation time curves would not have been linear.

When studying the chemical effects produced by



$\gamma$ -rays on aqueous ferrous sulphate Miller<sup>22</sup> observed that very little oxygen was required to keep the solutions effectively oxygen saturated. The commercial quality gases used to sweep out the  $\alpha$ -irradiation cells probably contained sufficient oxygen to keep the solutions effectively aerated. The small amount of ozone formed from this oxygen would be swept from the cell before it could be absorbed in the solution.

An attempt was made to deaerate a ferrous sulphate solution by bubbling carbon dioxide through the solution for thirty minutes. An aliquot of the solution was transferred to the irradiation cell and  $\alpha$ -irradiated with a stream of carbon dioxide passing through the cell. The results indicated that very little deaeration had occurred. It was presumed that either the carbon dioxide contained sufficient oxygen to keep the solution effectively aerated, or alternatively that the solution had become reaerated during its transfer to the irradiation cell. The results obtained in airfree and in carbon dioxide saturated solutions irradiated with an internal source, will be discussed in a later section.

(6) A Study of the Decrease in Ferrous Ion  
Oxidation Yield observed at Low Ferrous  
Ion Concentrations.

It was shown in section (1) that the oxidation yield observed when a stirred solution of ferrous sulphate was irradiated in an air filled cell, decreased as the initial concentration of ferrous ion was decreased, below  $5 \times 10^{-4}M$ . This decrease of yield with decreasing initial ferrous ion concentration is a similar effect to that observed for X- and  $\gamma$ -rays<sup>35,38</sup> where the yield began to decrease at a ferrous ion concentration of  $10^{-4}M$ . Using cells through which carbon dioxide was passed, experiments were made to confirm the observations of section (1) and to provide a mechanism for the decreased yields observed at ferrous ion concentrations below  $5 \times 10^{-4}M$ . These experiments were as follows:-

(a) Irradiations made on unstirred solutions.

A study was made of the ferrous ion oxidation yield as a function of initial ferrous ion concentration between  $2 \times 10^{-5}M$  and  $5 \times 10^{-3}M$ . Curves were plotted (Figure 8) in which the amounts of ferrous ion oxidised were expressed as a function of the irradiation time. The source (approximately 13 m.c.) was not sufficiently powerful to observe the oxidation

FIGURE 8.

Ferrous ion oxidation as a function  
of time

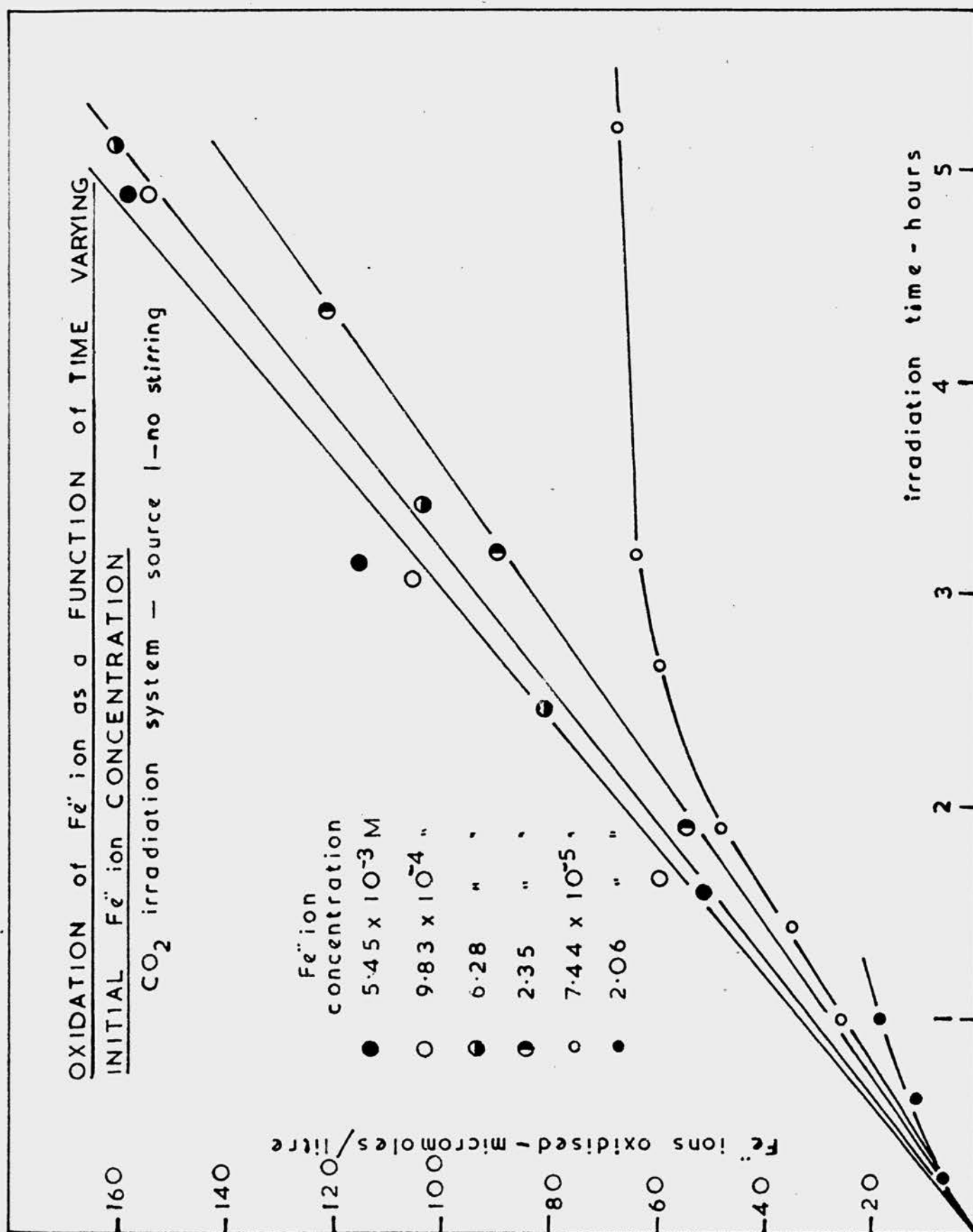
Unstirred 0.8N sulphuric acid solutions  
of ferrous sulphate.

Irradiation cell swept with carbon dioxide.

Strength of source  $\sim 13$  mc.

Source-solution distance 2.74 mm.

FIGURE 8.



to completion of the more concentrated solutions. The curves did, however, appear to be linear over the initial part of the oxidation. With the  $7.44 \times 10^{-5} \text{M}$  solution, it was possible to follow the complete course of the oxidation; the rate of oxidation decreased at approximately 60% oxidation. The ferrous ion oxidation yields, expressed as molecules/100 e.v., were obtained from the initial slopes of the curves in Figure 8, and from ionisation measurements which will be described in a later section. The ferrous ion oxidation yield was expressed as a function of initial ferrous ion concentration (Figure 9, curves A and C) and was found to be independent of initial concentration above  $10^{-3} \text{M}$ . Below  $10^{-3} \text{M}$ , the ferrous ion oxidation yield decreased gradually as the initial ferrous ion concentration was decreased.

Dewhurst<sup>38</sup> showed that for  $\gamma$ -irradiated solutions in the concentration dependent region, the decreased oxidation yield could be restored to the value obtained in the concentration independent region, by heating the irradiated solution for a few minutes prior to analysis. The decrease in the ferrous ion oxidation yield in the concentration dependent region was attributed to the slow rate of reaction between the ferrous ions and the hydrogen peroxide. The effect

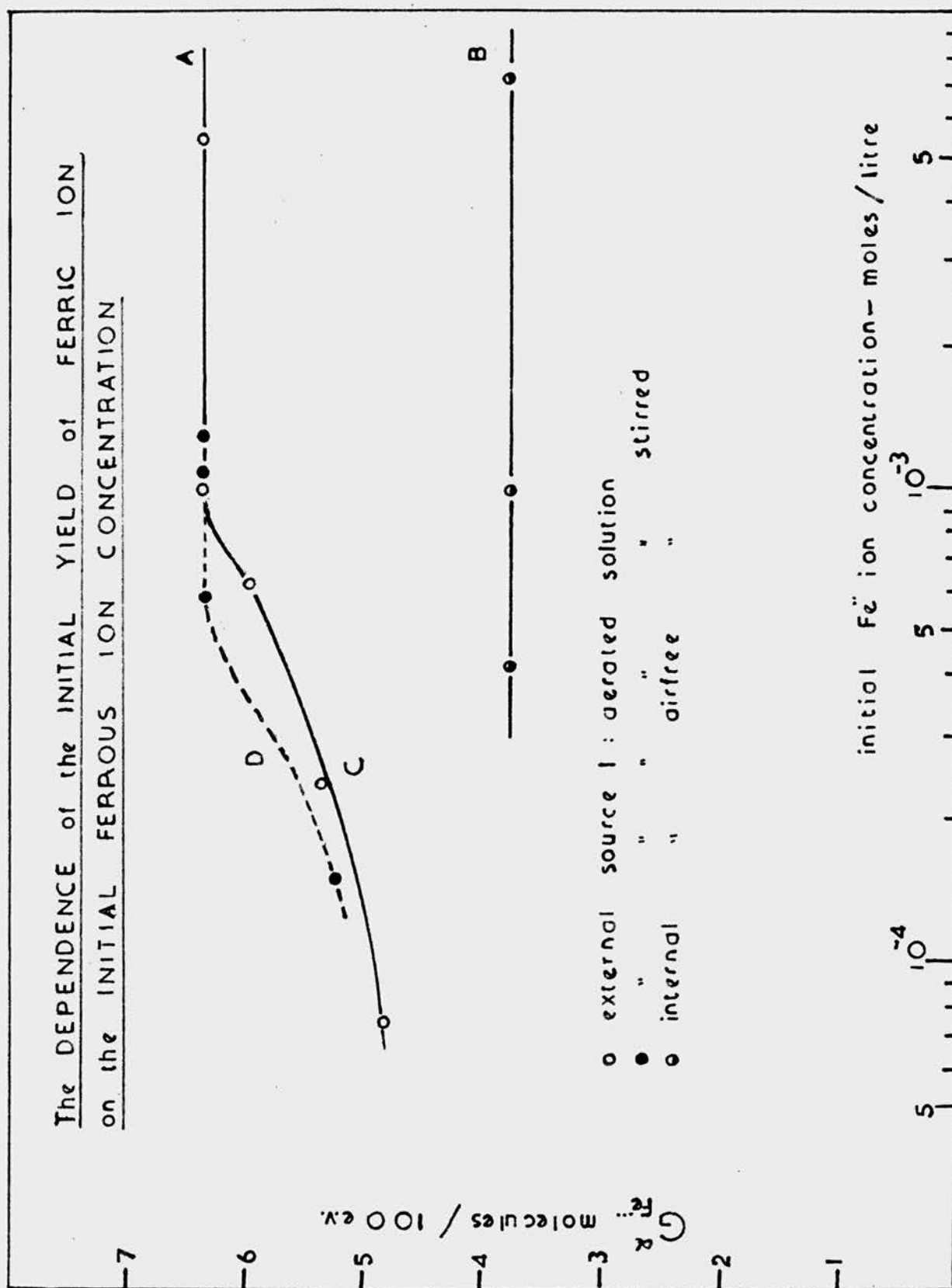
FIGURE 9.

The Dependence of the Initial Yield of  
Ferric Ion on the Initial Ferrous Ion  
Concentration.

0.8N Sulphuric acid solutions of ferrous  
sulphate.

Curves A and C	Unstirred aerated solution; external source
Curve D	Stirred " " " "
Curve B	Airfree solutions; internal source.

FIGURE 9.



of the heat was to increase this rate and so restore the oxidation yield to its normal value.

Heat was applied to  $\alpha$ -irradiated solutions of ferrous sulphate whose concentrations were less than  $5 \times 10^{-4}M$ . No increase of the oxidation yield was observed. This indicated that the slow rate of the ferrous-peroxide reaction at low concentrations of the ferrous ion, was not the cause of the concentration dependent region observed for  $\alpha$ -irradiations.

(b) Irradiations made on stirred solutions.

A study was made of the ferrous ion oxidation yield as a function of initial ferrous ion concentration between  $1.5 \times 10^{-4}M$  and  $1.3 \times 10^{-3}M$ . The solutions were stirred at a rate of two revolutions per second. The ferrous ion oxidation/irradiation time curves are shown in Figure 10. The ferrous ion oxidation yield was expressed as a function of the initial ferrous ion concentration (Figure 9, Curves A and D). The ferrous ion oxidation yield was independent of initial ferrous ion concentration above  $5 \times 10^{-4}M$ . Below  $5 \times 10^{-4}M$ , as in the air filled cells, the ferrous ion oxidation yield was found to decrease as the initial ferrous ion concentration was decreased.

These results indicated that the decrease in ferrous ion oxidation yield with decreasing initial

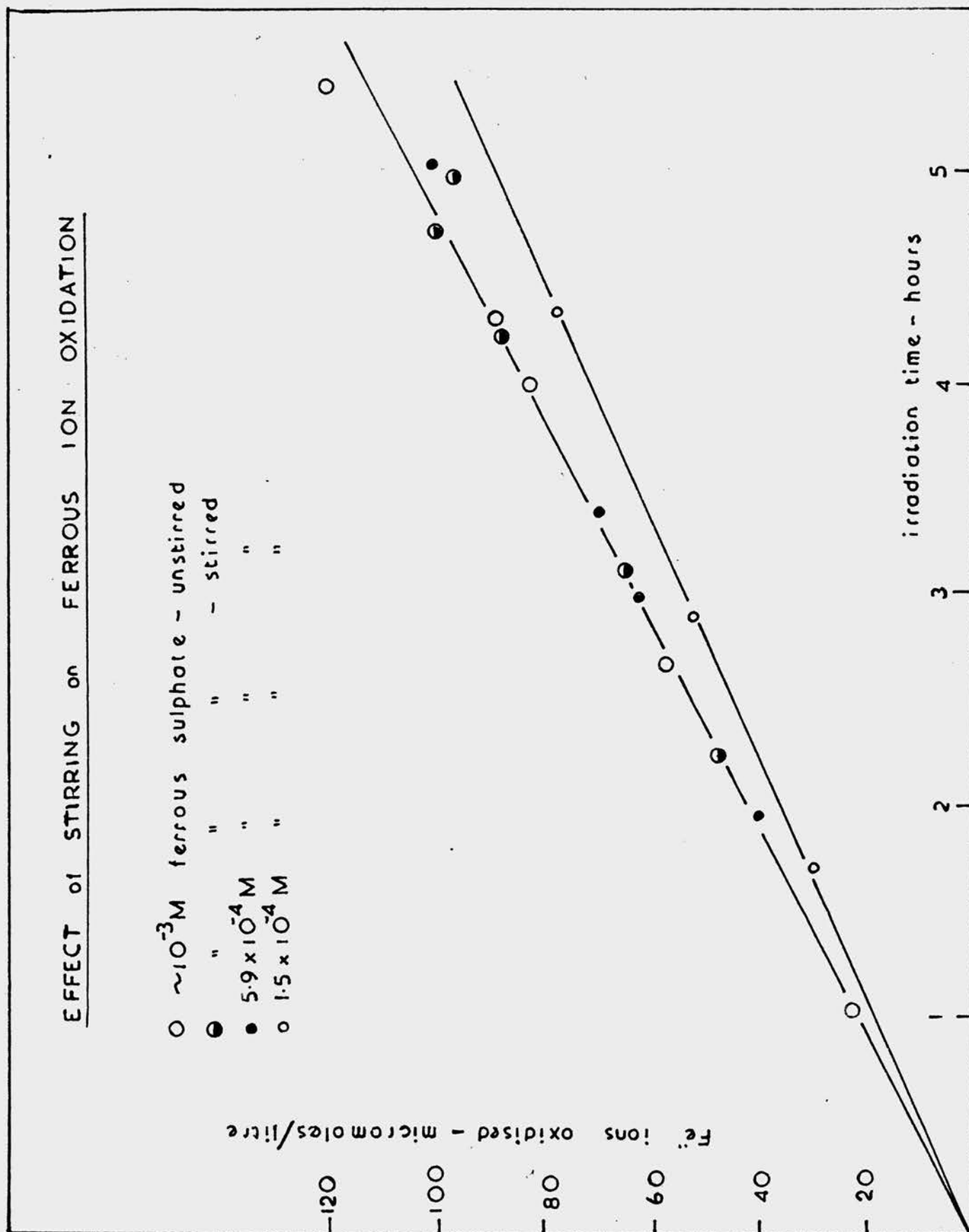


FIGURE 10.

Effect of Stirring on Ferrous Ion  
Oxidation.

Ferrous sulphate in 0.8N sulphuric acid solution  
Irradiation cell swept with carbon dioxide  
Strength of source ~ 6 mc.  
Source-solution distance 2.74 mm.

FIGURE 10 .



ferrous ion concentration was due to inefficient stirring of the solutions. Nurnberger<sup>25</sup>, who used an internal source, observed that the oxidation of ferrous sulphate solutions was linear with time up to 100% oxidation. The irradiations with an external source on unstirred solutions indicated that the oxidation was linear with time only up to approximately 60% oxidation. With an internal source the ionisation products are distributed throughout the solution which, as a result, needs no stirring (Figure 9, Curve B). With an external source, as discussed in a previous section, the  $\alpha$ -particles are absorbed in the surface layer of the solution. The observation that the concentration independent region could be extended from  $10^{-3}M$  to  $5 \times 10^{-4}M$  initial ferrous ion concentration by stirring the solution, indicated that above  $10^{-3}M$  diffusion was sufficient to keep the surface layer replenished with ferrous ions. Below this ferrous ion concentration, diffusion is apparently not sufficient and the solution must be stirred.

For this reason most of the studies of the chemical effects produced by the  $\alpha$ -particles from external sources were made using ferrous sulphate solutions of concentration  $10^{-3}M$  or higher. Stirring at these concentrations is not required. Solutions

irradiated with internal sources of polonium also appear to require no stirring. The ferrous ion oxidation yield observed in airfree solution irradiated with an internal source (Figure 9B), was independent of initial ferrous ion concentration between  $7 \times 10^{-3}M$  and  $4 \times 10^{-4}M$ .

(7) The Effect of  $\alpha$ -rays on Ferrous Sulphate  
Solutions which Contained Ammonium or  
Neodymium Ions.

It has been suggested<sup>65</sup> that different values for  $G_{Fe^{2+}}^{X,\gamma}$  might be observed using different brands of reagents. This was shown later<sup>20</sup> not to be the case. Solutions of approximately  $10^{-3}M$  ferrous sulphate and  $10^{-3}M$  ferrous ammonium sulphate were irradiated with  $\alpha$ -rays from an external source. The ferrous ion oxidation/irradiation time curve is shown in Figure 11. As in solutions irradiated with X- and  $\gamma$ -rays the presence of the ammonium ion had no effect on the ferrous ion oxidation yield.

The polonium solution used as an internal  $\alpha$ -source contained approximately 5 mg/ml of neodymium. Usually 0.1 ml of this solution was added to 8 ml of ferrous sulphate solution. To determine any possible effects produced by the neodymium, the following

FIGURE 11.

The Effect of Neodymium and Ammonium  
Ions on Ferrous Ion Oxidation.

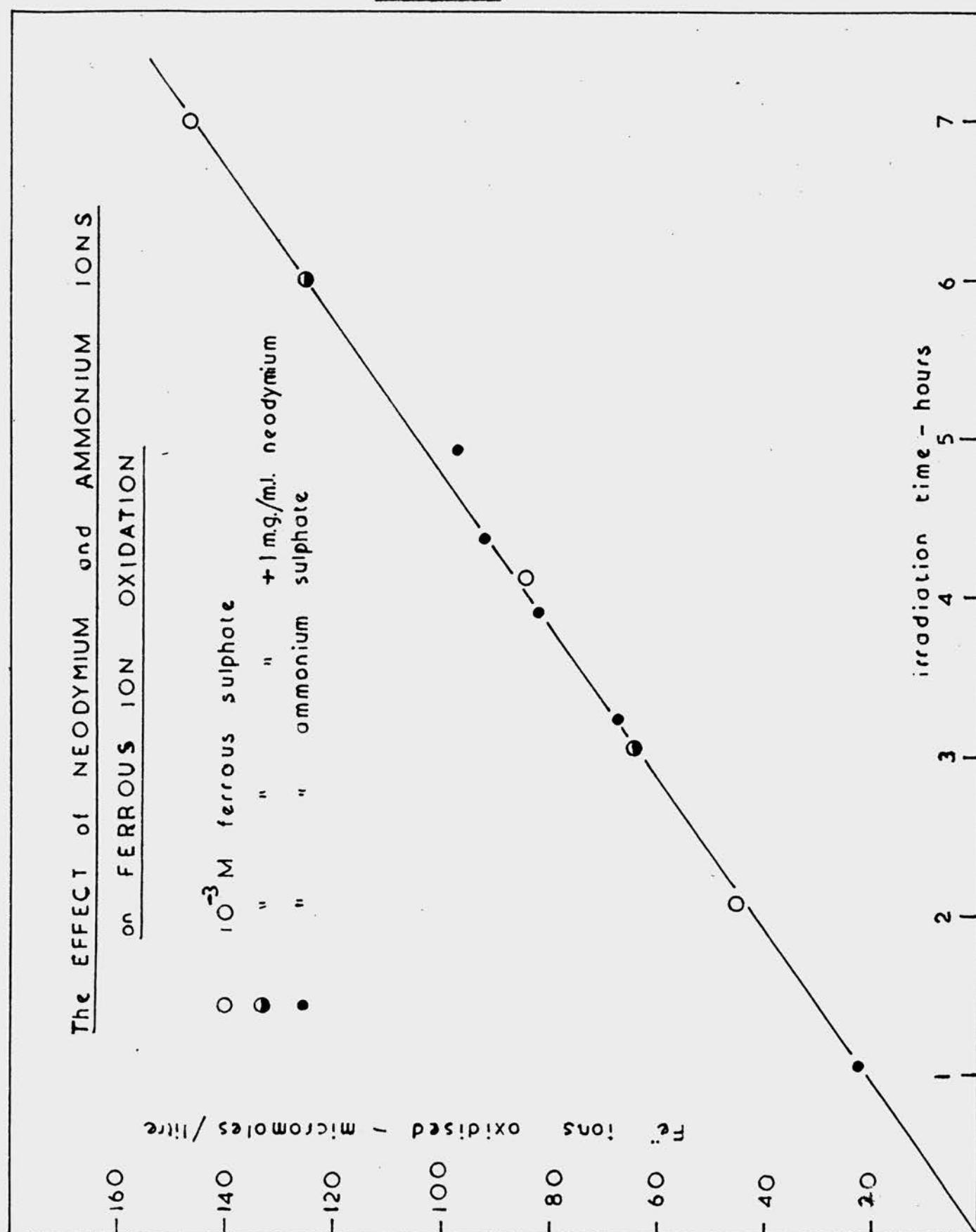
$\sim 10^{-3}$ M ferrous sulphate in 0.8N sulphuric acid.

Irradiation cell swept with carbon dioxide.

Strength of source  $\sim 6$  mc.

Source-solution distance 2.74 mm.

FIGURE 11.



experiments were made.

(a) A ferrous sulphate solution containing 1 mg/ml of neodymium was examined spectrophotometrically at a wavelength of 304 m. $\mu$ . The percentage transmission of the solution did not change with time.

(b) An aliquot of the same solution was irradiated with  $\alpha$ -particles from the external source. The ferrous ion oxidation/irradiation time curve is shown in Figure 11. The ferrous ion oxidation yield was the same as that obtained on irradiation of solutions containing no neodymium.

(c) The solutions irradiated with the internal source contained approximately 0.06 mg/ml of neodymium. 8 ml of a  $5 \times 10^{-3}M$  ferrous sulphate solution containing approximately 0.06 mg/ml of neodymium, were irradiated with X-rays. The solution was de-aerated and irradiated once more with X-rays. As in a solution where no neodymium was present the ratio of Ferrous ions oxidised in aerated solution " " " " airfree " was found to be equal to two (Table 4).

The solution was re-aerated and irradiated once more. The ferrous ion oxidation yield was the same as in the original aerated solution.

These experiments indicated that the presence of neodymium ions had no effect on the ferrous ion oxidation yield in either aerated or airfree solution.

Before proceeding to discuss the use of ferrous sulphate as a chemical dosimeter for  $\alpha$ -rays, it may be useful to summarise the conclusions drawn from the sections just described, as follows:-

1. For a protracted series of experiments, the use of an internal  $\alpha$ -particle source is not to be recommended.
2. The use of external polonium sources introduces many experimental difficulties associated with the gaseous phase. Irradiations must be made in a stream of inert gas or alternatively in the absence of any gaseous phase.
3. A region exists where the ferrous ion oxidation yield is independent of the initial concentration of ferrous ions in the irradiated solution. In this region no stirring is required. For solutions of ferrous ion concentration less than  $10^{-3}M$ , stirring is necessary.
4. The chemical effects produced by secondary light emission are negligible.
5. The presence of neodymium or ammonium ions in the irradiated solution has no effect on the ferrous ion oxidation yield.



#### 4. PHYSICAL MEASUREMENTS.

##### (1) Introduction.

As stated in a previous section the principal object of the work undertaken in this thesis was to determine, accurately, the absolute yield for  $\alpha$ -induced oxidation of ferrous sulphate, i.e. to compare the chemical change produced in a solution of ferrous sulphate with the amount of  $\alpha$ -particle energy absorbed in the solution. Most estimates of the energy emitted by  $\alpha$ -sources are based on measurement of the amount of ionisation produced in a gas filled ionisation chamber. The result for the absolute oxidation yield of ferrous ions depends directly, therefore, on the value assumed for W, the energy released per ion pair formed, for  $\alpha$ -particles in the gas. Gray<sup>56</sup> showed that in air the value of W varied with the energy of the  $\alpha$ -particle. (Table 8)

In hydrogen and the rare gases there is no such variation of W with the energy of the  $\alpha$ -particle and the amount of energy required to produce an ion pair is constant along the whole track. Stetter<sup>57</sup> tabulated useful values of W for polonium  $\alpha$ -particles in various gases. (Table 9)

The best value of W for polonium  $\alpha$ -particles

in air, was calculated by Gray<sup>56</sup> from his modification of Gerbes' formula<sup>58</sup> The value of  $W_{\text{air}} = 35.6 \text{ ev}$  was the average for slowing down the  $\alpha$ -particle to zero energy over the whole length of the track. This result was subsequently confirmed<sup>57,59</sup> and has been generally accepted. Although the average value for  $W_{\text{air}}$  is known accurately, ionisation measurements are not usually made in air filled chambers on account of the poor saturation properties exhibited by air owing to the presence of oxygen. With the type of polonium source used in the present work,  $\alpha$ -particles entered the ionisation chamber with energies depending on the angle at which they were emitted from the source. It is necessary therefore, to employ a gas in which  $W$  is constant over the whole track. Most measurements are made in argon filled chambers owing to the excellent saturation properties of this gas. The value of  $W_{\text{argon}}$  has been determined by comparing the values of the saturation currents obtained in an argon filled ionisation chamber, with those obtained when the chamber was filled with air. The ratio of  $W_{\text{air}}/W_{\text{argon}}$  varies with the energy of the  $\alpha$ -particle. A certain amount of confusion exists in the literature as to the best value to be taken for this ratio. The results obtained by various groups of workers who used

TABLE 8.

The Variation of  $W_{air}$  with  $\alpha$ -Particle Energy.

$\alpha$ -particle energy M.e.v.	1	2	3	4	5	6	7	8
$W_{air}$ e.v.	38.6	37.3	36.5	36.0	35.7	35.4	35.2	35.0

TABLE 9.

The Values of  $W$  for various gases, obtained with Polonium  $\alpha$ -particles.

Gas	Air	Nitrogen	Hydrogen	Helium	Neon	Argon	Krypton	Xenon	Carbon Dioxide
$W_{ev.}$	35.6	37.1	36.0	30.0	29.7	28.2	26.2	23.6	33.9

TABLE 10.  
Determinations of the Ratio of Wair/Wargon for  
Polonium  $\alpha$ -Particles

Residual Range of the $\alpha$ -particle. cm.	Wair e.v.	Wair/ Wargon	Wargon e.v.	Observers
Whole track	35.6	1.26	28.2	Gray <sup>56</sup> Stetter <sup>57</sup> Alder Huber and Metzger <sup>59</sup>
"	35.7			
"	35.9 (corrected for lack of saturation)	1.43	24.9 (recalculated using Wair = 35.6 e.v. 26.1	Schmieder <sup>60</sup>
"	35.2	1.35		Livingstone <sup>61</sup> Valentine <sup>62</sup> McInally <sup>63</sup> Jesse <sup>64</sup> Gurney <sup>64a</sup>
1.9		1.36		
1.25		1.36		
0.7		1.32	26.4 $\pm$ 0.15	
0.4		1.34		
		1.38		
		1.41		

different parts of the polonium  $\alpha$ -track, are given in Table 10.

Ionisation chambers are, in general, of two types:-

- (i) Pulse chambers, in which the ionisation produced by individual particles is detected.
- (ii) Current chambers in which the ion current through the chamber is allowed to flow through some suitable measuring device, for example, a sensitive galvanometer or a resistor to which is connected an electrometer valve to give the integrated effect.

A current chamber is the type most suitable for measuring the ionisation produced by the polonium sources used in the present work. The rate at which energy is dissipated by a source is estimated by measuring the saturation current. The chief problem with current ionisation chambers is saturation. Two of the important factors which affect saturation are recombination and electron attachment processes whereby negative ions are formed. These effects are not serious in the rare gases, provided that they are pure and not contaminated with gases, such as oxygen, which have high electron affinity. \*

Powerful sources produce large saturation

\*On account of the trace of oxygen present in the commercial quality argon used in ionisation current measurements, the saturation characteristics of the chamber were not entirely reproducible (Fig 15 and Fig 23).

currents and very high chamber fields are required to obtain saturation. A parallel plate ionisation chamber was known to have good saturation properties and was considered to be suitable for the present work. In order to eliminate spurious effects due to discharges across the insulating surface reaching the collecting electrode, the latter is usually provided with a guard-ring which also renders the collecting field more uniform over the collecting volume.

The measurement of the saturation currents produced by the polonium sources, in an argon-filled, parallel plate ionisation chamber, are described in the following section.

## (2) The Ionisation Chamber.

The ionisation chamber (Figure 12) consisted of two plastic discs 0.6 cm in thickness and 17 cm in diameter clamped together with eight brass bolts across a brass cylinder, 3 cm in depth and 14.5 cm internal diameter. The chamber had a volume of approximately 500 ml and was fitted with gas inlet and outlet tubes. The upper disc was of perspex, the central part of which was cut away to receive the ionisation chamber head. The cut-away section was well coated with "aqua-dag" so that there should be good contact

FIGURE 12.

Ionisation Chamber.

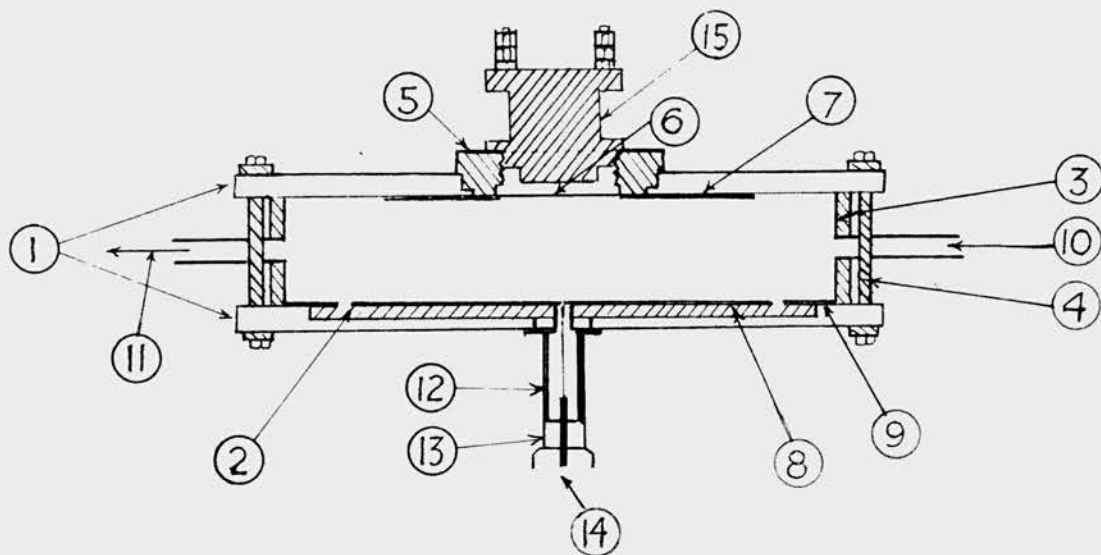
A The Ionisation chamber

- 1 perspex discs
  - 2 polystyrene inlay
  - 3 brass cylinder, earthed
  - 4 brass bolts
  - 5 ionisation chamber head
  - 6 gold leaf-nylon window } H.T. electrode
  - 7 aluminium foil }
  - 8 " " collecting electrode.
  - 9 " " guard ring
  - 10, 11 gas inlet and outlet tubes
  - 12 brass tube, earthed
  - 13 coaxial plug
  - 14 lead to galvanometer
  - 15 polonium source holder (See Figure 5A)
- B Circuit used for measuring ionisation current.
- G sensitive galvanometer

FIGURE 12.

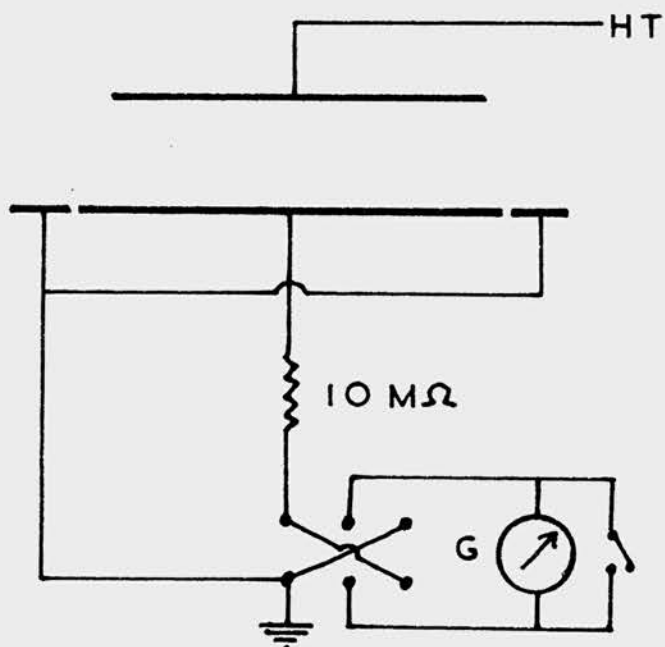
IONISATION CHAMBER

A



scale = half full size

B





between the chamber head and the high tension electrode. The H.T. electrode consisted of an annular sheet of aluminium foil 9.5 cm in diameter, attached to the perspex disc with perspex cement. The lower disc, which was well coated with "aqua-dag" on all surfaces, was made from perspex inlaid with polystyrene. The latter is a better insulator than perspex. The collecting electrode was a sheet of aluminium foil 11 cm in diameter and was surrounded by a guard ring made from the same material. The dimensions of the chamber were such that all ions formed in the chamber were collected. This was demonstrated by a preliminary experiment. With a polonium source in a fixed position in the ionisation chamber head, the depth of the chamber was increased from 3 cm to 5 cm. No change was observed in the value of the saturation current. The diameter of the H.T. electrode was increased from 9.5 cm to 11 cm also with no effect on the saturation current.

To ensure that the saturation current represented, in the ionisation chamber, the rate of absorption of  $\alpha$ -particle energy in an irradiated solution, the top of the ionisation chamber (Figure 5, D and E) was designed to correspond to the conditions in the irradiation cell. The gold leaf stretched across

the ionisation chamber head represented, in the ionisation chamber, the surface of the solution in the irradiation cell. The gold leaf was the same area as the surface of the irradiated solution. To render the window more stable, the gold leaf was backed with a thin nylon film. The amount of  $\alpha$ -particle energy absorbed by the window was very small (equivalent to approximately 0.5 mm of air). The space between the window and the source which was threaded into the ionisation chamber head, was the same in volume as that between the source and the solution in the irradiation cell. There was no collection of the ions produced in this space, as the source and the ionisation chamber head were at the same potential as the H.T. electrode. The ions formed in this space corresponded to those formed between the source and the solution in the irradiation cell and which had no chemical effect on the solution if precautions were taken against the formation of oxidising substances in the gaseous phase. The rate at which  $\alpha$ -particle energy was absorbed in the ionisation chamber was the same as that absorbed by an irradiated solution. In certain experiments, it was necessary to measure the rate at which energy was absorbed in the whole irradiation cell, i.e. in both liquid and gaseous phases. This

was done by measuring the saturation current with no window present in the chamber. Solutions were irradiated at varying source-solution distances. The distance between the source and the window in the ionisation chamber, could be varied by inserting suitable washers between the source and the ionisation chamber head.

The gas inlet and outlet tubes on the brass source holder enabled gases to be circulated between the source and the window. Ionisation measurements could be made therefore, under identical conditions to those existing in the irradiation cells. Owing to the delicate nature of the gold leaf window, it was not possible to fill the chamber with argon by the usual method, i.e., evacuating the chamber then admitting pure argon. Ionisation measurements were made therefore, with a continuous current of argon passing through the chamber, sufficient time being allowed for the displacement of air. Care had to be taken when adjusting the rates of flow of argon through the chamber, and the gas through the chamber head, that the gold leaf window did not bulge, thereby altering the source-window distance. This was demonstrated experimentally by passing currents of argon of varying speeds through the ionisation chamber and through the

chamber head, simultaneously. The values of the saturation currents obtained varied with the speeds of the gases to the extent of  $\pm 6\%$ . With reasonable care, however, the speeds of the gases could be adjusted so that errors due to distortion of the gold leaf window were reduced to  $\pm 1\%$ .

The irradiation of solutions in which sheets of mica were interposed between the source and the solution will be discussed in a later section. The corresponding ionisation measurements were made under similar conditions. The gold leaf-nylon window was replaced by one of mica which was attached to the chamber head with picein wax. Since mica is a non-conductor, the chamber side of the window was covered with gold leaf.

The ionisation currents produced by the polonium sources were of sufficient magnitude to be measured without amplification using a sensitive galvanometer. A thin wire from the collecting electrode passed through a small hole in the perspex disc and was connected to the galvanometer through a protecting resistance of 10 megohms. A galvanometer of sufficient sensitivity was selected according to the strength of the polonium source to be measured. The galvanometer employed for the measurement of the

FIGURE 14.

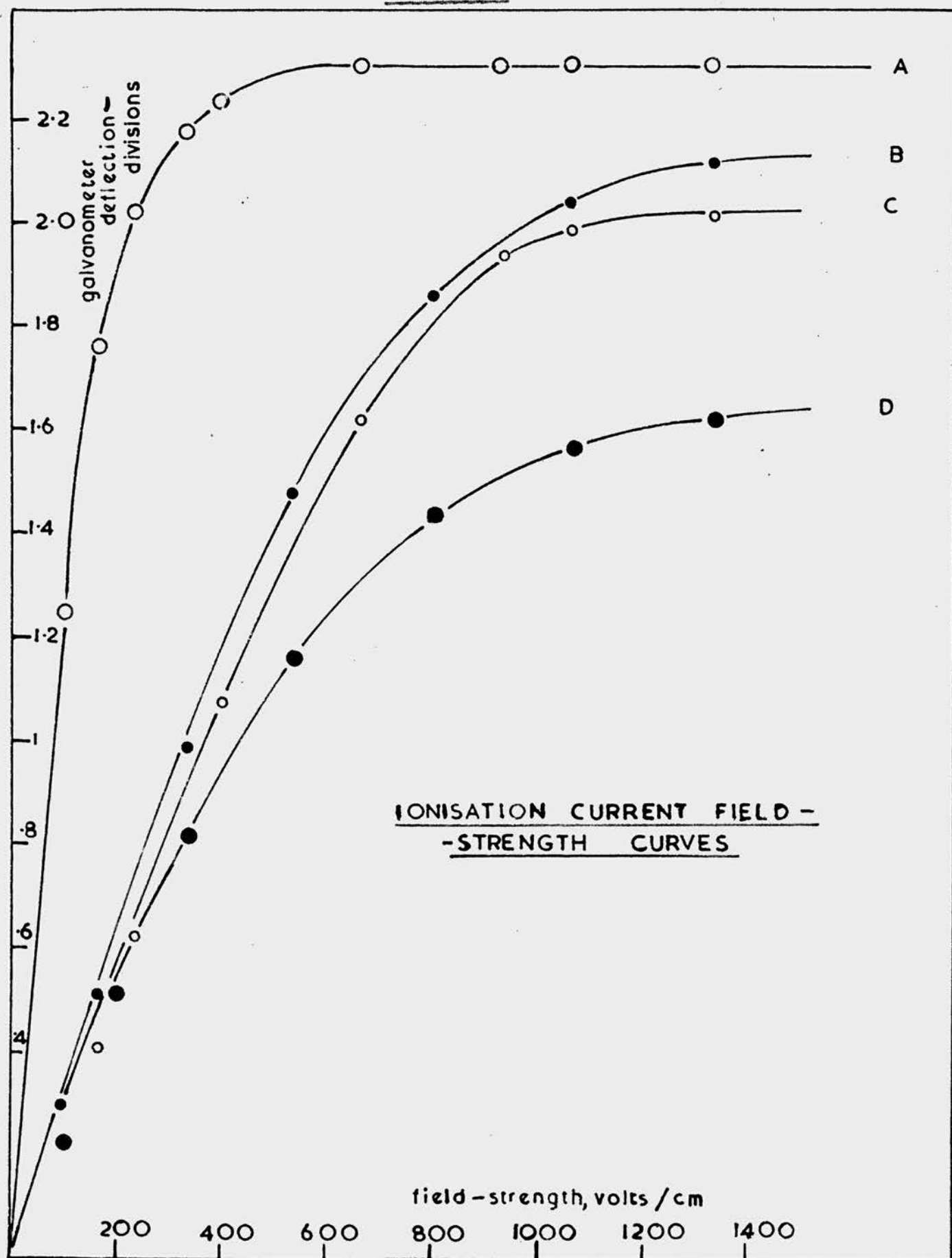
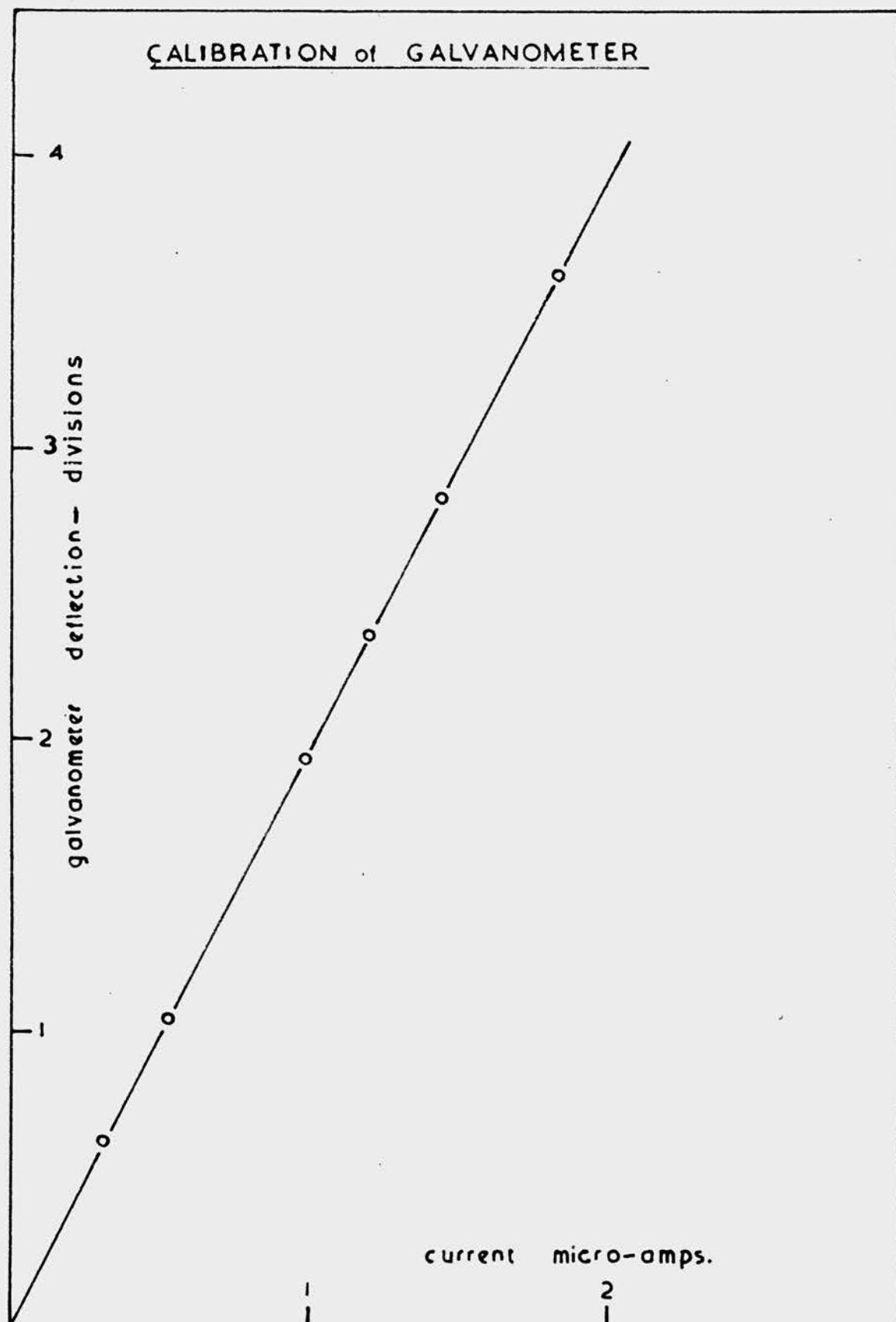


FIGURE 13.



currents produced by the stronger sources used in dosimetry experiments, was calibrated over the range of current using a standard megohm and an accurate potentiometer. The galvanometer deflections observed were expressed as a function of the current (Figure 13) and a calibration of  $1.96 \pm 1\%$  scale divisions/ $\mu\text{a}$ . was recorded. It was possible to read the galvanometer to  $\pm 0.01$  scale divisions and errors were reduced by using a reversing switch. The high tension was supplied by a Power Unit Type 200 (Dynatron Radio Ltd., Maidenhead) and a voltage of 4 kV could be applied to the H.T. electrode. The maximum chamber field of 1333 volts/cm obtained was sufficient to produce saturation when the source strength was approximately 6 mc or less.

(3) Measurements using the Ionisation Chamber.

(a) Saturation Characteristics.

When the evaluation of  $G_{\text{Fe}}^{\infty}$  was first attempted it was intended that the rate at which ferrous ions were oxidised in a gas-filled irradiation cell should be compared with the saturation current produced by the same source in an ionisation chamber filled with the same gas. By using the value of W appropriate to the gas employed, the value of G could be calculated. It was hoped, initially, that irradiations could be made

FIGURE 14.

Ionisation Current - Field Strength Curves.

Chamber shown in Figure 12A.

gold leaf-nylon window.

strength of source  $\sim 6$  mc

source-window distance 3.5 mm.

galvanometer calibration 1.96 div/ $\mu$ a.

Curve A - chamber filled with argon: source-window gap filled  
with argon.

" B - " " " " : source-window gap filled  
with air.

" C - " " " " : source-window gap filled  
with carbon dioxide.

" D - " " " " air : source-window gap filled  
with air.



in air, or carbon dioxide-filled cells, in order to save expense on argon.

Irradiations were made in cells swept with argon (these will be discussed in a later section) and the corresponding ionisation measurements were made with currents of argon passing through ionisation chamber and through the chamber head. A typical saturation curve obtained by a measurement of this kind is shown in Figure 14, curve A. An excellent plateau was obtained.

Irradiations were made in air-filled cells. The corresponding saturation curves were plotted using a chamber with air on both sides of the gold leaf window. A typical curve is shown in Figure 14, curve D. The plateau was not quite reached at the maximum field strength of 1333. volts/cm, and the value of the saturation current was obtained by extrapolation. With carbon dioxide on both sides of the window much worse saturation characteristics were exhibited, and it was not found possible to reach the plateau.

It was decided, therefore, that all measurements should be made in an argon-filled chamber with the gas used in the irradiation cell passing through the ionisation chamber head. By this method it was possible to have maximum saturation and yet preserve the conditions

obtaining in the irradiation cell. For irradiations made in argon-filled cells, ionisation measurements were made with argon on both sides of the window (Figure 14A). When air or carbon dioxide were passed through the irradiation cell, measurements were made with the same gases passing through the ionisation chamber head. A field-strength of 1333 volts/cm was not quite sufficient to obtain saturation (Figure 14 Curves B and C). The extrapolated values of the saturation currents obtained when air or carbon dioxide were passed through the chamber head were lower than that obtained when argon was used. The reasons for the different values of the saturation currents are as follows.

- (i) The stopping power of air and carbon dioxide, for  $\alpha$ -particles, is greater than that of argon<sup>(64b)</sup>. This would decrease the energy of the  $\alpha$ -particles entering the chamber through the gold leaf window.
- (ii) Air and carbon dioxide diffuse through the window into the ionisation chamber. Since the values of  $W_{\text{air}}$  and  $W_{\text{carbon dioxide}}$  are greater than  $W_{\text{argon}}$  (Table 9), the diffusion of these gases into the chamber would account for the lower values of the saturation currents. The presence of air or carbon dioxide in the chamber would also alter the shape of the saturation curve. The curve obtained in the

FIGURE 15.

Ionisation Current - Field Strength Curves.

Chamber shown in Figure 12A.

Mica window  $1.17 \text{ mg/cm}^2$  in thickness

strength of source  $\sim 6 \text{ mc.}$

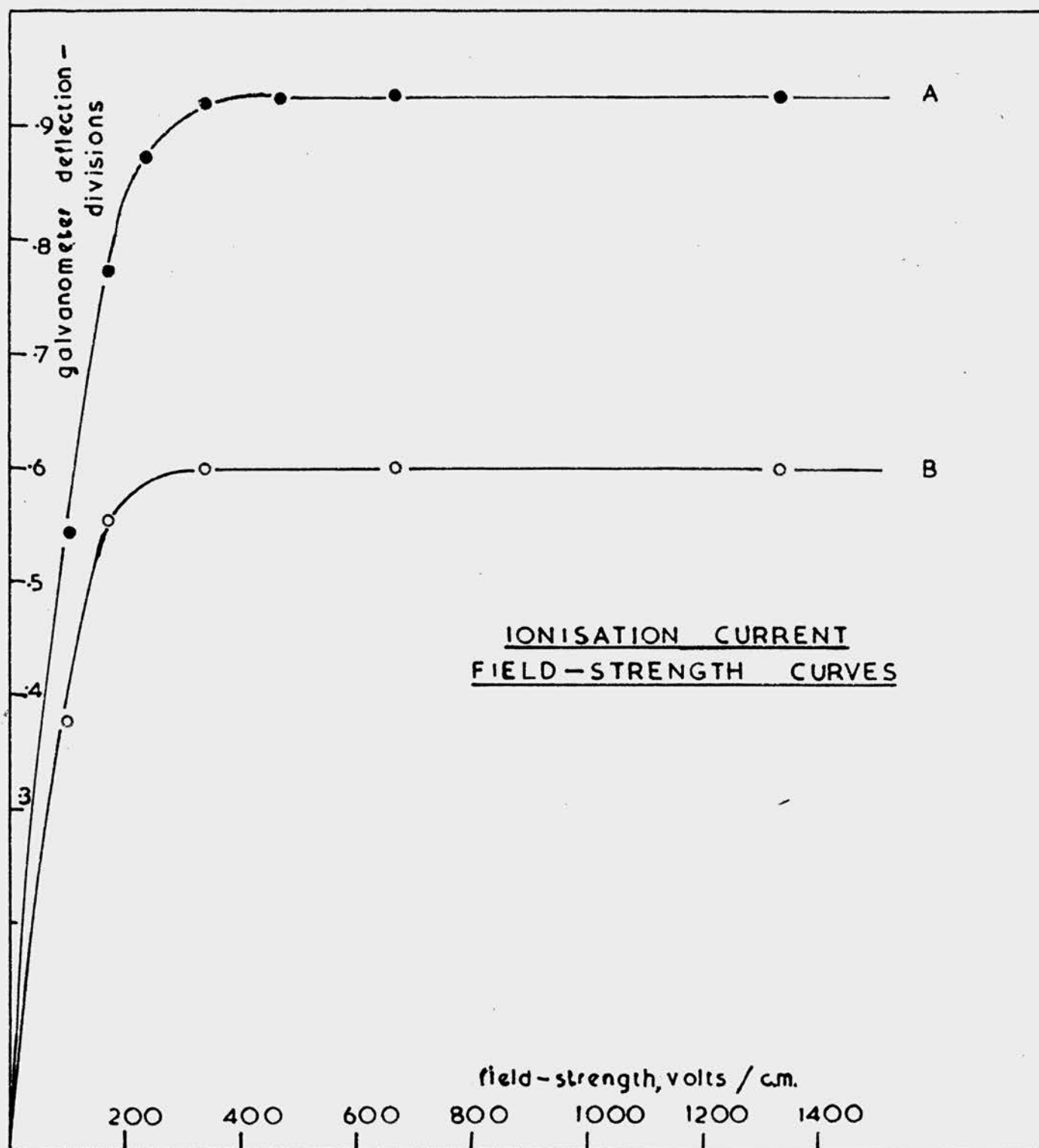
source-window distance 5.65 mm

galvanometer calibration  $1.96 \text{ div/}\mu\text{a.}$

Curve A - chamber filled with argon: source-window gap  
filled with air,

Curve B - " " " " : source-window gap  
filled with carbon  
dioxide.

FIGURE 15.



argon-filled chamber into which air had diffused (Figure 14 Curve B) shows more resemblance to the curve obtained when air was present on both sides of the window (Figure 14 Curve D) than to that obtained in pure argon (Figure 14 Curve A). It was found possible to lower the rate of diffusion of gas into the chamber by increasing the rate of flow of argon through the chamber and decreasing the rate of flow of the gas through the chamber head. However, as discussed in a previous section, the rates of flow of gases through the chamber and the chamber head must be closely regulated to avoid distortion of the gold leaf window.

It was obvious, therefore, that owing to the difficulties outlined above, the only accurate measurement that could be used for the purposes of chemical dosimetry, was that in which argon was present on both sides of the gold leaf window.

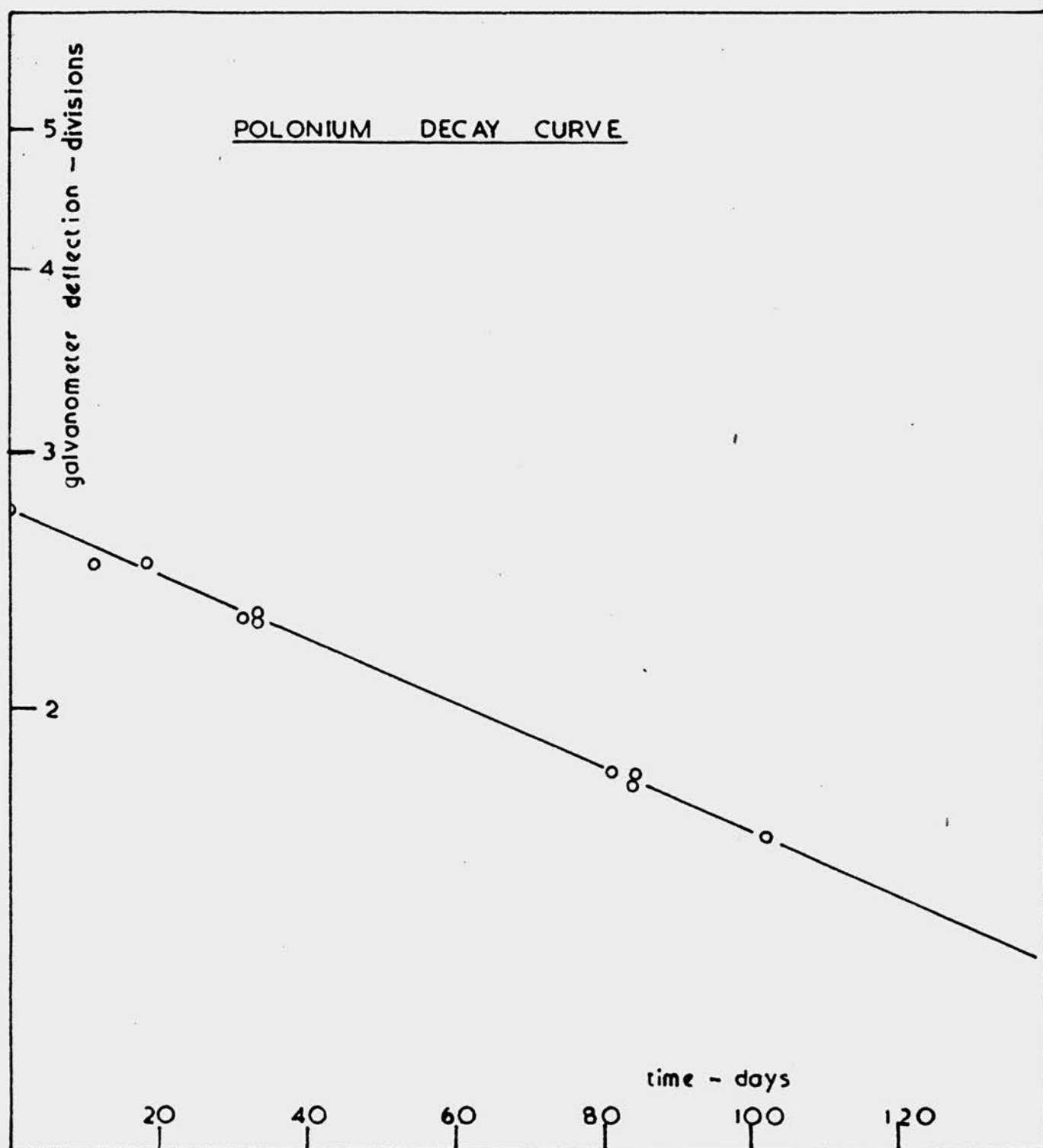
When ionisation measurements were made in chambers fitted with gold leaf-mica windows, diffusion difficulties did not arise owing to the windows being effectively gas-tight. Ionisation measurements were made in argon-filled chambers with the chamber head filled first with air and then with carbon dioxide (Figure 15 Curves A and B). In contrast to the results obtained in the chamber

FIGURE 16.

Polonium Decay Curve.

Saturation current measurements made at a field strength  
of 1333v/cm  
chamber shown in Figure 12A  
gold leaf-nylon window  
source-window distance 3.5 mm  
source strength ~ 6 mc, initially  
galvanometer calibration 1.96 div/pa.  
chamber filled with argon; source-window gap filled with  
argon.

FIGURE 16.



fitted with a gold leaf-nylon window, saturation was obtained. This indicated that no leakage of gas into the chamber had occurred. The lower value of the saturation current obtained when carbon dioxide filled the chamber head, relative to that obtained in air, was due to the greater stopping-power of carbon dioxide for  $\alpha$ -particles.

(b) Polonium Decay Curve.

The reproducibility of the ionisation measurements was demonstrated in the following way. With argon present on both sides of the gold leaf window, saturation current measurements were made over a period of 102 days, the source being placed in the same position each time. The half-life of polonium obtained from the decay curve (Figure 16) was found to be approximately 138 days.

(c) Measurements made at Varying Source-Window Distance.

It was not always convenient to adjust the source-window distance in the ionisation chamber to correspond exactly to the source-solution distance in the irradiation cell. The saturation current at any given distance was obtained from a curve in which saturation current was expressed as a function of source-window distance. Such curves, constructed over



the range of irradiation distances used, are included with the corresponding chemical measurements in the dosimetry section, which will be discussed later.

By comparing the value of the saturation current obtained in a chamber in which argon was present on both sides of the gold leaf window, with that obtained in air, a value for the ratio of  $W_{\text{air}}/W_{\text{argon}}$  may be calculated.\* The approximate values of the saturation currents measured in an air-filled chamber were obtained by extrapolation of the ionisation curves, as discussed previously. The values of the saturation currents obtained in air and argon-filled chambers at varying source-window distances are given in Table II.

TABLE II.

Source-Window Distance mm.	Saturation Current Galvanometer Deflection - scale divisions ( $1 \mu\text{a} = 1.96 \text{ div.}$ )		$W_{\text{air}}/$ $W_{\text{argon}}$
	Argon	Air (extra- polated value)	
1.5	2.065	1.525	1.35
2.5	1.935	1.423	1.36
3.5	1.800	1.300	1.38
5.66	1.535	1.080	1.42

\* This calculation is made assuming as a first approximation that the relatively small difference between the stopping powers of the air and argon layers between the source and the membrane can be neglected.

As the source-window distance is increased the energy of the  $\alpha$ -particles entering the chamber is decreased. Since the value of  $W_{\text{air}}$  increases with decreasing  $\alpha$ -particle energy (Table 8) and since  $W_{\text{argon}}$  is constant over the whole  $\alpha$ -track, the ratio of  $W_{\text{air}}/W_{\text{argon}}$  increases as the source-window distance is increased.

(4) Discussion.

The measurement of saturation current by the ionisation chamber method described in the previous sections, was considered to be a fairly reliable means of estimating the rate at which energy was absorbed by a solution irradiated with  $\alpha$ -particles.

Owing to the design of the chamber, it was not possible to measure saturation currents with the accuracy obtained in recent determinations where the ionisation chambers used could be evacuated and filled with purified argon. The measurement of the half-life of polonium did demonstrate, however, that reproducible results of fair accuracy, could be obtained. In addition, the approximate values obtained for the ratio of  $W_{\text{air}}/W_{\text{argon}}$  were in fair agreement with the more recent published values (Table 10).

The determination of the ratio of  $W_{\text{air}}/W_{\text{argon}}$  was merely intended as an indication of the best value to be accepted from the literature. The residual ranges

of the  $\alpha$ -particles entering the ionisation chamber through the gold leaf window, were of all values up to a maximum of approximately 2.7 cm in air. No recent determinations of the ratio of  $W_{\text{air}}/W_{\text{argon}}$  have been made for  $\alpha$ -particles of this residual-range. Gurney<sup>(64(a))</sup> obtained values for  $\alpha$ -particles of residual-range 0.4 cm to 1.9 cm. Livingstone<sup>61</sup> used a modified Segré-type ionisation chamber which had many features in common with the chamber used in the present work. Using the whole of the polonium  $\alpha$ -particle track, Livingstone obtained a value for the ratio of  $W_{\text{air}}/W_{\text{argon}} = 1.35$ . This value, which has been substantially confirmed recently<sup>62,63,66</sup>, was very close to the value obtained in the present work where the source was 1.5 mm to 2.5 mm from the gold leaf; solutions were usually irradiated at source-solution distances of 1.9 mm to 2.9 mm. A value for the ratio of  $W_{\text{air}}/W_{\text{argon}} = 1.36$  was therefore adopted. This corresponds to a value for  $W_{\text{argon}} = 26.2$  ev. The values for  $G_{\text{Fe}}^{\alpha}$  obtained in the present work were calculated assuming this value for  $W_{\text{argon}}$ .

5. CHEMICAL DOSIMETRY

(1) Introduction.

Many of the difficulties associated with the quantitative study of the chemical effects produced by  $\alpha$ -particle irradiation of ferrous sulphate solutions, have been discussed previously in Section III (3 and 4). The main point which resulted from the preliminary experiments was that the oxidation produced in ferrous sulphate solutions was largely dependent on the nature of the gaseous phase present in the irradiation cell. In a quantitative study, therefore, it was essential that the effects produced in solution, owing to the presence of a gaseous phase, should be measured or eliminated completely. This problem was investigated by three different methods.

- (a) Solutions were irradiated in air-filled cells. The effects were observed in solution as the source-solution distance was decreased and the results were extrapolated to zero air thickness.
- (b) Solutions were irradiated under conditions where there was little contact between the solution and the gaseous phase.
- (c) Solutions were irradiated in cells through

which currents of inert gases were passed. For each of these irradiation methods, a corresponding measurement was made in the ionisation chamber. The three methods for evaluating  $G_{Fe}^{\alpha \dots}$  are described in the following sections.

## (2) Irradiations in Air-Filled Cells.

The experiments described in this section were made at a time when only weak sources of polonium ( $< 0.5$  m.c.) were available. The method for evaluating  $G_{Fe}^{\alpha \dots}$  was very approximate and since more accurate methods were evolved subsequently, the measurements described in this section were not considered to be of sufficient importance to be repeated more accurately with the stronger sources. The method did give, however, an approximate value for  $G_{Fe}^{\alpha \dots}$ , and in addition, it was possible to make an approximate estimation of  $G_{O_3}^{\alpha}$ , the yield for ozone formation in  $\alpha$ -irradiated air.

### (a) Chemical measurements.

A solution of approximately  $10^{-3}M$  ferrous sulphate in 0.8N sulphuric acid was irradiated, without stirring, in an air-filled cell using a polonium source (4) of about 0.4 m.c. Irradiations were made

FIGURE 17

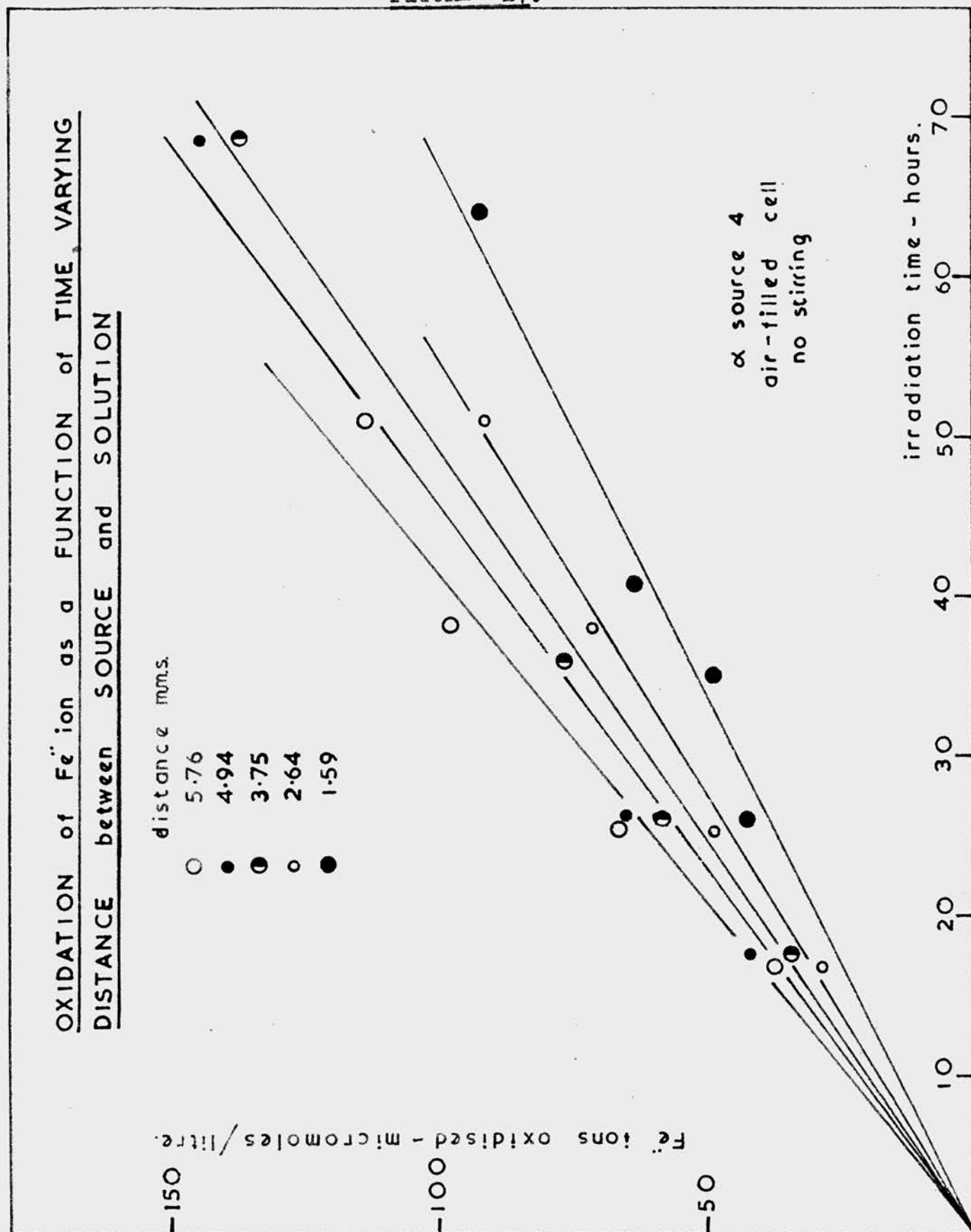
Oxidation of ferrous ion as a function of  
irradiation time.

Unstirred,  $\sim 10^{-3}$ M ferrous sulphate in 0.8N  
sulphuric acid.

air-filled irradiation cell.

strength of source  $\sim 0.4$  mc

FIGURE 17.



at source-solution distances varying from 1.59 mm to 5.76 mm and a ferrous ion oxidation/irradiation time curve was plotted at each distance (Figure 17). The amount of ferrous ion oxidised was found to be a linear function of irradiation time. The slopes of the curves, which gave the rates of ferrous ion oxidation, were found to increase as the source-solution distance was increased.

(b) Physical measurements.

Ionisation measurements were made in an argon-filled ionisation chamber. The space between the source and the gold leaf was filled with air. The distance between the source and the window was varied. At a field strength of 1333 volts/cm, the saturation current was obtained for each source-window distance. The saturation current was expressed as a function of the distance between the source and the gold leaf (Figure 18, Curve B).

The gold-leaf window was removed so that the  $\alpha$ -particles had direct access to the chamber. Saturation currents were obtained with the source in the same positions as in the measurements when the window was present. The value of the saturation current observed, was found to decrease slightly as the distance between the source and the body of the



## FIGURE 18.

Variation of Ionisation Current with  
source-window distance.

Saturation current measurements made at a field strength of 1333v/cm.

Chamber shown in Figure 12A.

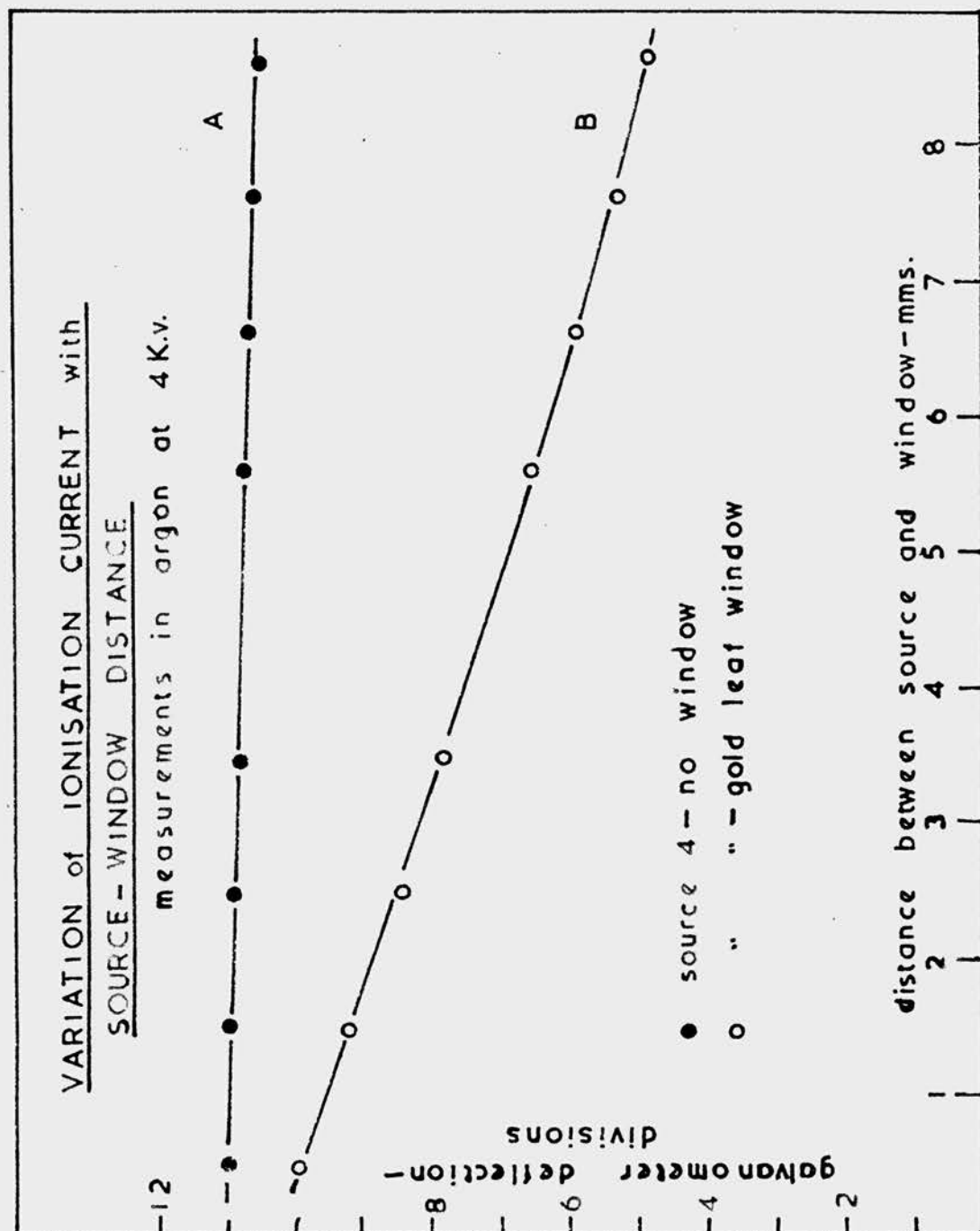
Galvanometer calibration: 12.45 div/ $\mu$ a.

Strength of source  $\sim 0.4$  mc

Curve A. Chamber filled with argon: no window present.

Curve B.        "        "        "        " : gold leaf-nylon  
window present,  
source-window gap  
filled with air.

FIGURE 18.



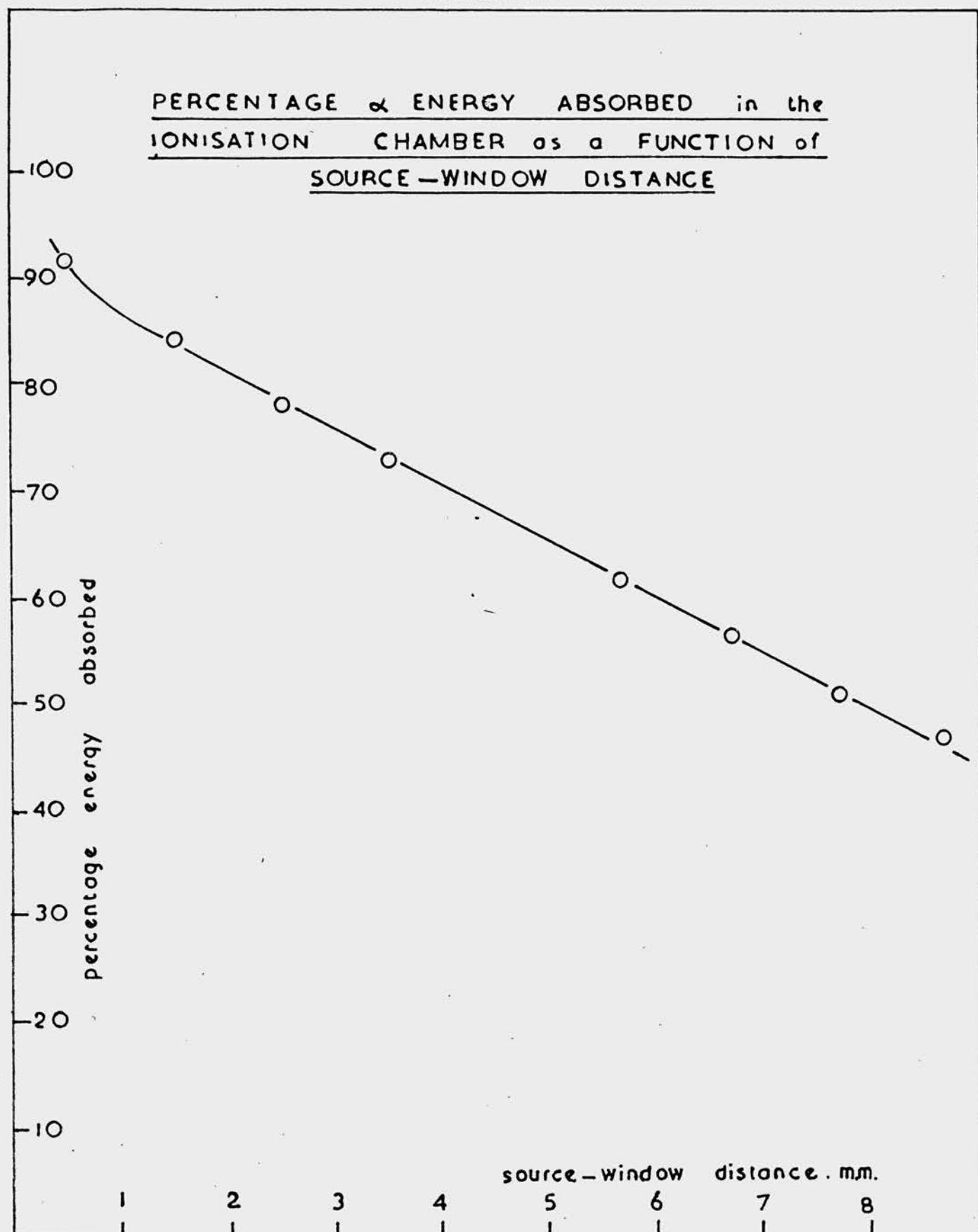
chamber was increased (Figure 18, Curve A). This was probably due to loss of  $\alpha$ -particles by collision with the sides of the ionisation chamber head.

The value of the saturation current, obtained in the chamber when the gold-leaf window was in position, represented the rate at which energy was absorbed in the irradiated solution. In the windowless chamber, the saturation current represented the rate at which energy was absorbed in the whole irradiation cell, i.e. the solution and the gaseous phase. At each source-window distance, the energy absorbed in the chamber (i.e. in the solution) was calculated as a percentage of the total energy absorbed (i.e. in the solution and the gaseous phase). The percentage of energy absorbed in the chamber was expressed as a function of the source-window distance (Figure 19). From this curve, it was possible to obtain the percentage of energy absorbed in an irradiated solution, at any given source-solution distance.

(c) The evaluation of  $G_{Fe}^{\alpha}$  and  $G_{O_3}^{\alpha}$

The effects produced in a ferrous sulphate solution, irradiated in an air-filled cell, have been described previously (III, 3, (1)). The ferrous sulphate is oxidised, partly due to radicals produced in solution by the  $\alpha$ -particles, and partly due to

FIGURE 19.



the ozone, produced by the  $\alpha$ -irradiation of air, absorbed in the solution. The rate of ferrous ion oxidation in the solution may be compared with the saturation current observed in the chamber with the window present. In this case, the whole chemical effect observed in the solution, is attributed to the  $\alpha$ -particle irradiation of the solution alone. A value for the "apparent"  $G_{Fe}^{\alpha}$  was calculated at each source-solution distance. The results are given in Table 12. (The method of calculating G is given in Appendix I). The "apparent"  $G_{Fe}^{\alpha}$ , calculated at each source-solution distance, was expressed as a function of the percentage energy absorbed in the solution at that distance (Figure 20, Curve A).

Had the oxidation in solution been due entirely to the effect of the  $\alpha$ -particles on the solution, the value for G would have been independent of the source-solution distance. The curve indicated, however, that the value for G increased rapidly as the distance between the source and the solution was increased. This was a clear indication that the ozone, produced by the  $\alpha$ -irradiation of the air above the solution, was being absorbed by the solution. At large source-solution distances, a greater proportion of the total  $\alpha$ -energy is dissipated in forming ozone,

FIGURE 20.

$G_{Fe}^{\alpha}$  expressed as a function of the energy absorbed in the irradiated solution.

Curve A: "apparent"  $G_{Fe}^{\alpha}$  calculated from the rate of ferrous ion oxidation in solution and the  $\alpha$ -particle energy absorbed in solution.

Curve B: "total"  $G_{Fe}^{\alpha}$  calculated from the rate of ferrous ion oxidation in solution and the  $\alpha$ -particle energy absorbed in the solution and in the air between the source and the solution.

FIGURE 20

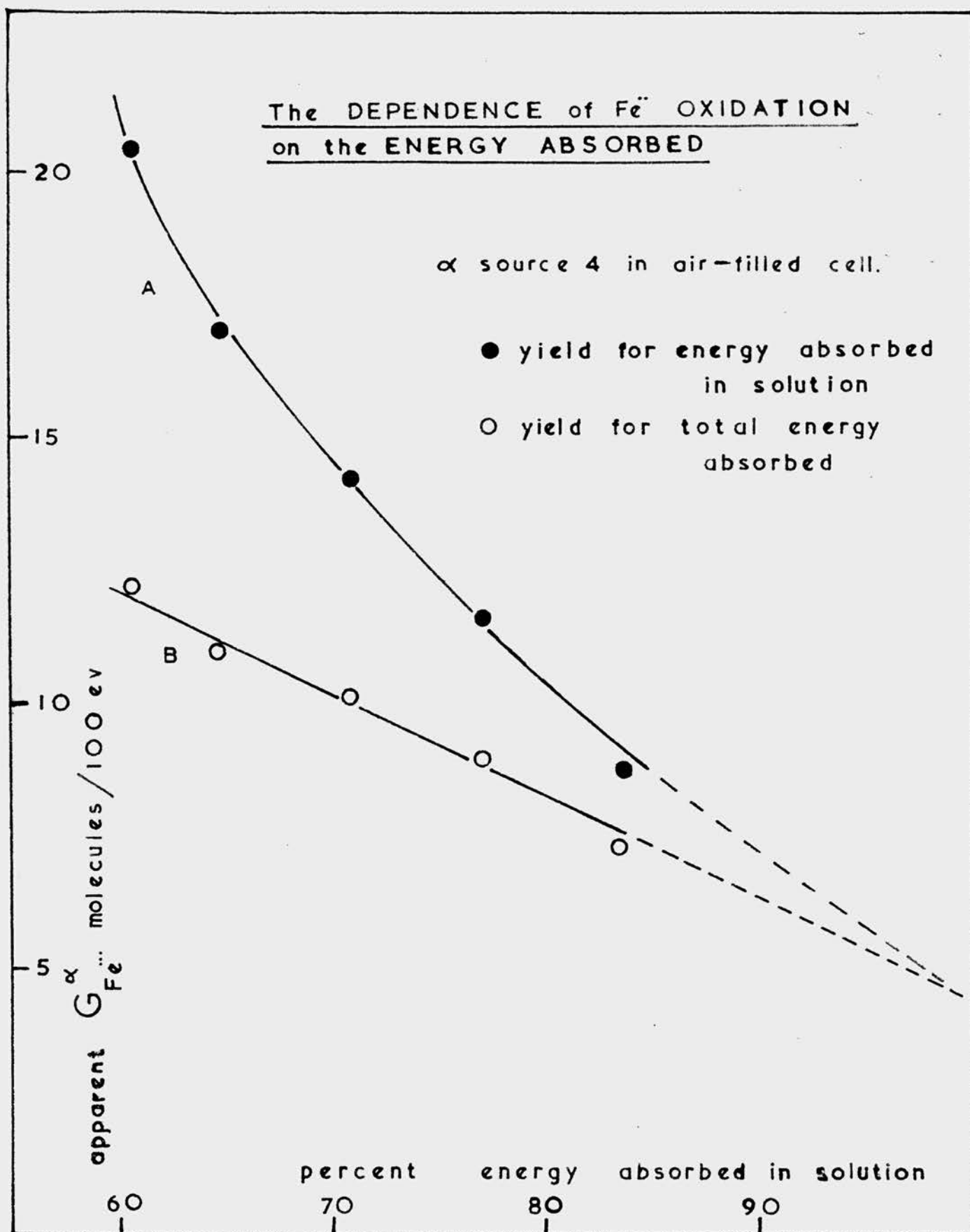


TABLE 12.

The evaluation of "apparent"  $G_{Fe}^{\alpha}$  and "total"  $G_{Fe}^{\alpha}$  at varying source-solution distance.

Source - Solution distance mm.	% Energy absorbed in the solution	Ferrous ion oxidation yield $\mu M$ /hour	Saturation Current (with window present) $\mu a$	"Apparent" $G_{Fe}^{\alpha}$ molecules/ 100 e.v.	Saturation Current (with win- dowless chamber) $\mu a$	"Total" $G_{Fe}^{\alpha}$ molecules/ 100 e.v.
5.76	60.65	2.44	0.0512	20.4	0.0855	12.2
4.94	64.75	2.20	0.0544	17.0	0.0860	10.9
3.75	70.95	2.05	0.0618	14.2	0.0868	10.1
2.64	77.15	1.84	0.0678	11.6	0.0876	8.9
1.59	83.50	1.50	0.0735	8.7	0.0882	7.3



than at small distances. Consequently, as the source-solution distance is increased, a greater proportion of the oxidation observed in solution is due to the ozone absorbed by the solution.

It was necessary, therefore, to compare the chemical change produced in the solution with the  $\alpha$ -particle energy dissipated in both the solution and in the gaseous phase. The rate of ferrous ion oxidation in the solution was compared with the saturation current observed in the windowless chamber, and a value for "total"  $G_{Fe}^{\alpha}$  was calculated at each source-solution distance. The results are given in Table 12. The "total"  $G_{Fe}^{\alpha}$ , at each source-solution distance, was expressed as a function of the percentage energy absorbed in the solution, at that distance (Figure 20, Curve B).

The value of the "total"  $G_{Fe}^{\alpha}$  increased as the source-solution distance was increased. This indicated that  $\alpha$ -particle energy dissipated in the air produced more oxidation in the solution, than the same amount of energy absorbed directly in the solution. This observation is not surprising since the values of  $G_{Fe}^{\alpha}$  and  $G_{O_3}^{\alpha}$  are similar, and unless the ozone absorbed in the solution is removed by reaction with hydroxyl radicals<sup>67</sup>, one ozone molecule is capable of

oxidising two ferrous ions.

On extrapolation of the  $G_{Fe}^{\alpha}$  /percentage energy absorbed in solution curves to zero air thickness (i.e. 100%  $\alpha$ -energy absorbed in the solution), a value for  $G_{Fe}^{\alpha} \approx 5$  molecules/100 ev. was obtained.

From the value of "total"  $G_{Fe}^{\alpha}$  at any given source-solution distance, it was possible to make an approximate estimate of  $G_{O_3}^{\alpha}$ . For source-solution distances of 1.59 mm to 5.76 mm, the corresponding values for  $G_{O_3}^{\alpha}$  were  $\approx 6$  molecules/100 ev. to  $\approx 10.6$  molecules/ev. (The method of calculation is given in Appendix II). The value for  $G_{O_3}^{\alpha}$  obtained by this method is of the same order of magnitude as that obtained by Lind and Bardwell<sup>52</sup>. ( $G_{O_3}^{\alpha} = 6-7$  molecules/100 ev.)

(3) Irradiations made in cells where contact between the solution and the gaseous phase was effectively eliminated.

(a) Chemical measurements.

A method was evolved for irradiation of solutions which were effectively out of contact with the gaseous phase, as follows. The thickness of a mica sheet (approximately 1.5 mg/cm<sup>2</sup>) was determined exactly, by weighing. The sheet was then placed between two

brass discs 3.3 cm in diameter. The mica which projected beyond the discs was cut away with a razor blade. The mica disc, 3.3 cm in diameter was cleaned by steeping overnight in a concentrated solution of ceric sulphate in N-sulphuric acid. The disc was washed with distilled water, then with purified water and allowed to dry. The mica disc, supported on a thin pyrex glass ring, was carefully lowered into the glass base of an irradiation cell so that the mica floated on the solution without any solution getting on top of the mica. The mica disc covered approximately 90% of the surface of the solution. The plastic cap was placed in position and the source holder was threaded into the cell. The source-mica distance was kept small so that all the  $\alpha$ -particles which entered the solution passed through the mica; this was to correspond to the measurements made in the ionisation chamber, where all particles entering the chamber passed through the mica window. The irradiation was made in an air-filled cell, but since the source-mica distance was small, the amount of ozone produced would also be small. Since the area of contact between the solution and the air was small, the rate of ferrous ion oxidation in solution owing

to the absorption of ozone, was very small, relative to that produced by the  $\alpha$ -particles. This was demonstrated experimentally and will be described later in this section. At the end of the irradiation, the mica was carefully lifted from the cell and the amount of ferric ion produced in the solution was estimated. Control experiments indicated that no chemical effect was produced in a 0.8N sulphuric acid solution of ferrous sulphate, as a result of its contact with mica. Owing to the pyrex ring, which was used to lift the mica sheet from the irradiation cell, it was not possible to stir the solution. Unstirred solutions of ferrous sulphate of varying concentration were irradiated at an average source-mica distance of 2.75 mm. The oxidation of the ferrous ion was found to be linear with irradiation time. Between initial ferrous ion concentrations of approximately  $10^{-3}M$  and  $6 \times 10^{-3}M$ , the ferrous ion oxidation yield was independent of ferrous ion concentration. Below  $10^{-3}M$ , the ferrous ion oxidation yield decreased as the initial concentration of ferrous ion was decreased. The curves obtained for irradiations made in the concentration-dependent region are given in Figure 21. The results are in agreement with those obtained previously (III, 3, (6)),

FIGURE 21.

Oxidation of Ferrous Ion as a Function of  
Irradiation Time.

Unstirred solutions of ferrous sulphate in  
0.8N sulphuric acid.

Solutions irradiated through a mica disc  $1.65 \text{ mg/cm}^2$   
in thickness.

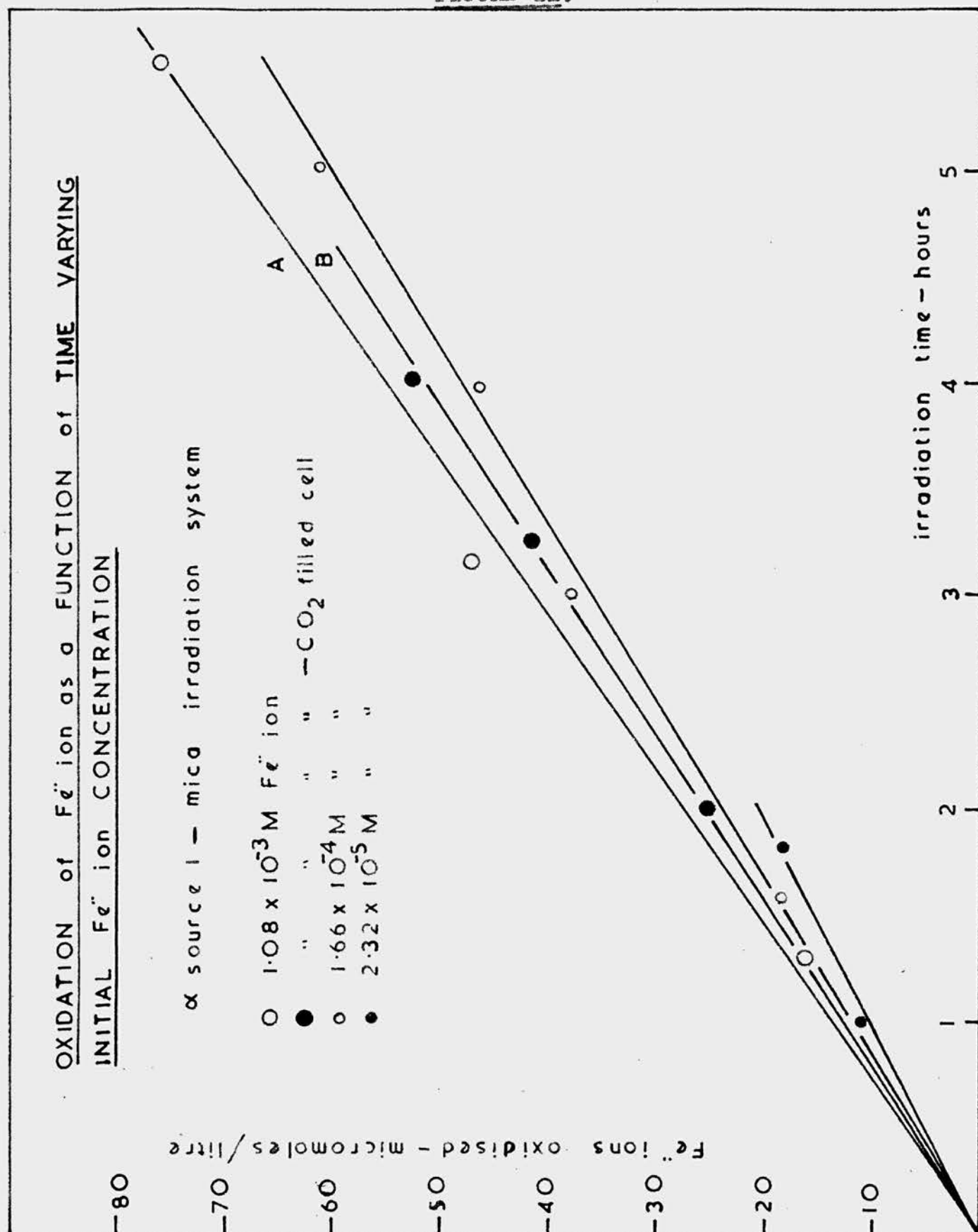
Strength of source  $\sim 13 \text{ mc.}$

Source-mica distance 2.75 mm.

Curve A: source-mica gap filled with air

Curve B:       "       "       "       "       "       carbon dioxide.

FIGURE 21.



where unstirred solutions were irradiated in cells swept with carbon dioxide.

Owing to the fragile nature of the mica, it was usually not possible to accomplish more than a dozen irradiations before the disc disintegrated. Since the mica sheets were not uniform in thickness, it was necessary to construct a curve in which ferrous ion oxidation yield was expressed as a function of mica thickness. The polonium source (1) (strength, approximately 13 mc.) was used at a source-mica distance of 2.75 mm. Solutions of approximately  $10^{-3}M$  ferrous sulphate were irradiated through mica discs, from  $1.4 \text{ mg/cm}^2$  to  $1.65 \text{ mg/cm}^2$  in thickness. The ferrous ion oxidation yield was found to be a linear function of mica thickness (Figure 22). It was possible, therefore, to obtain the ferrous ion oxidation yield for an irradiation made through any given sheet of mica, using source (1).

(b) Physical measurements.

The values of the saturation currents were obtained in an argon-filled ionisation chamber under conditions which corresponded to those in the irradiation cells. Measurements made in chambers fitted with mica windows have been described previously (III, 4, (3)). It was found that the value of the

FIGURE 22.

Oxidation of Ferrous Ion as a function of Mica  
Thickness.

Unstirred solutions of  $\sim 10^{-3}$  M ferrous sulphate in  
0.8N sulphuric acid.

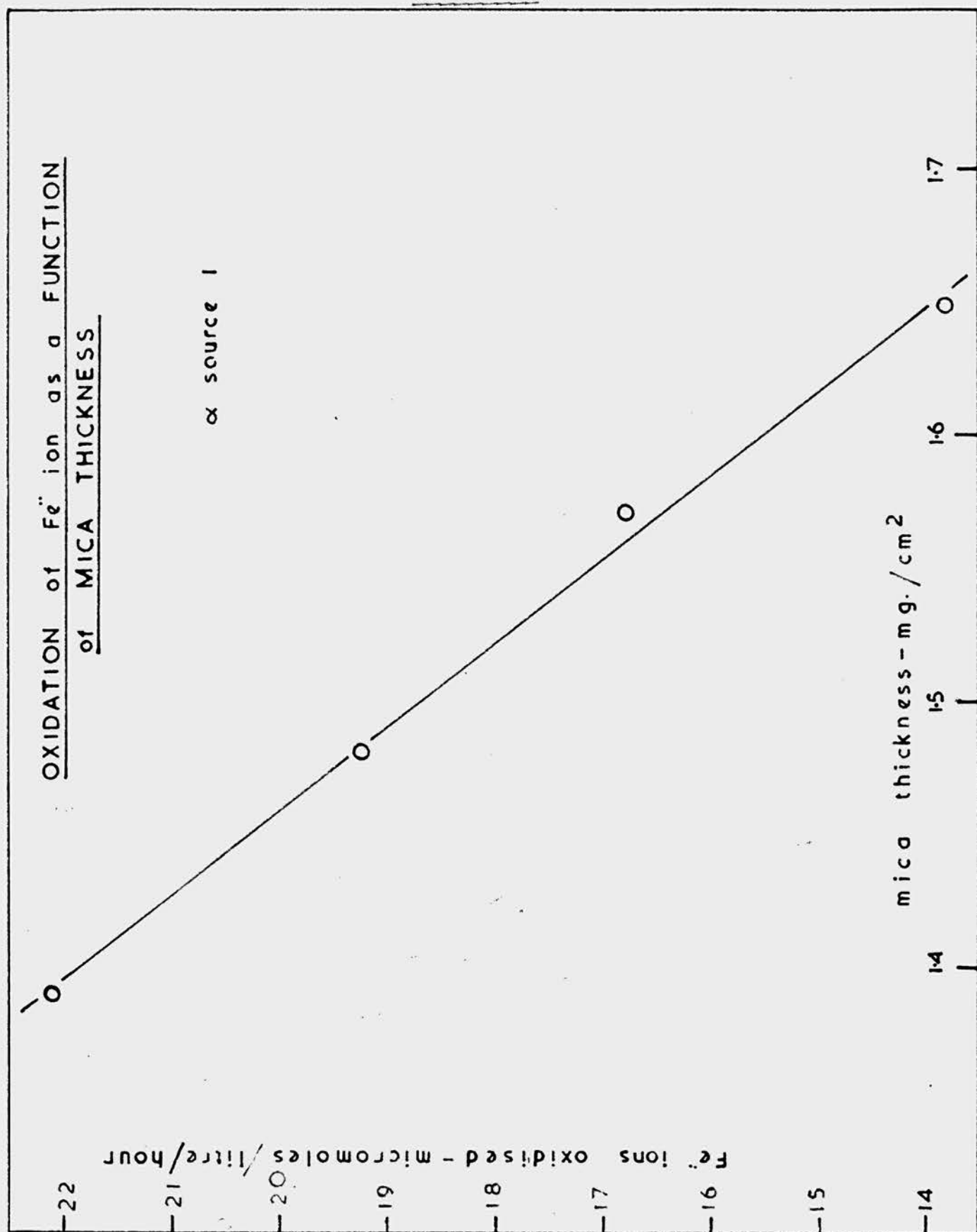
Strength of source  $\sim 13$  mc.

Source-mica distance 2.75 mm.

Source-mica gap filled with air.



FIGURE 22.



saturation current obtained in an argon-filled chamber fitted with a mica window  $1.17 \text{ mg/cm}^2$  in thickness, was only 30% of that obtained with a gold leaf window, the position of the source being the same in both measurements. The effect of interposing a sheet of mica between a source and an irradiated solution is to increase, considerably, the average linear ion density of the radiation entering the solution.

(c) The efficiency of the irradiation system.

In order to demonstrate that the whole of the chemical effect observed in an irradiated solution was produced by the  $\alpha$ -particles which penetrated the mica, the following experiment was made.

Using polonium source (1) ( $\sim 13 \text{ mc}$ ), an approximately  $10^{-3} \text{ M}$  ferrous sulphate solution was irradiated through a mica sheet  $1.65 \text{ mg/cm}^2$  in thickness. The space between the source and the mica was filled with air and the distance between the source and the mica was 2.75 mm. The ferrous ion oxidation/irradiation time curve is shown in Figure 21, Curve A. The irradiation was repeated with a slow current of carbon dioxide passing between the source and the mica-covered solution (Figure 21, Curve B). The effect of the carbon dioxide was to lower the ferrous

ion oxidation yield to 93% of that obtained when the cell was filled with air. The corresponding measurements made in an argon-filled ionisation chamber showed that the effect of carbon dioxide passed through the chamber head was to reduce the value of the saturation current to 93% of that obtained when the chamber head was filled with air. Had ozone played any part in the ferrous ion oxidation, the effect of the carbon dioxide would have been greater in the irradiation experiment than in the ionisation chamber measurement. The decrease in the ferrous ion oxidation yield was the same as that observed in the saturation current measurements and could be attributed to the greater stopping-power of carbon dioxide, for  $\alpha$ -particles.

The method of preventing contact between the solution and the gaseous phase in the cell was therefore considered to be effective, for irradiation purposes.

(d) The evaluation of  $G_{Fe}^{\alpha}$ ...

A solution of approximately  $10^{-3}M$  ferrous sulphate in sulphuric acid was irradiated through a mica disc which floated on its surface, in a cell filled with air. Two polonium sources ((1)  $\sim 13$  mc and (2)  $\sim 7$  mc) were used and the source-mica distance

FIGURE 23.

Ionisation Current Field Strength  
Curves.

Chamber shown in Figure 12A.

Mica window  $1.51 \text{ mg/cm}^2$  in thickness.

Source-window distance 2.5 mm.

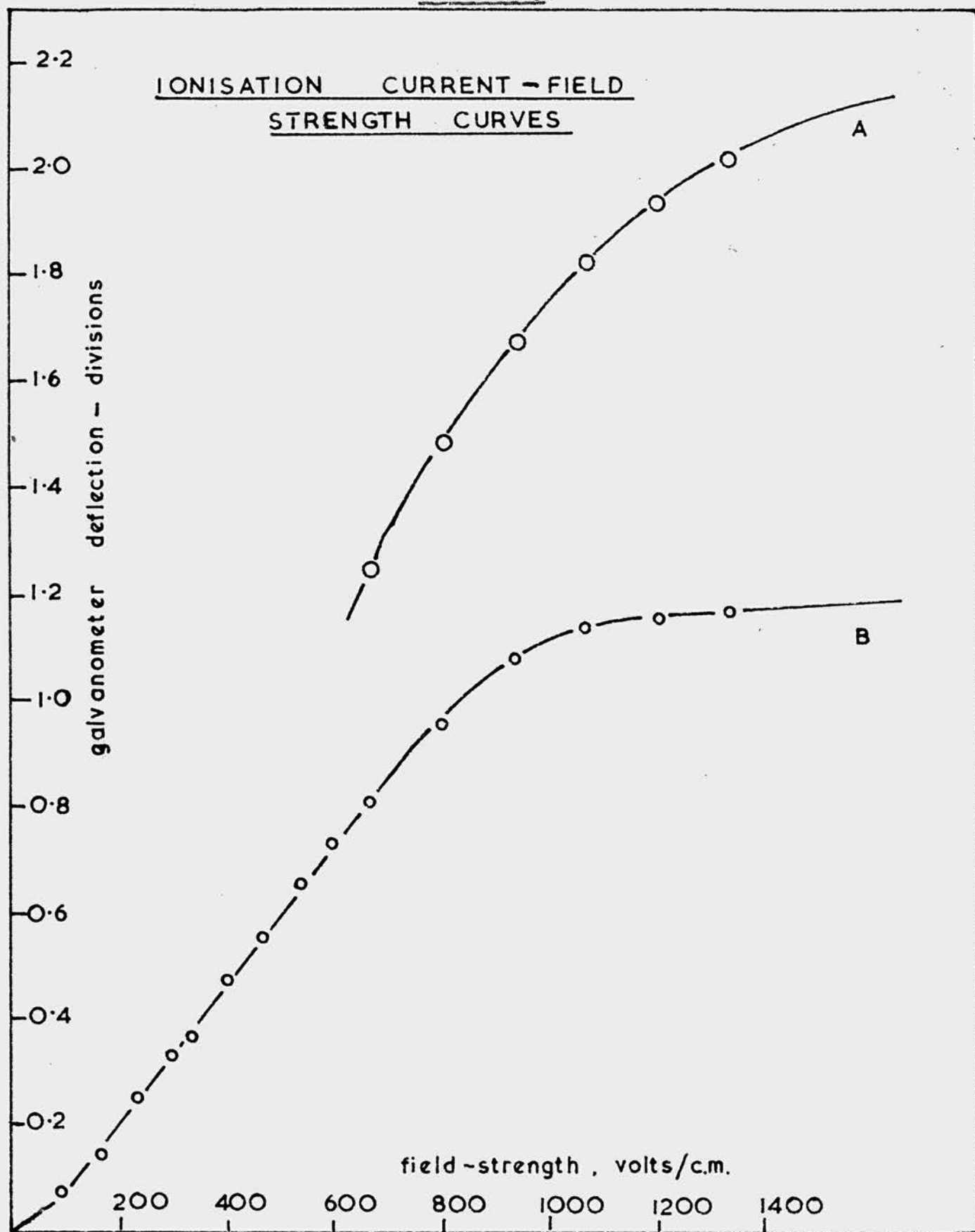
Chamber filled with argon: source-window gap filled  
with air.

Galvanometer calibration  $1.96 \text{ div/}\mu\text{a}$ .

Curve A : strength of source  $\sim 13 \text{ mc}$ .

Curve B :       "       "       "        $\sim 7 \text{ mc}$ .

FIGURE 23.



was 2.75 mm. For source (2), mica of thickness  $1.44 \text{ mg/cm}^2$  was used. The ferrous ion oxidation was a linear function of irradiation time and the ferrous ion oxidation yield for a solution irradiated with source (1) through mica  $1.44 \text{ mg/cm}^2$  in thickness, was obtained from the curve in which ferrous ion oxidation yield was expressed as a function of mica thickness (Figure 22).

The corresponding physical measurements were made in an argon-filled ionisation chamber fitted with mica windows of thickness  $1.407 \text{ mg/cm}^2$  and  $1.510 \text{ mg/cm}^2$ . Using the  $1.510 \text{ mg/cm}^2$  mica and each source in turn, curves were plotted in which the ionisation current was expressed as a function of field-strength (Figure 23)\*. The curve obtained with source (2) (Curve B) just reached the plateau and the value of the saturation current was obtained by a small extrapolation. The strength of source (1) was so great that a large extrapolation of the curve (curve A) was required in order to obtain a value for the saturation current.

At the maximum field-strength of 1333 volts/cm, the values obtained for the ionisation currents were expressed as a function of the source-mica distance. The curves obtained for the two sources using the two mica windows, are given in Figure 24. It was assumed \*The saturation characteristics shown in Fig 23 are different to those shown in Fig 15. This was due to the measurements having been made using argon from two different cylinders which probably contained different amounts of oxygen as impurity.

FIGURE 24.

Variation of Ionisation Current  
with Source-Window Distance.

Ionisation current measurements made at a field-strength  
of 1333v/cm.

Chamber shown in Figure 12A.

Mica windows  $1.407 \text{ mg/cm}^2$  and  $1.510 \text{ mg/cm}^2$  in thickness

Chamber filled with argon.

Source-window gap filled with air.

Galvanometer calibration  $1.96 \text{ div}/\mu\text{a}$ .

Strength of sources, (1)  $\sim 13 \text{ mc}$ , (2)  $\sim 7 \text{ mc}$ .

Broken line represents ionisation current expressed as  
a function of the source-window distance, for a mica  
window of thickness  $1.44 \text{ mg/cm}^2$ .

FIGURE 24.

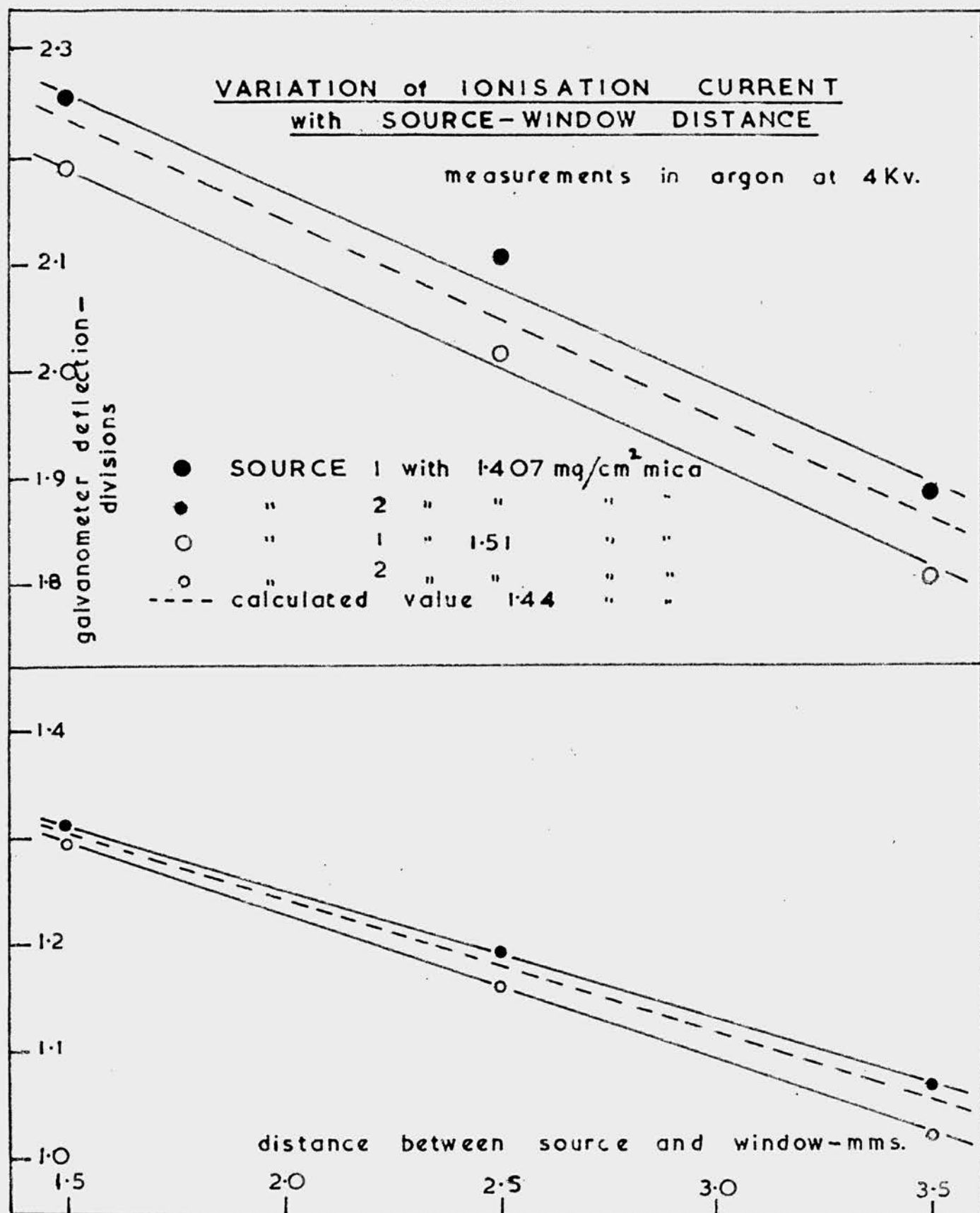




TABLE 13.

The evaluation of  $G_{Fe}^{\alpha}$  for irradiations made through mica.

Source No.	Approx. strength mc.	Source-solution distance mm	Galvanometer Deflection (scale divisions) for mica				Ionisation current for 1.44 mg/cm <sup>2</sup> mica. $\mu$ a (1 $\mu$ a = 1.96 div.)	Ferrous ion oxidation yield for 1.44 mg/cm <sup>2</sup> mica $\mu$ M/hour	$G_{Fe}^{\alpha}$ molecules/100 e.v.
			1.51 mg/cm <sup>2</sup> (observed) source-window distance 2.5 mm	1.44 mg/cm <sup>2</sup> (calculated) source-window distance 2.75 mm	At 1333 V/cm	Extrapolated value			
1	13	2.75	2.015	2.2	2.01	2.2	1.12	17.37	6.32
2	7	2.75	1.16	1.19	1.146	1.175	0.598	9.40	6.40

that ionisation current, like ferrous ion oxidation yield, was a linear function of mica thickness, and a curve which corresponded to measurements made with mica  $1.44 \text{ mg/cm}^2$  in thickness, was calculated. From this curve, it was possible to obtain the values of the ionisation currents (at a field-strength of 1333 volts/cm), which corresponded to the chemical measurements made in the irradiation cells. The values of the corresponding saturation currents were calculated by multiplying the values of the ionisation currents obtained from Fig. 24) by the ratio of the value of the saturation current obtained by extrapolation, to the value of the ionisation current obtained at a field strength of 1333 volts/cm (obtained from Figure 23).

By comparing the ferrous ion oxidation yields with the saturation currents produced by the sources placed 2.75 mm from a mica window  $1.44 \text{ mg/cm}^2$  in thickness, it was possible to calculate values for  $G_{\text{Fe}}^{\alpha}$ . (The method of calculation is given in Appendix I). The results obtained with the two polonium sources are given in Table 13.

(4) Irradiations made in Cells Swept with Inert Gases.

The preliminary experiments described previously (III, 3, (4)) indicated that the effects produced in

solution due to ozone could be suppressed by irradiating the solution in a cell swept with carbon dioxide. Quantitative studies of the  $\alpha$ -induced oxidation of ferrous sulphate solutions were made therefore, using carbon dioxide, and values for  $G_{Fe}^{\alpha}$  were obtained. As discussed in Section III, 4, (3), however, the accuracy with which a saturation current may be estimated is somewhat decreased owing to the diffusion of carbon dioxide through the gold leaf window. This difficulty may be eliminated by using argon as the inert gas;  $\alpha$ -particles are known to have no chemical effect on argon. The determination of  $G_{Fe}^{\alpha}$  was repeated with greater accuracy using argon.

(1) The Evaluation of  $G_{Fe}^{\alpha}$  using carbon dioxide-filled cells.

(a) Chemical measurements.

Unstirred solutions of approximately  $10^{-3}M$  ferrous sulphate in 0.8N sulphuric acid were irradiated in cells through which a slow current of carbon dioxide was passed. The irradiations were made using three sources; (1) ( $\sim 13$  mc), (2) ( $\sim 7$  mc), (3) ( $\sim 4$  mc) and later (1) ( $\sim 6$  mc). The source-solution distances, which were determined before and after every irradiation, varied from 1.93 mm

FIGURE 25.

Ionisation Current - Field strength  
Curves.

Chamber shown in Figure 12A.

Gold leaf-nylon window.

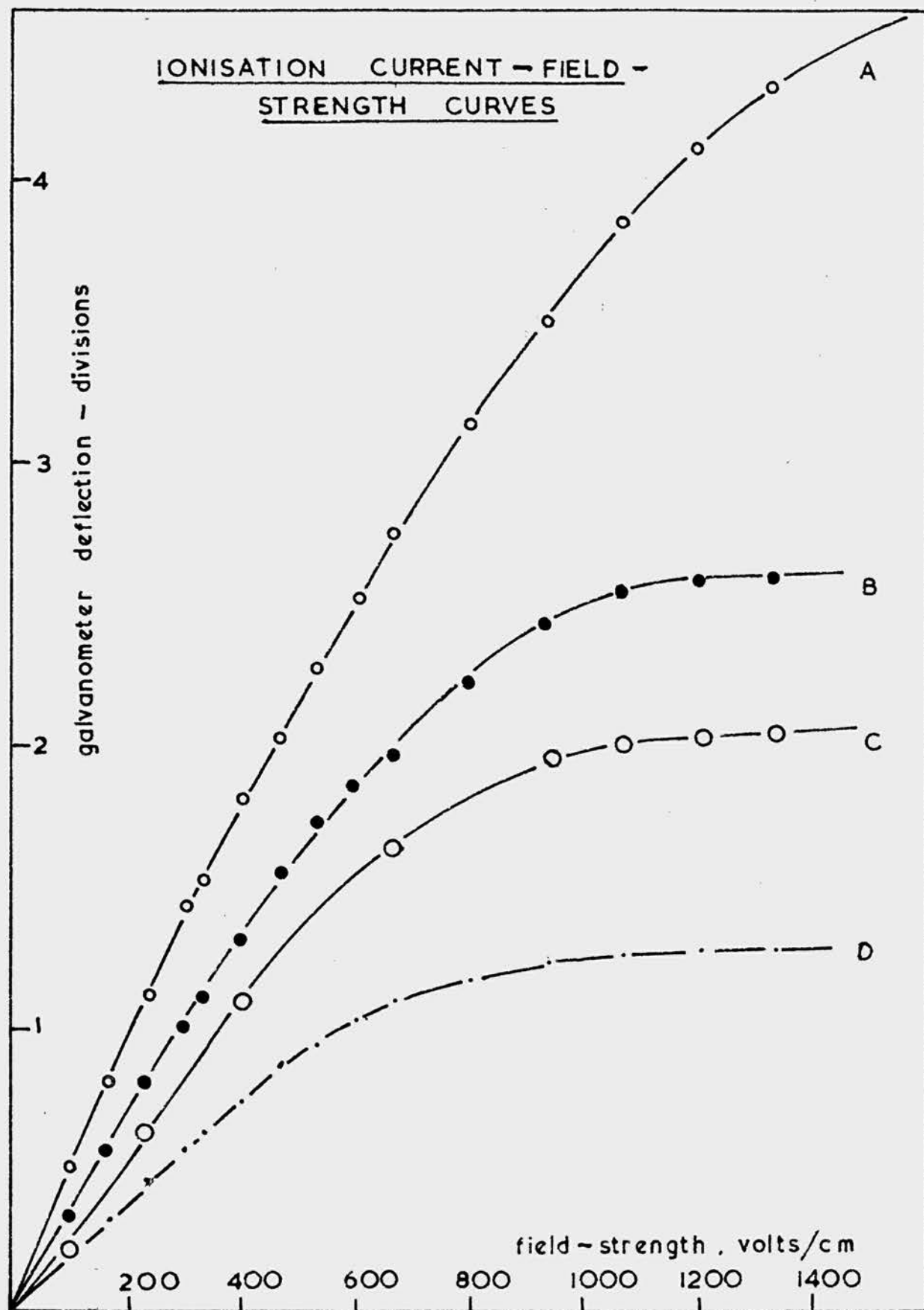
Chamber filled with argon.

Source-window gap filled with carbon dioxide.

Galvanometer calibration 1.96 div/na.

Curve A:	Strength of source	~13 mc:	source-window	
			distance	1.5 mm.
" B:	"	" ~ 7 :	"	2.5 mm.
" C:	"	" ~ 6 :	"	3.5 mm.
" D:	"	" ~ 4 :	"	3.5 mm.

FIGURE 25.



to 2.88 mm. Ferrous ion oxidation/irradiation time curves were plotted. A typical ferrous ion oxidation/irradiation time curve is given in Figure 11, where source (1) ( $\sim 6$  mc) was used. The oxidation of ferrous ion was a linear function of the irradiation time. The ferrous ion oxidation yields were obtained from the slopes of the curves. The yield obtained with each source is given in Table 14.

(b) Physical measurements.

The corresponding physical measurements were made in an argon-filled ionisation chamber fitted with a gold leaf-nylon window. A slow stream of carbon dioxide was passed between the source and the window. For each source, a curve was drawn in which ionisation current was expressed as a function of field-strength (Figure 25). With the exception of source (3), the values of the saturation currents had to be obtained by extrapolation. At a field-strength of 1333 volts/cm. the value of the ionisation current obtained with each source, was expressed as a function of the source-window distance (Figure 26). The method of calculating the saturation current, at a given source-window distance, was the same as that described in the previous section. For a given source, the value of the ionisation current, at the required source-

FIGURE 26.

Ionisation Current as a Function of Source-  
Window Distance.

Ionisation current measurements made at a field-strength  
of 1333v/cm.

Chamber shown in Figure 12A.

Gold leaf-nylon window.

Chamber filled with argon

Source-window gap filled with carbon dioxide.

Galvanometer calibration 1.96 div/ $\mu$ a.

Curve A: Strength of source  $\sim$  13 mc.

" B: " " "  $\sim$  7 mc.

" C: " " "  $\sim$  6 mc.

" D: " " "  $\sim$  4 mc.

FIGURE 26.

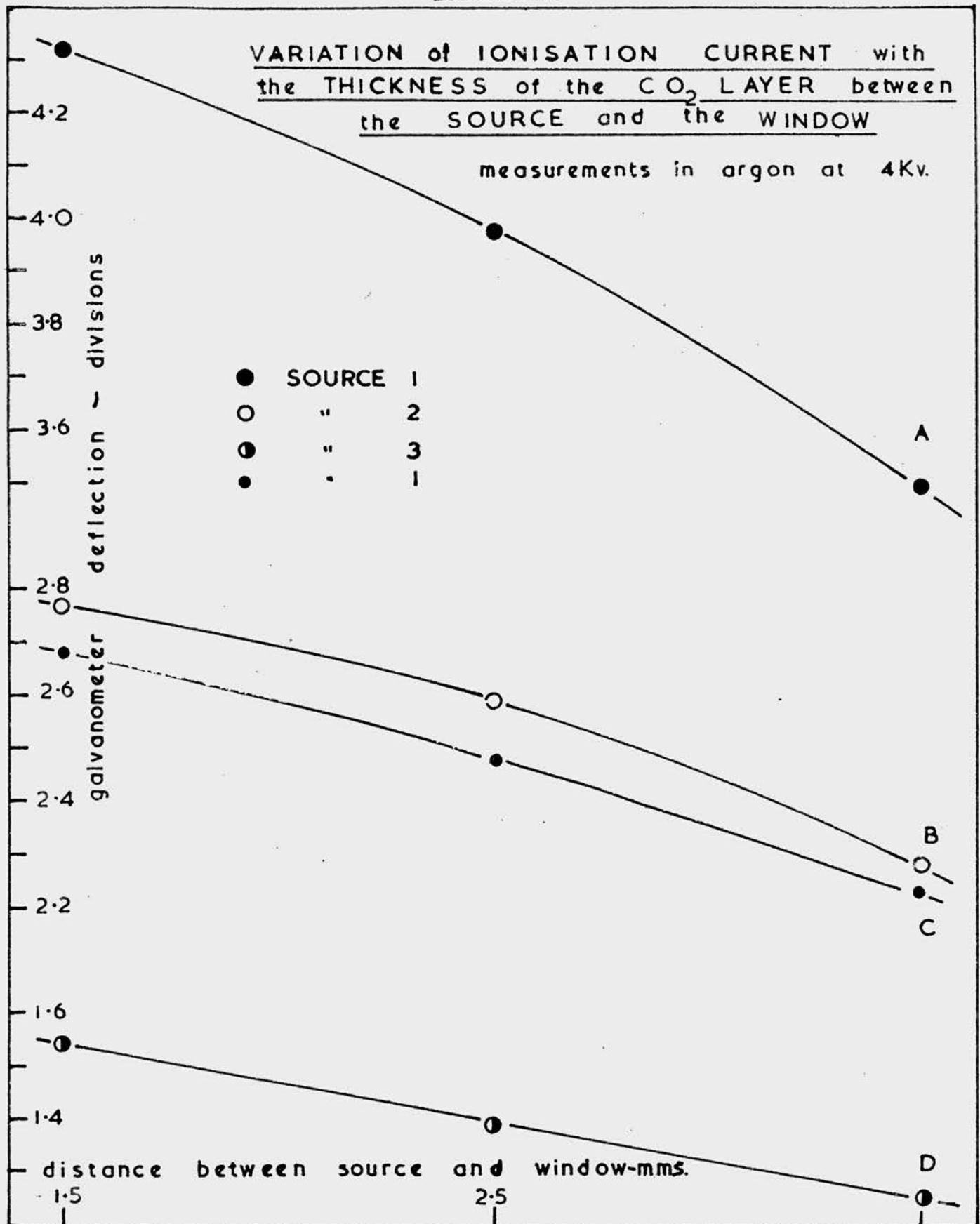




TABLE 14.

The evaluation of  $G_{Fe}^{\alpha}$  for irradiations made in carbon dioxide-filled cells.

Source No.	Approx. strength mc.	Source-window distance mm.	Galvanometer deflection scale divisions		Source-solution distance mm.	Galvanometer deflection scale divisions		Ionisation *current $\mu$ a (1 $\mu$ a = 1.96 div.)	Ferrous ion oxidation yield $\mu$ M/hour	$G_{Fe}^{\alpha}$ molecules/100 e.v.
			At 1333 V/cm	Extrapolated value		At 1333 V/cm	Extrapolated value			
1	13	1.5	4.32	4.75	1.93	4.18	4.60	2.35	32.9	5.70
2	7	2.5	2.585	2.61	2.88	2.48	2.51	1.28	21.1	6.70
3	4				1.93	1.46		0.75	11.7	6.35
1	6	3.5	2.015	2.035	2.74	2.415	2.44	1.25	20.9	6.82

\*The value of the ionisation current has been corrected for absorption of  $\alpha$ -energy by the gold leaf-nylon window.

solution irradiation distance, was obtained from the relevant curve (Figure 26). This value was then multiplied by the ratio of the value of the saturation current obtained by extrapolation, to the value of ionisation current at a field-strength of 1333 volts/cm, obtained with the same source.

By comparing the ferrous ion oxidation yield with the saturation current, it was possible to calculate a value for  $G_{Fe}^{\alpha}$ . The results obtained in the four determinations using the three sources, are given in Table 14.

(ii) Evaluation of  $G_{Fe}^{\alpha}$  using Argon-filled Cells.

(a) Chemical Measurements.

Unstirred solutions of approximately  $10^{-3}M$  ferrous sulphate in 0.8N sulphuric acid, were irradiated in cells through which a current of argon was passed. Source (1) ( $\sim 6$  mc) and later ( $\sim 4$  mc) was used throughout, at a mean source-solution distance of 2.74 mm. The ferrous ion oxidation/irradiation time curves obtained for the source at the two strengths, are given in Figure 27. The ferrous ion oxidation yields were obtained from the slopes of the curves.

(b) Physical Measurements.

An ionisation chamber was used in which argon was present on both sides of the gold leaf-nylon window.

FIGURE 27.

Ferrous Ion Oxidation as a Function of  
Irradiation Time.

Unstirred solution of  $\sim 10^{-3}M$  ferrous sulphate in  
0.8N sulphuric acid.

Argon-swept irradiation cell .

Source-solution distance 2.74 mm. .

Curve A: Strength of source  $\sim 6$  mc.

" B: " " "  $\sim 4$  mc.

FIGURE 27.

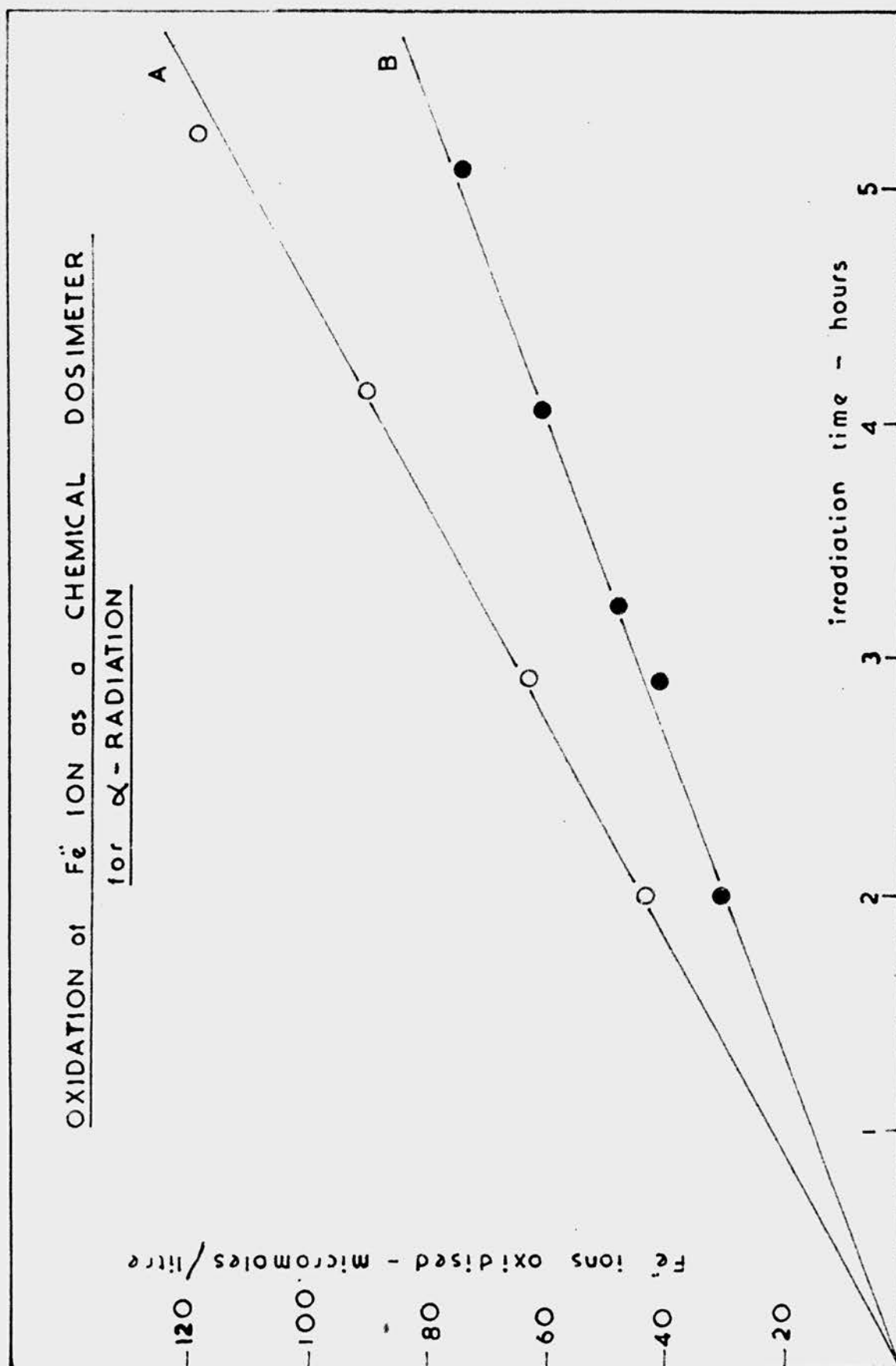


TABLE 15.

The evaluation of  $G_{Fe}^{\alpha}$  for irradiations made in argon-filled cells.

Approximate strength of source mc	Galvanometer deflection at 1333V/cm scale divisions	Ionisation * current $\mu a$ ( $1 \mu a = 1.96 \text{ div}$ )	Ferrous Ion oxidation yield $\mu M/\text{hour}$	$G_{Fe}^{\alpha}$ molecules/100 ev.
6	2.73	1.4	22.0	6.42
4	1.89	0.97	14.94	6.30

\*The value of the ionisation current has been corrected for absorption of  $\alpha$ -energy by the gold leaf-nylon window.

It was possible to obtain saturation with both strengths of source, and ionisation current/field-strength curves were obtained which were similar to that shown in Figure 14, Curve A. Saturation current was expressed as a function of the source-window distance and curves were obtained which were similar to those shown in Figure 26.

By comparing the ferrous ion oxidation yields with the corresponding saturation currents, values for  $G_{Fe}^{\alpha}$  were calculated. The results obtained in the two determinations with source (1), are given in Table 15.

#### (5) Summary of Results

The values for  $G_{Fe}^{\alpha}$  obtained by the methods described in the previous sections are listed, in order of importance, in Table 16.

The results obtained in the argon irradiation system were considered to be the most reliable since undetermined errors were eliminated; for example errors in the value of the saturation current produced by the diffusion of carbon dioxide into the ionisation chamber. It was possible to obtain saturation with both strengths of source used. A weight of three was assigned to the measurement. For

TABLE 16.

The absolute determination of  $G_{Fe}^{\alpha}$ .

Irradiation system used	Source-Solution distance mm	Approximate strength of source mc	$G_{Fe}^{\alpha}$ Molecules/ 100 ev	Weight
argon	2.74	6	6.42	3
"	"	4	6.30	3
mica	2.75	7	6.40	2
"	"	13	6.32	2
carbon-dioxide	1.93	4	6.35	2
"	2.74	6	6.82	1
"	2.88	7	6.70	1
"	1.93	13	5.70	1

Weighted Mean value for  $G_{Fe}^{\alpha}$  = 6.37 molecules/100 ev.  
Standard deviation = 0.09

the determinations made in the mica irradiation system, there was no error due to diffusion but the strengths of the sources were such that the values of the saturation currents had to be obtained by extrapolation. A weight of two was assigned to the measurement. For the determinations made in the carbon dioxide irradiation system there was an undetermined error in the value of the saturation current owing to the diffusion of carbon dioxide into the ionisation chamber. With the exception of the 4 mc. source, it was not possible to obtain saturation and the values of the saturation currents were obtained by extrapolation. A weight of 2 was assigned to the measurement made with the 4 mc source and a weight of 1 to those made with the stronger sources.

The value of the standard deviation seems somewhat lower than would have been expected from the maximum error allowed for each measurement. The possible sources of error are discussed in the following section.

(6) Possible Sources of Error.

When calculating the value for  $G_{Fe}^{\alpha}$  no account was taken of possible errors in the assumed value for



$W_{\text{argon}} = 26.2 \text{ ev.}$  Since the value of  $G_{\text{Fe}}^{\alpha}$  depends directly on the value taken for  $W_{\text{argon}}$ , a final result cannot be given until a more accurate value for  $W_{\text{argon}}$  has been determined.

(a) Chemical

The errors in the determination of the ferrous ion oxidation yield were from two sources: analytical errors and irradiation errors.

The error allowed for the spectrophotometric estimation of ferric ion is 1%. Additional analytical errors introduced by the technique of transferring an irradiated solution to a 5 ml. graduated flask possibly amounted to 1%; an error from this source would result in a slightly low value for  $G_{\text{Fe}}^{\alpha}$ . This technique did eliminate, however, errors due to evaporation of the solution when inert gases were passed through the cell. The ferric ion content of the stock solution was determined before and after every irradiation and a suitable correction was applied to the ferrous ion oxidation yield. This eliminated errors due to the slow atmospheric oxidation of the solution during the period of an irradiation.

Although the errors in the ionisation chamber measurements are reduced when weak sources are used,

longer irradiations are necessary to oxidise a reasonable proportion of the ferrous sulphate solutions. With strong sources, short irradiation times may be used. For the most part the ferrous ion oxidation/irradiation time curves were linear and an error of 2 - 3% in the oxidation yield was considered adequate to cover the spread of the results.

(b) Physical.

The physical errors were from several sources. Errors common to all the measurements of saturation current were those of the galvanometer calibration and the galvanometer reading errors. The former amounted to 1%. The galvanometer could be read to 0.01 scale-divisions.

Other saturation current errors were those introduced by variations in the source-solution distance. This distance was determined before and after every irradiation and the mean value was taken. The distance was averaged over a large number of irradiations and the standard deviation was calculated at 0.03 mm. The saturation current at any given source-solution distance was obtained from the curve in which saturation current was expressed as a function of the source-window distance. An error of 0.03 mm in the source-solution distance gave an error of 0.1 - 0.3% in the saturation current.

For irradiations made in gas-swept cells, the errors in the corresponding saturation current measurements due to the distortion of the gold leaf-nylon window could be reduced to 1%, by careful regulation of the gas flow. When carbon dioxide was used, an error was introduced due to diffusion through the window. This error was not determined and the results for  $G_{Fe}^{\alpha}$ ... , quoted for determinations made in carbon dioxide swept cells, may be a little high on this account.

The gold leaf-nylon window absorbs a small amount of the  $\alpha$ -particle energy. The gold leaf and the nylon were each taken to be equivalent to 0.25mm of air, for  $\alpha$ -particles. The decrease in saturation current due to  $\alpha$ -particle energy absorbed by the window was calculated and allowed for. All saturation currents given in the preceding tables were corrected for absorption by the window.

The largest errors in the saturation current measurements were observed when sources of strengths greater than 6 mc, were used. The value of the saturation current was obtained by extrapolation of the ionisation current/field strength curve and for the 13 mc source an error of 2 - 3% was possible.

The mica thickness was determined by measuring

the area of the sheet and weighing. The error was very small.

(7) Ferrous Sulphate as a Chemical Dosimeter for  
Mixed Radiation.

The use of the ferrous sulphate system as a chemical dosimeter for X-,  $\gamma$ -, and  $\beta$ -radiation was outlined in the introduction (Section I, 2 (b)). The present work indicated that the system could also be used for  $\alpha$ -radiation. For sources such as radon, however, where radiations other than  $\alpha$ -particles are emitted, it is important to know whether the effects produced simultaneously in the solution by the different radiations, are additive.

Preliminary experiments were made in which ferrous sulphate solutions undergoing  $\alpha$ -irradiation from internal polonium sources, were irradiated simultaneously with X-rays. 8 ml. of an approximately  $10^{-3}M$  solution of ferrous sulphate in 0.8N sulphuric acid containing approximately 0.1 mc/ml of polonium, were placed in the bulb of the vessel shown in Figure 4. The production of ferric ion was expressed as a function of the irradiation time (Figure 28). After a suitable irradiation time, the vessel was clamped so that the bulb could be mounted reproducibly, 3 cm above the end of the X-ray tube. The solution was

FIGURE 28.

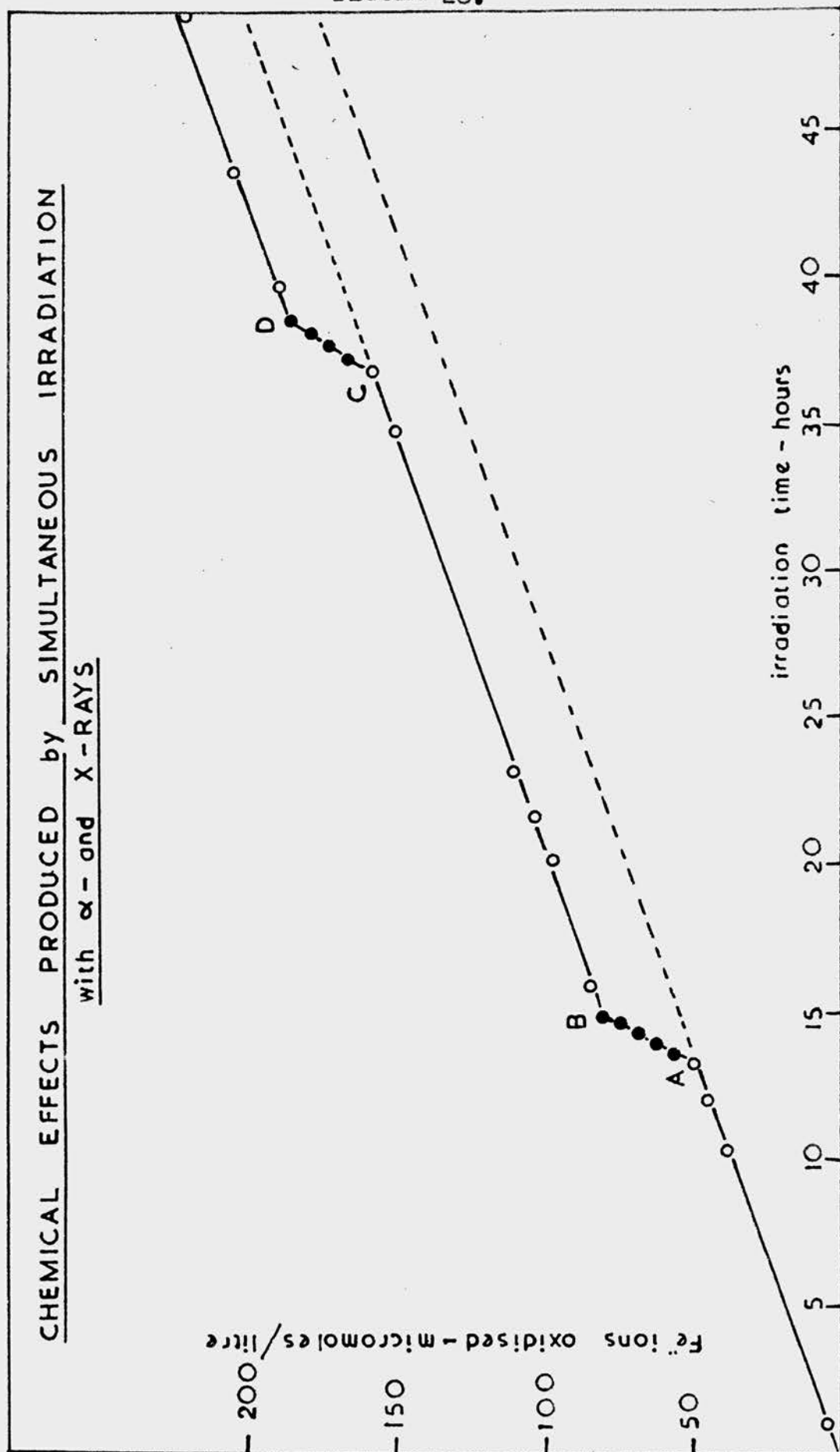
Chemical Effects Produced by Simultaneous  
Irradiation with  $\alpha$ - and X-rays.

Solution of  $\sim 10^{-3}M$  ferrous sulphate in 0.8N  
sulphuric acid, containing 0.1 mc/ml of polonium.

At points A and C the solution was irradiated with  
50 kV peak X-rays at 0.3 ma.

- |       |   |  |
|-------|---|--|
| -A    | } | Ferrous ion oxidation, due to $\alpha$ -rays<br>alone, expressed as a function of time.                                |
| B - C |   |  |
| D-    |   |  |
| A - B | } | Ferrous ion oxidation, due to X- and $\alpha$ -<br>rays.<br>acting simultaneously, expressed as a<br>function of time. |
| C - D |   |  |

FIGURE 28.



irradiated with 50 kV peak X-rays at a tube-current of 0.3 ma (point A, Figure 28). The total X-irradiation time of 25 minutes was spaced over approximately 1.5 hours and the amount of ferric ion produced was estimated after each 5 minute X-irradiation. The production of ferric ion by the X- and  $\alpha$ -rays acting simultaneously was expressed as a function of irradiation time. The X-irradiation was stopped (point B, Figure 28) and the production of ferric ion due to the  $\alpha$ -particles alone was expressed as a function of time. The solution was irradiated again with X-rays (point C, Figure 28) and then the oxidation due to the  $\alpha$ -particles alone was allowed to continue (point D, Figure 28). The slope of each section of the curve shown in Figure 28, represented the ferrous ion oxidation yield due to the  $\alpha$ -particles alone, or with superimposed X-rays. The rate of ferrous ion oxidation by the X-rays was determined in a separate experiment; a solution of approximately  $10^{-3}M$  ferrous sulphate was irradiated using the same irradiation geometry and the same tube current. The dose rates, in ergs/gramme-minute, of the X-rays and the  $\alpha$ -rays were calculated from the respective ferrous ion oxidation yields (Appendix III). The ferrous ion oxidation yield due to the X-rays was subtracted from the yield obtained

with the X- and  $\alpha$ -rays acting simultaneously. The results, which show the ferrous ion oxidation yield due to the  $\alpha$ -particles acting first alone, then during the X-irradiation, and finally alone again, are given in Table 17.

TABLE 17.

The chemical effects produced by simultaneous irradiation with X- and  $\alpha$ -rays.

Approx. Dose Rate ergs/g. min.		Ferrous Ion Oxidation Yield due to the $\alpha$ -particles $\mu$ M/hour		
X	$\alpha$	Before X-	During X-	After X-
4700	900	3.78	3.74	3.65
4700	900	3.65	3.79	3.37
4700	1080	4.37	4.13	4.19

The dose-rate of the X-rays was about five times as great as that of the  $\alpha$ -rays. Since  $G_{Fe^{2+}}^{X\gamma} = 20$  molecules/100 ev, the ferrous ion oxidation yield for the X-rays was approximately fifteen times as great as that for the  $\alpha$ -rays. The results did indicate, however, that the  $\alpha$ -induced ferrous ion oxidation yield was not significantly affected when the solution was irradiated



with X-rays, and that the effects produced by the X- and  $\alpha$ -rays were additive.

This experiment would appear to support the use of ferrous sulphate as a chemical dosimeter for mixed radiation.

(8) Discussion of the Results.

The quantitative studies of the chemical effects produced by  $\alpha$ -particles, discussed in the previous sections, were made using an external polonium source from which  $\alpha$ -particles were emitted with an average energy considerably less than that of  $\alpha$ -particles emitted from an internal polonium source. Experiment showed that, within the limits studied, the value for  $G_{Fe}^{\alpha}$  was independent of the energy of the incident  $\alpha$ -particle. The value for  $G_{Fe}^{\alpha}$  obtained in an argon, or carbon dioxide filled cell, remained unchanged when the average energy of the  $\alpha$ -particles entering the solution was reduced by interposing a sheet of mica between the solution and the source.

Recent work,<sup>68,69</sup> in which internal polonium sources were used, confirmed substantially the values for  $G_{Fe}^{\alpha}$  obtained in the present work and also supported the use of the ferrous sulphate system as a chemical

dosimeter for  $\alpha$ -particles of varying energy.

Hart<sup>68</sup> used an internal polonium source and determined the energy input by an absolute counting technique. A value for  $G_{Fe}^{\alpha\cdots} = 6.25$  molecules/100 ev, was obtained.

Haïssinsky<sup>69</sup> also used an internal polonium source. The energy input was determined by evaporating an aliquot of the irradiated solution on a foil and measuring the saturation current in an ionisation chamber. A value for  $G_{Fe}^{\alpha\cdots} = 6.2$  molecules/100 ev. was obtained.

These results are a little low compared with the value obtained in the present work, although they are within the experimental error. This may be due to the value assumed for  $W_{argon} = 26.2$  ev.

Jesse<sup>66</sup> recently published a value for  $W_{argon} = 26.4 \pm 0.15$  ev. If this value is used when calculating  $G_{Fe}^{\alpha\cdots}$  results very close to those of Hart and Haïssinsky, may be obtained.

The present work indicated that not only was  $G_{Fe}^{\alpha\cdots}$  independent of the energy of the incident  $\alpha$ -particle, but also of the intensity of the source used. Polonium sources, of strengths which varied from 0.4 mc to 13 mc were used without producing a significant change in the value for  $G_{Fe}^{\alpha\cdots}$ . The value for  $G_{Fe}^{\alpha\cdots}$  remained constant when the distance between the source and the irradiated

solution was varied.

The quantitative studies made by Nurnberger<sup>25</sup> are not considered to be particularly accurate. Most of the irradiations were made on ferrous sulphate solutions which were so concentrated that oxidation due to direct action probably took place. In the concentration independent region, different values for  $G_{Fe}^{\alpha}$  were obtained when internal and external sources were used. In addition, the ratio of the yield for ferrous ion oxidation to that for <sup>molecular</sup> hydrogen evolution = 1:1, is not in accordance with the mechanism for the  $\alpha$ -induced oxidation of ferrous sulphate solutions discussed in a later section.

Attempts have recently been made<sup>70</sup> to determine the value for  $G_{Fe}^{\alpha}$  by irradiating ferrous sulphate solutions containing boric acid, in a nuclear reactor.

$\alpha$ -particles are produced by the  $B^{10} (n, \alpha) Li^7$  reaction. These determinations are still in the preliminary stage, however. The oxidation produced in the solution was due to the  $\alpha$ -particles, recoil lithium atoms and the  $\beta$ - and  $\gamma$ -rays from the decaying fission products and  $(n, \gamma)$  isotopes, in the pile. It was assumed that the effects produced by the different types of radiation were additive. For irradiations made in the centre of the pile, values were

obtained for  $G_{Fe}^{\alpha} = 3.9$  molecules/100 ev. If the value for  $G_{Fe}^{\alpha}$  obtained in the present work is correct, it would appear that the effects produced by mixed radiations are not additive. However, when irradiations were made in the thermal column of the pile, where the proportion of the chemical change due to the  $\alpha$ -particles was considerably higher than in the centre of the pile, values for  $G_{Fe}^{\alpha}$  approaching 6 molecules/100 ev. were obtained. It was probable that the high background intensity of  $\beta$ - and  $\gamma$ - rays in the centre of the pile was responsible for the low value observed for  $G_{Fe}^{\alpha}$ . The result obtained in the thermal column of the pile would tend to support the preliminary observation (Section (5)) that the ferrous sulphate system can be used as a chemical dosimeter for mixed radiations and that the effects produced by the different radiations are additive.

## Appendix I

### The Evaluation of $G^\alpha$

Data supplied by experiment:-

I - the saturation current ( $\mu\text{a}$ )

N - rate of chemical change in solution  
( $\mu\text{M}/\text{hour}$ ).

V - volume of solution irradiated (ml).

Data assumed:-

W - energy released/ion pair formed (ev).

To be calculated:-

$G^\alpha$  (molecules/100 ev).

In the ionisation chamber, a saturation current of

$$1\mu\text{a} = 6.281 \times 10^{12} \times W \text{ ev/sec.}$$

$$= 6.281 \times 10^{12} \times W \times 3600 \text{ ev/hour.}$$

In the irradiated solution, a chemical change of

$$1\mu\text{M}/\text{hour} = 6.03 \times 10^{23} \times 10^{-6} \text{ molecules/litres/hour.}$$

$$= 6.03 \times 10^{23} \times 10^{-6} \times 10^{-3} \times V \text{ molecules/Vml/hour.}$$

$$G^\alpha = \frac{6.03 \times 10^{14} \times V \times N}{6.281 \times 10^{12} \times W \times 3600 \times I} \times 100 \text{ molecules/100 ev.}$$

$$\therefore G^\alpha = \frac{N \cdot V}{I \cdot W} \times 2.667 \text{ molecules/100 ev.}$$

When 4 ml of solution are irradiated and the saturation current, I is determined in an argon-filled ionisation chamber where a value for  $W_{\text{argon}} = 26.2 \text{ ev}$  is assumed

$$G^\alpha = \frac{N}{I} \times \frac{4 \times 2.667}{26.2} = \frac{N}{I} \times 0.4075 \text{ molecules/100 ev.}$$

## Appendix II.

### The Evaluation of $G_{O_3}^{\alpha}$

Ferrous ion oxidation in solution is due partly to the effects produced by the  $\alpha$ -particles in solution, and partly to the ozone absorbed from the  $\alpha$ -irradiated air. One ozone molecule is capable of oxidising two ferrous ions.

At a source-solution distance of 1.59 mm :-

% $\alpha$ -energy absorbed in the air = 16.5%

% $\alpha$ -energy absorbed in the solution = 83.5%

"total"  $G_{Fe}^{\alpha}$  = 7.3 molecules/100 ev.

"total"  $G_{Fe}^{\alpha}$  =

$$\left[ (\text{fraction of } \alpha\text{-energy absorbed in solution}) \times \text{"absolute" } G_{Fe}^{\alpha} \right] + \left[ (\text{fraction of } \alpha\text{-energy absorbed in air}) \times 2 G_{O_3}^{\alpha} \right]$$

The value for the "absolute"  $G_{Fe}^{\alpha}$  was obtained from the determinations described in Section III 5(5)

Table 16 :  $G_{Fe}^{\alpha}$  = 6.37 molecules/100 ev.

$$\therefore 7.3 = \left( \frac{83.5}{100} \times 6.37 \right) + \left( \frac{16.5}{100} \times 2 \times G_{O_3}^{\alpha} \right)$$

$$= 5.31 + 0.33 G_{O_3}^{\alpha}$$

$$\therefore G_{O_3}^{\alpha} = 6.0 \text{ molecules/100 ev.}$$


---

A similar calculation at a source-solution distance of 5.76 mm gives a value for  $G_{O_3}^{\alpha}$  = 10.6 molecules/100 ev.

---

### Appendix III

#### The Calculation of the Dose-rate for X- and $\alpha$ -rays from the Ferrous Ion Oxidation Yields.

##### X-rays.

A solution of ferrous sulphate irradiated with 50 kV peak X-rays at a tube-current of 0.3 ma was oxidised at a rate of  $0.995 \mu\text{M}/\text{minute}$ .

$$G_{\text{Fe}}^{\text{X}} = 20 \text{ molecules}/100 \text{ ev, or } 19.7 \mu\text{M}/1000 \text{ roentgens.}$$

$$\begin{aligned} \therefore \text{Dose-rate} &= \frac{0.995}{19.7} \times 1000 \text{ r/minute} \\ &= 50.5 \text{ r/minute} \\ &= 50.5 \times 93.12 \text{ ergs/g. minute.} \end{aligned}$$

$$\therefore \text{X-ray dose-rate} = 4705 \text{ ergs/g. minute.}$$

-----

##### $\alpha$ -rays.

8 ml of an  $10^{-3}\text{M}$  ferrous sulphate solution containing 0.1 mc/ml of polonium is oxidised at a rate of  $3.65 \mu\text{M}/\text{hour}$ .

8 ml of a solution, 0.8N in sulphuric acid, weighs

$$8 \times 1.025 = 8.2 \text{ g.}$$

$$G_{\text{Fe}}^{\alpha} = 6.37 \text{ molecules}/100 \text{ ev.}$$

Ferrous ion oxidation yield =  $3.65 \mu\text{M}/\text{hour}$

$$= 3.65 \times 8 \times 6.023 \times 10^{23} \times 10^{-6} \times 10^{-3} \text{ molecules/hour}$$

$$= \frac{3.65 \times 8 \times 6.023 \times 10^{14}}{60} \text{ molecules/minute}$$

$$\therefore \alpha\text{-ray dose rate} = \frac{3.65 \times 8 \times 6.023 \times 10^{14} \times 100}{60 \times 6.37} \text{ ev/minute.}$$

$$= \frac{3.65 \times 8 \times 6.023 \times 10^{14} \times 100 \times 1.6 \times 10^{12} \text{ ergs/}}{60 \times 6.37 \times 8.2} \text{ g.minute.}$$

$$\therefore \underline{\alpha\text{-ray dose rate} = 900 \text{ ergs/g. minute.}}$$



6. THE MECHANISM OF THE CHEMICAL EFFECTS PRODUCED  
IN AQUEOUS SOLUTIONS BY  $\alpha$ -PARTICLES.

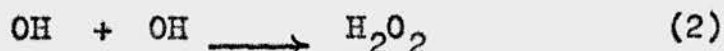
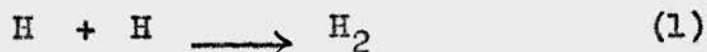
1. Introduction.

It was realized from the earliest observations made in the field of radiation chemistry, that different chemical effects were produced in solutions irradiated with different types of radiation.  $\alpha$ -rays were shown to decompose pure water<sup>1</sup> with the evolution of hydrogen and the production of hydrogen peroxide in solution. X-rays, on the other hand, produce relatively little decomposition of pure water<sup>5</sup>. Much attention has been drawn recently to the effects produced in water<sup>71</sup> and in aqueous solutions<sup>33</sup> irradiated with particles of different energies.

It is generally accepted that when ionising radiation is absorbed in water, free radicals are produced as a result of ionisation. The number of free radicals formed by the dissociation of excited water molecules, is very small due to the recombination of radicals in the "solvent cage". The chemical effects produced by different types of radiation have been explained by the different distribution of free radicals along the tracks of the ionising particles

The mechanism of the radiation-induced effects

produced in solution has been approached by two methods. The first, due to Allen<sup>5</sup> explained the effects produced by different radiations on a basis of the ion density along the track of the incident particle. Cloud-chamber studies of the tracks produced in gases by ionising particles indicated that ions are formed in clusters along the tracks. The formation of ions in clusters along the track of the ionising particle was also considered to take place in solutions. The spacing of the clusters along the track is dependent on the energy of the ionising particle. With X- and  $\gamma$ -rays, the ion clusters are relatively widely spaced along the tracks of the ejected photoelectrons or Compton electrons and the radicals produced become widely distributed throughout the solution. In the absence of a solute, the bulk of the radicals recombine to give water. The small yields of hydrogen and hydrogen peroxide observed were attributed to the following combination reactions.



These reactions were alleged to occur in the regions of high ion density at the ends of the

electron tracks. The activation energy of reaction (2) was estimated at 5.5 cal/mole <sup>5(a)</sup>. The production of hydrogen peroxide by the combination of two hydroxyl radicals was considered to take place in regions of high free radical density owing to the formation of the free radicals in an excited state. For more densely ionising radiation such as  $\alpha$ -particles, the ion clusters are formed in close proximity, and result in a high density of free radicals along the track. These conditions favour the combination reactions (1) and (2) and the yields of hydrogen and hydrogen peroxide produced by the  $\alpha$ -irradiation of water are high compared with those produced by X-rays.

The physical picture of the distribution of the radicals along the track of an ionising particle has been developed by Lea<sup>49</sup> and Gray<sup>72</sup>. The resultant effect of the electrons ejected in the primary ionisation of water molecules is the creation of free hydroxyl radicals close to the track, and free hydrogen atoms in a cylinder which is coaxial with the track. It has been estimated that the hydroxyl radicals and the hydrogen atoms are formed in cylinders of radii  $8\text{\AA}$  and  $150\text{\AA}$ , respectively. The density of the radicals in the cylinders is greater

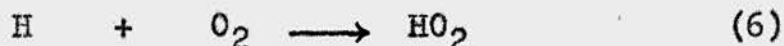
the smaller the energy of the incident particle.

The production of hydrogen and hydrogen peroxide in regions of high ion density, such as the ends of electron tracks or along the tracks of  $\alpha$ -particles, was attributed to the "molecular decomposition" of water.



Evidence in support of this reaction has been presented by Allen<sup>5</sup>.

Many of the effects observed in irradiated solutions cannot be explained by this "molecular decomposition" theory. The production of hydrogen peroxide and the evolution of hydrogen and oxygen from irradiated water have been explained<sup>6,73</sup> on an alternative mechanism which does not involve the combination of two hydroxyl radicals.



From considerations of dipole attraction, reaction (4) is more probable than reaction (2).<sup>73</sup>

Hitherto, many of the chemical effects produced

in aqueous solutions by  $\alpha$ -particles have been attributed to the hydrogen peroxide formed by the "molecular decomposition" of water. The experiments described later in this section cannot, however, be explained on this mechanism and there is a good deal of evidence to show that the chemical effects produced by  $\alpha$ -particles are due to free radicals and not to products of a "molecular decomposition".

An effective mechanism for  $\alpha$ -induced reactions in aqueous solutions can be put forward only when all the chemical effects have been studied. This involves the investigation, not only of the effects on solutes, but of the gases evolved. The preliminary studies presented in this section are far from complete. It has been possible however to explain qualitatively some of the results obtained in ferrous sulphate solutions irradiated with  $\alpha$ -rays, by the free radical mechanisms derived for  $\gamma$ -rays.

## 2. Experimental and Results.

The experiments described in this section were made using both internal and external polonium sources. Since no determinations of  $G_{Fe}^{\alpha}$  were made in this section, the irradiations in which external sources were used were made in cells swept

FIGURE 29.

Effect of Ethanol on the Ferrous Ion Oxidation  
by  $\alpha$ -rays.

Unstirred, aerated solutions irradiated through a  
mica disc  $1.39 \text{ mg/cm}^2$  in thickness.

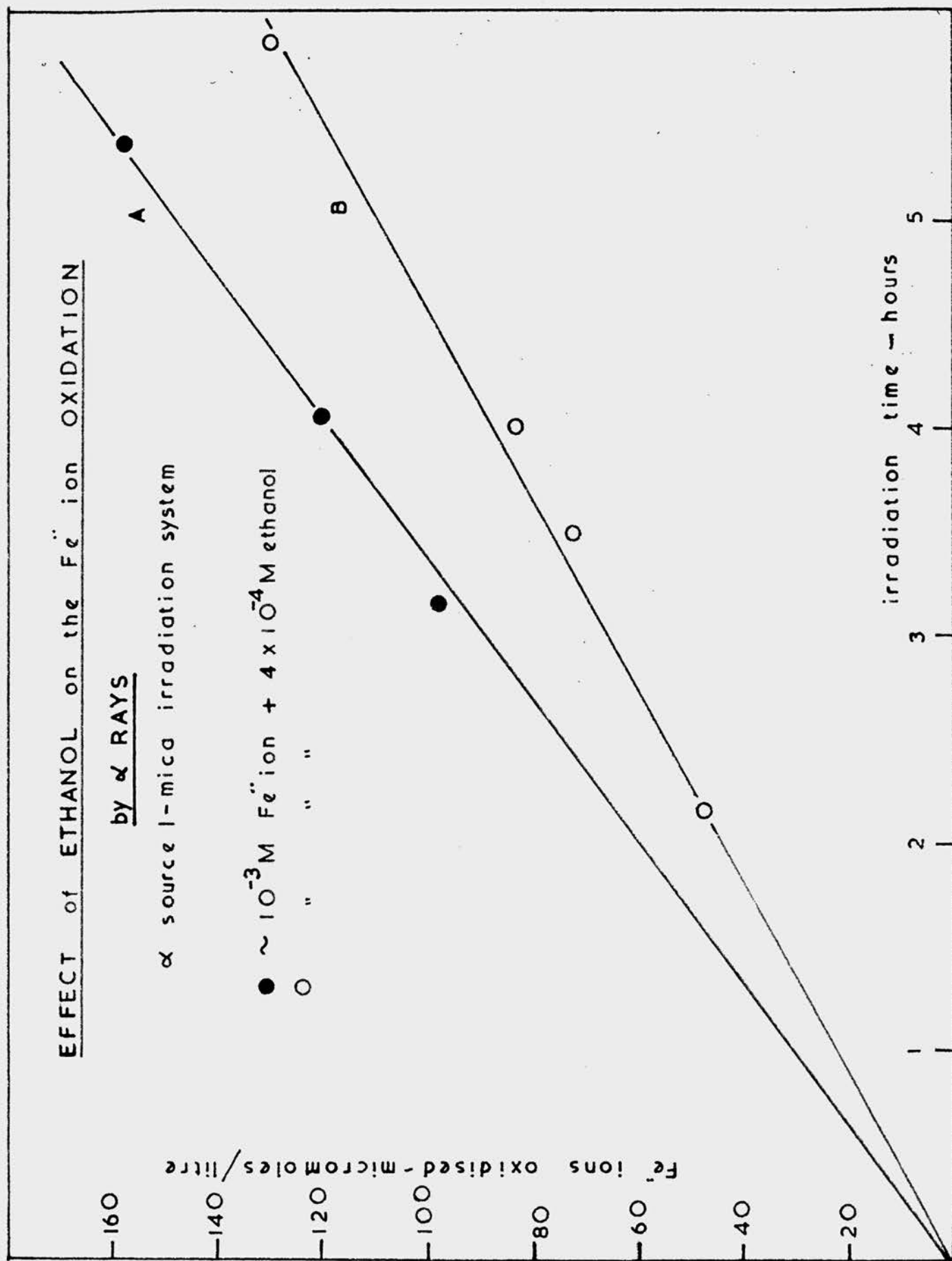
Strength of source  $\sim 13 \text{ mc.}$

Source-solution distance  $2.75 \text{ mm.}$

Curve A: Solution of  $\sim 10^{-3} \text{M}$  ferrous sulphate,  $4 \times 10^{-4} \text{M}$   
ethanol in  $0.8 \text{N}$  sulphuric acid.

Curve B: Solution of  $\sim 10^{-3} \text{M}$  ferrous sulphate in  $0.8 \text{N}$   
sulphuric acid.

FIGURE 29



with carbon dioxide. Carbon dioxide was used in preference to argon purely on account of cost.

- (i) The effect of  $\alpha$ -rays on aerated ferrous sulphate solutions containing ethanol.

The irradiations were made, first in a cell where a sheet of mica floated on the surface of the solution, next in a cell through which a current of carbon dioxide was passed, and finally using an internal source.

A 0.8N sulphuric acid solution of approximately  $10^{-3}M$  ferrous sulphate,  $4 \times 10^{-4}M$  in ethanol, was irradiated through a sheet of mica. The amount of ferrous ion oxidised was expressed as a function of the irradiation time (Figure 29, Curve A). The ferrous ion oxidation yield was compared with that obtained when a solution containing no ethanol was irradiated under the same conditions (Figure 29, Curve B). Aliquots of the same solutions were irradiated with  $\gamma$ -rays. The ferrous ion oxidation/irradiation time curves are given in Figure 30.

The  $\alpha$ -irradiations were repeated in a cell through which carbon dioxide was passed.

The result of these irradiations are given in Table 18.

The ferric ion production in an approximately  $10^{-3}M$  ferrous sulphate, 0.8N sulphuric acid solution



FIGURE 30.

Effect of  $\gamma$ -rays on ferrous sulphate solutions  
containing ethanol.

5 ml portions of the solutions irradiated with  
 $\gamma$ -rays from the 800 mc cobalt source in  
the vessel shown in Figure 1.

Curve A: Solution of  $\sim 10^{-3}M$  ferrous sulphate,  
 $4 \times 10^{-4}M$  ethanol in 0.8N sulphuric acid.

Curve B: Solution of  $\sim 10^{-3}M$  ferrous sulphate in  
0.8N sulphuric acid.

FIGURE 30.

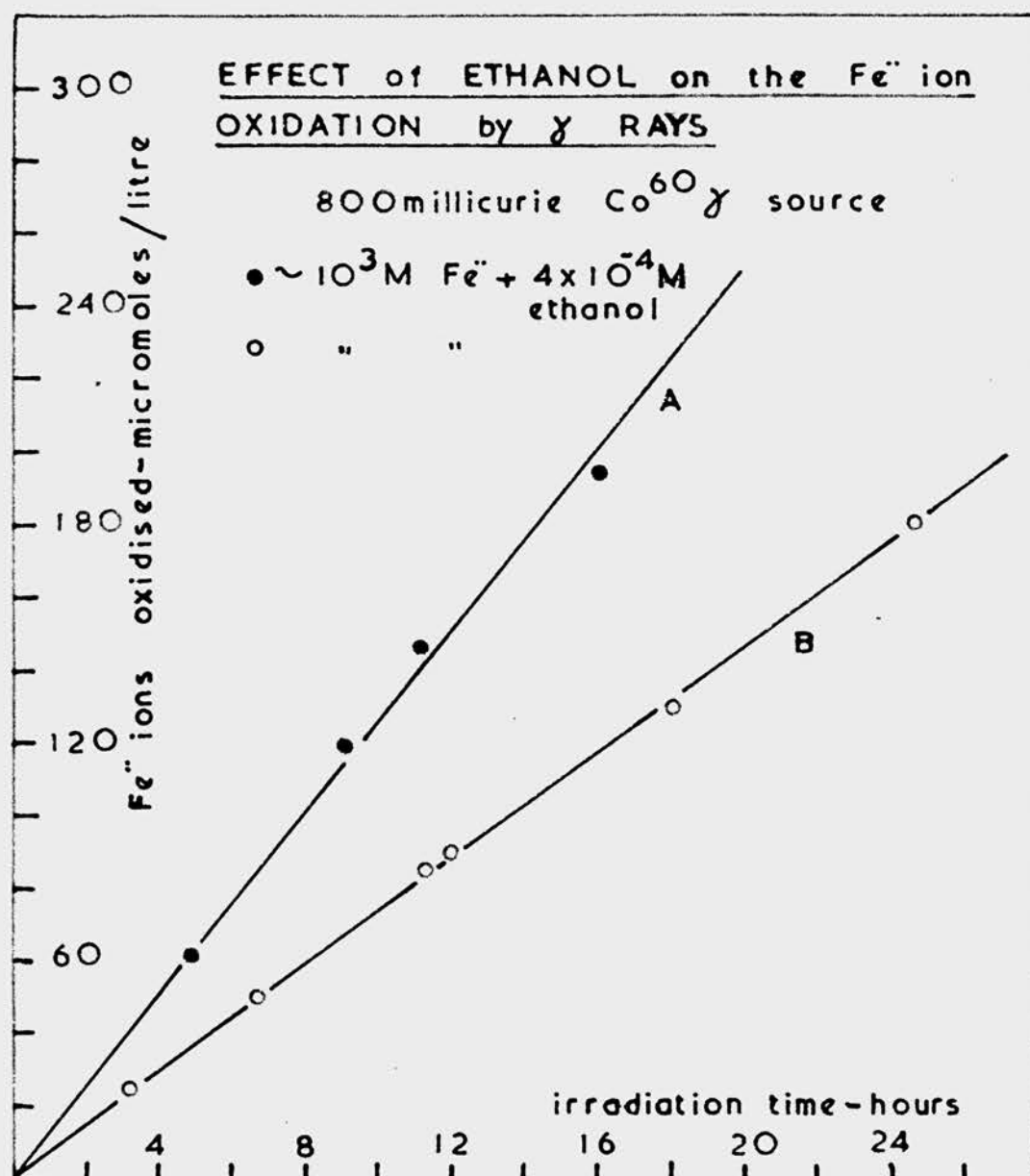


TABLE 18.

The Effect of ethanol on the radiation-induced oxidation of  
aerated ferrous sulphate solutions.

Irradiation system	Ferrous ion oxidation yield $\mu\text{M}/\text{hour}$		Ratio of yield in $\text{Fe}^{2+}$ ion + ethanol $\frac{\text{Fe}^{2+} \text{ ion}}{\text{solution}}$	Concentration of ethanol M
	$\sim 10^{-3}\text{M Fe}^{2+}$ ion	$\sim 10^{-3}\text{M Fe}^{2+}$ ion+ethanol		
Solution irradiated through mica using an external $\alpha$ - source	22.1	29.5	1.34	$4 \times 10^{-4}$
Solution irradiated in a cell swept with carbon dioxide	14.7	18.6	1.27	$6 \times 10^{-4}$
Solution irradiated using an internal $\alpha$ -source	5.63	9.25	1.64	$6 \times 10^{-4}$
Solution irradiated with $\gamma$ -rays	7.32	12.8	1.75	$4 \times 10^{-4}$

containing 0.1 mc/ml of polonium, was studied as a function of irradiation time (Figure 31). At point A, the solution was made  $6 \times 10^{-4}M$  in ethanol and the ferric ion production was again studied as a function of time. A suitable correction was applied for the increase in volume of the solution caused by the addition of the ethanol. At point B, the solution was made  $10^{-3}M$  in sodium chloride.

When ethanol was added to an aerated ferrous sulphate solution, the  $\alpha$ -induced oxidation yield was found to increase. The effect of adding sodium chloride was to reduce the yield to approximately the same value as that observed in the original solution before the ethanol was added.

The results of this experiment are given in Table 18.

The effects produced by adding alcohols to  $\gamma$ -irradiated aerated ferrous sulphate solutions, have been discussed by Dewhurst<sup>41</sup>. The competition between the alcohol molecules and the ferrous ions for the hydroxyl ions results in the formation of organic free radicals, according to the reaction



The organic free radical may then react with dissolved oxygen to produce an organic peroxide, which

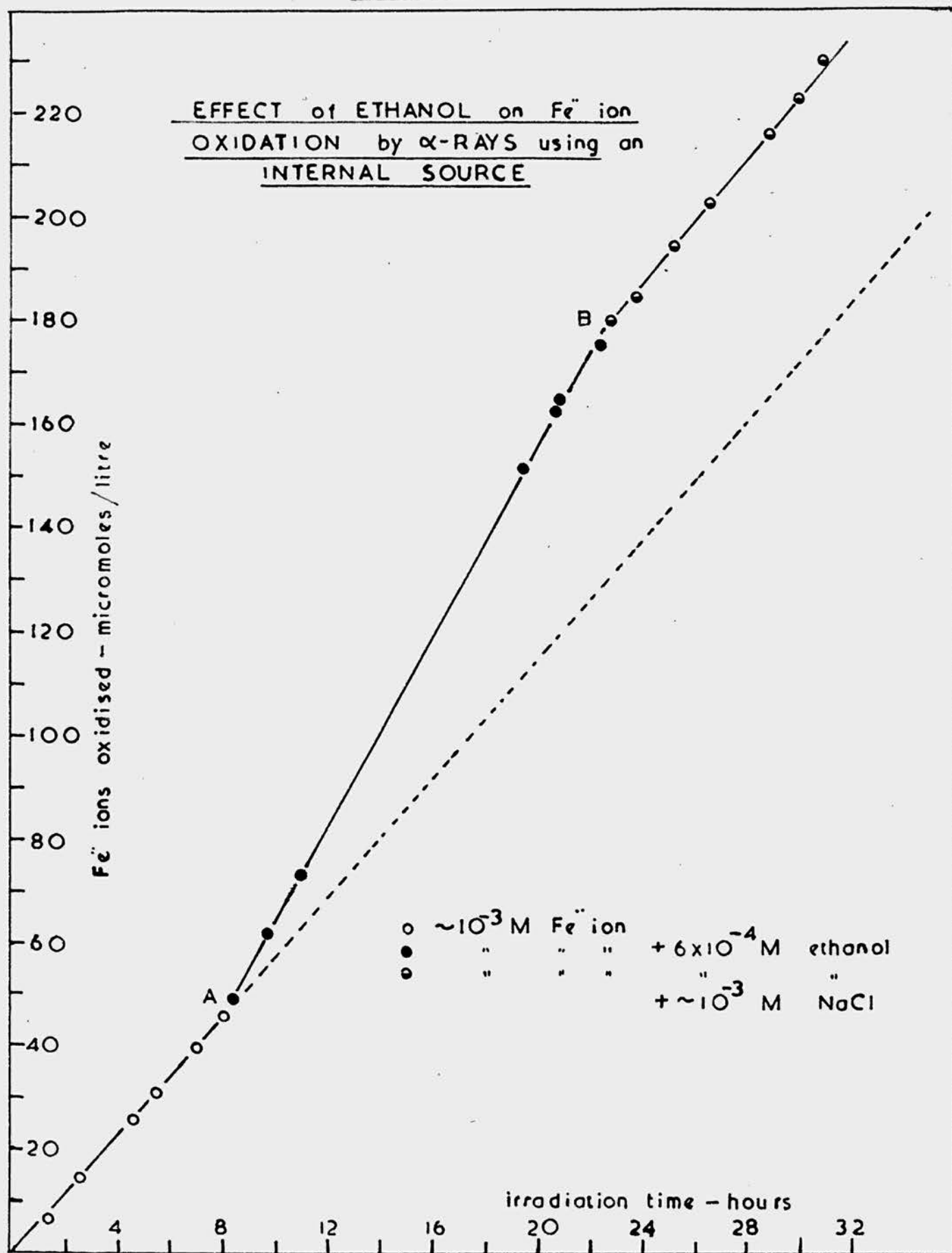
FIGURE 31.

Effect of Ethanol on Ferrous Ion Oxidation  
by  $\alpha$ -rays using an Internal Source.

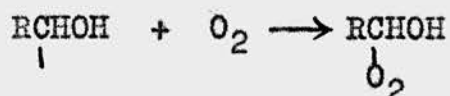
Solution of  $\sim 10^{-3}M$  ferrous sulphate in 0.8N sulphuric  
acid.  
Containing 0.1 mc/ml of polonium.

At point A, the solution was made  $6 \times 10^{-4}M$  in ethanol  
" " B " " " "  $10^{-3}M$  in sodium  
chloride.

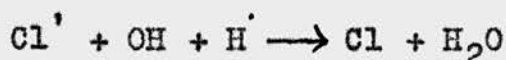
FIGURE 31



is capable of oxidising several ferrous ions.



Thus, the effect of an alcohol, is to increase the ferrous ion oxidation yield. The addition of chloride ions to a solution undergoing irradiation, suppresses the effect produced by the alcohol. Chlorine atoms are produced by the following reaction.



The chlorine atoms react with ferrous ions in preference to the alcohol. Organic peroxides are not formed and the ferrous ion oxidation yield is lowered to the value obtained in solutions containing no alcohol.

Since the enhanced ferrous ion oxidation yield is due, primarily to the reaction between the alcohol molecules and the hydroxyl ions, the addition of ethanol is a means of determining whether free hydroxyl radicals are produced in an irradiated solution. The enhanced ferrous ion oxidation yields observed in solutions irradiated with  $\alpha$ -particles, indicated that free hydroxyl radicals were present. The effect of the ethanol was more pronounced when the solution was irradiated

with an internal source than with an external source. This effect may be due to the surface layer of the externally irradiated, unstirred solution, becoming depleted in oxygen or ethanol, thus decreasing the formation of the organic peroxide and thereby the ferrous ion oxidation yield. When an internal  $\alpha$ -source is used, the irradiation products are more evenly distributed throughout the solution. This ensures maximum efficiency for the reactions leading to enhanced ferrous ion oxidation. The effect produced by the ethanol was of the same magnitude in the solution irradiated in a carbon dioxide-swept cell, as in that irradiated through mica. This observation provided additional evidence that an irradiated solution was not appreciably deaerated when an inert gas was passed over its surface (III, 3(5)). Had the surface layer of the solution been depleted in oxygen owing to the gas passing through the cell, the production of an organic peroxide would have been lowered, and as a result, the ferrous ion oxidation yield would not have been increased significantly on addition of ethanol.

The  $\alpha$ -induced ferrous ion oxidation yield was increased by a factor of 1.64 as against the



factor of 1.75 obtained with  $\gamma$ -rays. This result indicated that free hydroxyl radicals play almost as large a part in the  $\alpha$ -induced oxidation of ferrous sulphate, as in the oxidation induced by  $\gamma$ -rays.

- (ii) The effect of dissolved oxygen on the  $\alpha$ -induced oxidation of aqueous ferrous sulphate.

It was not possible to use the external source in vacuo for the reasons outlined previously (II, 2). Solutions were irradiated using an internal polonium source and the vessel shown in Figure 4. Ferrous sulphate solutions, approximately 8 ml in volume, containing 0.1 mc/ml of polonium, were used. The presence of the neodymium carrier in the polonium solution was shown to have no effect on the ferrous ion oxidation yield (III, 3, (7)).

The oxidation of the ferrous ion in aerated solution was studied as a function of time. The apparatus was attached to the pumping line (Figure 3) and dissolved gases were removed from the solution by the technique described previously (II, 5(c)). The solution was sealed off in vacuo and the radiation-induced oxidation of the ferrous ion in airfree solution was studied as a function of time.

(A control experiment showed that the ferric ion content of an airfree stock solution was small, and remained constant over a period of a month). The vessel was opened to the air and the solution was allowed to reaerate. The oxidation of the ferrous ion in the reaerated solution was studied as a function of time. Finally, the solution was made  $10^{-3}M$  in sodium chloride and the course of the oxidation was again followed. A typical ferrous ion oxidation/irradiation time curve for an irradiation of this kind, is given in Figure 32.

Irradiations were made on solutions of ferrous sulphate in 0.8N sulphuric acid. The ferrous ion oxidation yields obtained in aerated, and airfree solutions, were studied as a function of the initial ferrous ion concentration. Assuming a value for  $G_{Fe}^{\alpha} = 6.37$  molecules/100 ev., for an aerated solution, it was possible to calculate the value for  $G_{Fe}^{\alpha}$ , for an airfree solution. The results are given in Table 19(a).

The value for  $G_{Fe}^{\alpha}$ , in airfree solution, was expressed as a function of the initial ferrous ion concentration (Figure 9, Curve B). Over the concentration range  $8.1 \times 10^{-3}M$  to  $4.36 \times 10^{-4}M$  ferrous ion, the value for  $G_{Fe}^{\alpha}$ , in airfree solution, was

FIGURE 32.

Ferric Ion Production as a Function of Time  
of Irradiation in Aerated and Airfree Solution,  
Irradiating with an Internal Source.

Solution of  $\sim 10^{-3}M$  ferrous sulphate in 0.8N  
sulphuric acid containing 0.1 mc/ml of polonium.

At point A the solution was deaerated.

" " B " " " reaerated

" " C " " " made  $10^{-3}M$  in sodium  
chloride.

FIGURE 32.

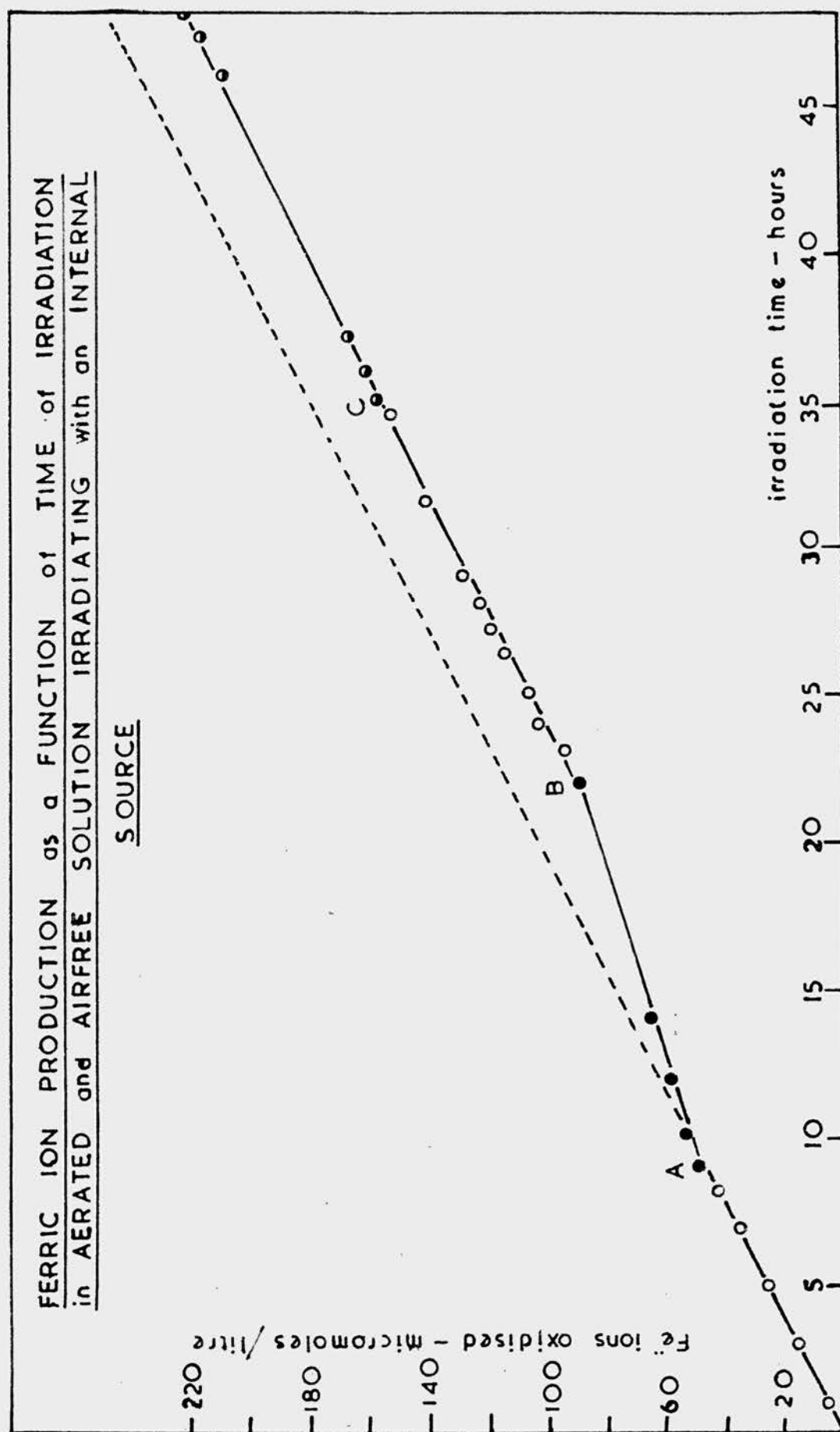


TABLE 19.

The oxidation of ferrous sulphate, in aerated and airfree solution, using an internal polonium source.

Initial Concentration of ferrous ion M	Sulphuric acid Concentration M	Ferrous ion oxidation yield $\mu\text{M}/\text{hour}$		Ratio of Yield in aerated Yield in airfree solution	$G_{\text{Fe}^{2+}}^{\alpha}$ molecules/ 100 ev. (airfree solution)	Ferrous ion oxidation yield in re-aerated solution $\mu\text{M}/\text{hour}$
		Aerated solution	Airfree solution			
(a) $8.10 \times 10^{-3}$ $9.62 \times 10^{-4}$ $4.36 \times 10^{-4}$	0.4	9.20	5.50	1.69	3.77	9.10
		5.20	3.08	1.69	3.77	4.95
		6.84	4.07	1.68	3.79	7.73
(b) $1.41 \times 10^{-3}$ $1.14 \times 10^{-3}$	1.0 0.01	5.73	3.52	1.63	3.90	6.11
		3.67	2.17	1.69	3.77	3.09

independent of the initial ferrous ion concentration.

The addition of sodium chloride to a reaerated solution produced no significant change in the ferrous ion oxidation yield. This indicated that no impurities had been introduced into the solution as a result of the deaeration process (II, 5(c)). The slight irregularities in the values of the ferrous ion oxidation yields, in reaerated solution, are difficult to explain.

The effect of dissolved oxygen on the radiation-induced oxidation of the ferrous ion is almost as pronounced for  $\alpha$ -rays as for X- and  $\gamma$ -rays.

When solutions of ferrous sulphate, with concentrations  $5 \times 10^{-3}M$  or greater, are irradiated with

$\gamma$ -rays, the ratio of the ferrous ion oxidation yield in aerated solution to that in airfree solution is  $2.0^{38}$ . The ratio obtained for an  $\alpha$ -irradiated solution is 1.69. This result indicated that a considerable fraction of the oxidation taking place in an aerated solution was due, as in  $\gamma$ -irradiated solutions, to the radical  $HO_2$ . The  $HO_2$  radicals are produced along the track of an  $\alpha$ -particle by the reaction between dissolved oxygen and the free hydrogen atoms formed as a result of the primary ionisation of water molecules.

The values of the ratios, 2.0 and 1.69, obtained for the aerated/airfree ferrous ion oxidation yields produced by  $\gamma$ - and  $\alpha$ -rays respectively, suggest that the oxidation produced in an  $\alpha$ -irradiated solution is not entirely due to the reactions involving the hydrogen atoms and the hydroxyl radicals. It is possible therefore, that a certain amount of oxidation takes place due to the hydrogen peroxide formed in the  $\alpha$ -particle track by the reactions (4) to (7), described previously in section (1). It would appear that about 10% of the total  $\alpha$ -induced oxidation in an aerated solution, is due to the hydrogen peroxide formed in the  $\alpha$ -tracks. In an airfree solution, the percentage would be higher.

It has been suggested<sup>29,39</sup> that the oxidation of ferrous ions in an airfree solution is produced by the hydroxyl radicals and the ion  $H_2^{\bullet}$ . In  $\alpha$ -irradiated, airfree solutions, oxidation probably occurs partly by the hydroxyl radicals and  $H_2^{\bullet}$  ions, and partly by the hydrogen peroxide produced along the  $\alpha$ -track.

For airfree solutions, the value for  $G_{Fe}^{\gamma}$  decreases as the initial ferrous ion concentration decreases below  $5 \times 10^{-3} M$ <sup>29,38</sup>. This effect has been attributed<sup>29</sup> to competition at low ferrous

ion concentration, between the reaction in which the ion  $\text{H}_2^{\cdot}$  is formed, and other reactions which result in removal of hydrogen atoms. For airfree solutions irradiated with  $\alpha$ -particles, however, the value for  $G_{\text{Fe}}^{\alpha}$  is independent of the initial ferrous ion concentration. The reason for this is not entirely clear. It would appear that the conditions along an  $\alpha$ -track are such, that the reactions resulting in the oxidation of the ferrous ions are efficient, even at low ferrous ion concentrations.

It has not been possible, in the present work to study the evolution of hydrogen from an airfree solution of ferrous sulphate, irradiated with  $\alpha$ -rays. It would be expected that the yield for hydrogen evolution would be half that for ferrous ion oxidation, according to the qualitative reaction



Nurnberger<sup>25</sup> observed that the yields for <sup>molecular</sup>hydrogen evolution and ferrous ion oxidation were approximately equal. However, the experimental conditions were such, that no reliance can be placed on this result. Garrison and his collaborators<sup>55</sup> observed that the ferrous ion oxidation yield in a solution saturated with carbon dioxide, and irradiated with 45 Mev helium ions, was double the yield for hydrogen.



evolution.

As the value for an airfree solution is  $G_{Fe}^{\alpha} = 3.77$  molecules/100 ev., the value for  $G_{H_2}^{\alpha}$  would be approximately 1.9 molecules/100 ev. It is of interest, that this value, for the yield of hydrogen evolved from an  $\alpha$ -irradiated airfree ferrous sulphate solution, is of the same order as the yield observed for hydrogen evolution in  $\alpha$ -irradiated water.<sup>79</sup>

(iii) The effect of acid concentration on the  $\alpha$ -induced oxidation of ferrous sulphate.

(a) In aerated solution.

Solutions of approximately  $10^{-3}M$  ferrous sulphate, in sulphuric acid of concentration varying from 0.4M to  $5 \times 10^{-4}M$ , were irradiated in cells swept with carbon dioxide, using the external source. The amount of ferrous ion oxidised was expressed as a function of the irradiation time (Figure 33). From the slopes of the ferrous ion oxidation/irradiation time curves, and the saturation current measurements made previously, the values for  $G_{Fe}^{\alpha}$  were calculated. The value for  $G_{Fe}^{\alpha}$ , obtained in aerated solution, was expressed as a function of the sulphuric acid concentration

FIGURE 33.

Dependence of Ferrous Ion Oxidation on Acid  
Concentration.

Solution of  $\sim 10^{-3}M$  ferrous sulphate.

Irradiations made in carbon dioxide-swept cells.

Strength of source  $\sim 6$  mc.

Source-Solution distance 2.74 mm.

FIGURE 33.

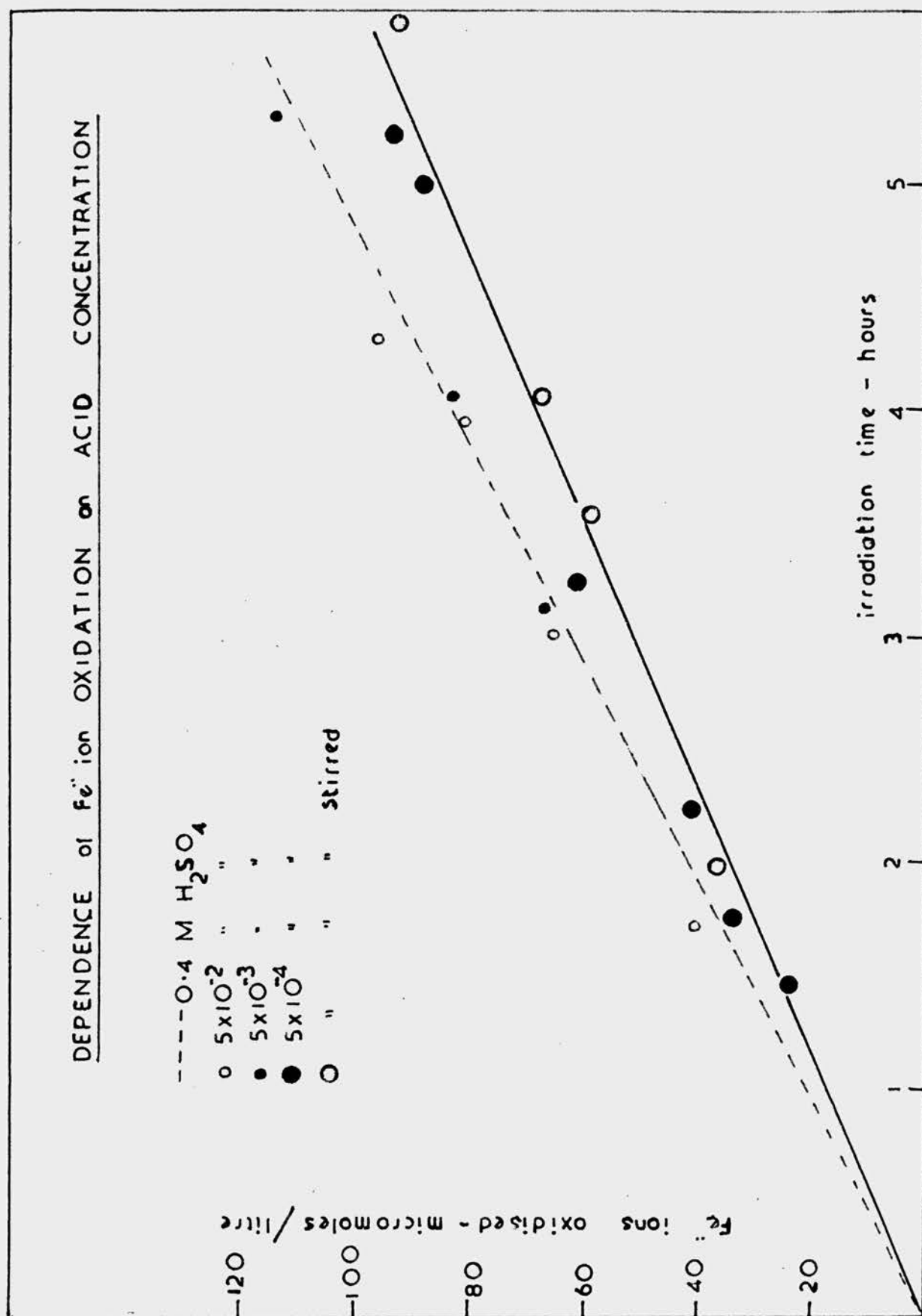


(Figure 34, Curve A). The value for  $G_{Fe}^{\alpha}$  was independent of the acid concentration down to  $5 \times 10^{-3}M$ ; below that, the value for  $G_{Fe}^{\alpha}$  appeared to decrease as the concentration of the acid was decreased. The value for  $G_{Fe}^{\alpha}$  appeared to be independent of stirring, at all acid concentrations.

The irradiations made in a carbon dioxide swept cell were repeated in an air-filled cell, with a mica disc floating on the surface of the solution. Similar results were obtained.

Spicer<sup>74</sup> showed that an aqueous solution of ferric chloride could be completely reduced due to the effects produced by the  $\alpha$ -particles from a 55 mc radon source. Experiments were made to determine whether any reduction occurred in the ferrous sulphate solutions irradiated with polonium  $\alpha$ -particles from an external source.

Solutions of approximately  $10^{-3}M$  ferric ammonium sulphate in 0.8N sulphuric acid, were irradiated for periods up to sixty hours. The ferrous ion content of the solution was determined before and after every irradiation with o-phenanthroline. No reduction of the ferric ion was observed. The irradiations were repeated in  $10^{-3}M$  sulphuric acid. Again, no reduction was observed.

FIGURE 34.

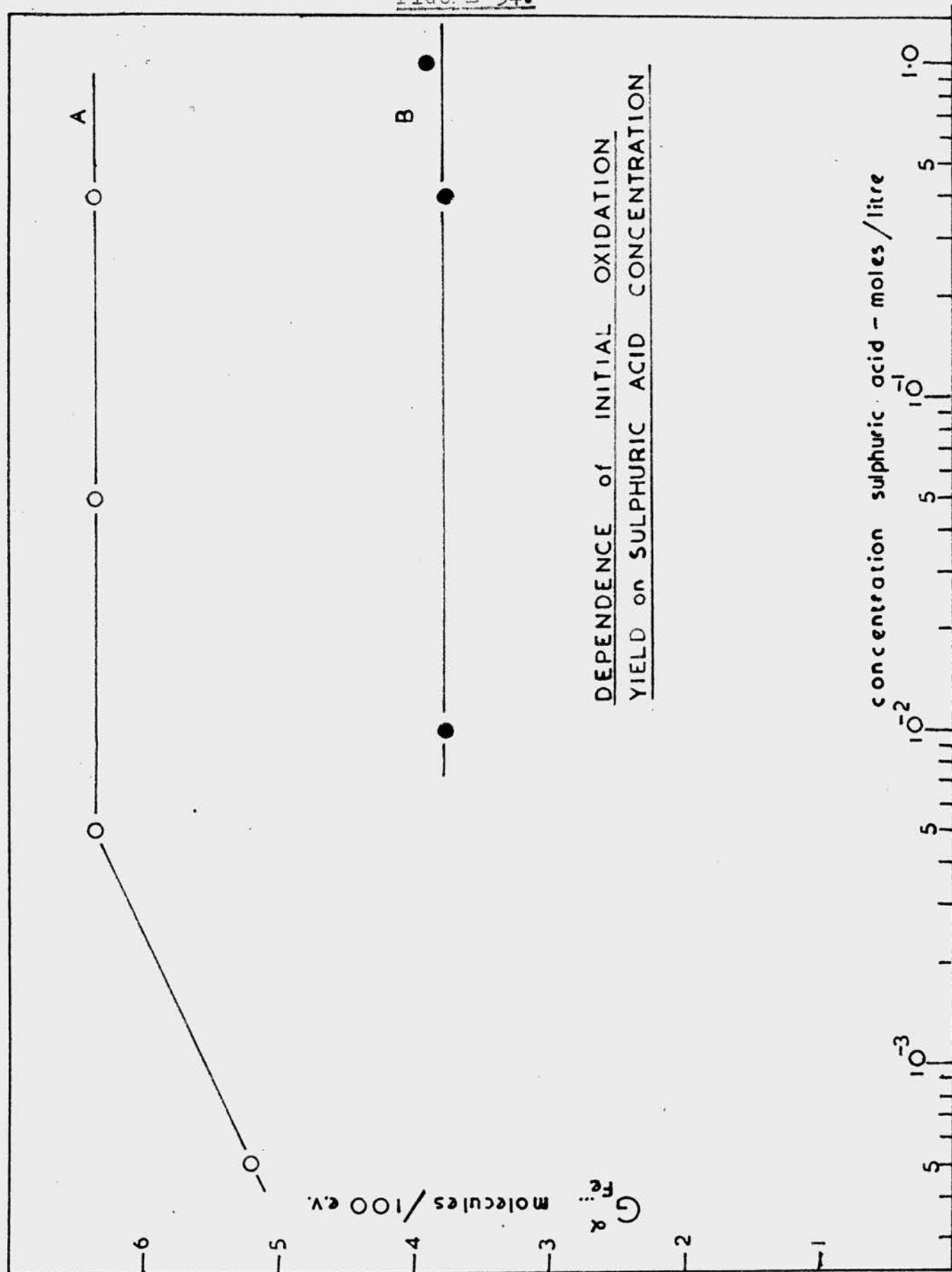
$\alpha$   
 $G_{Fe}$  expressed as a Function of Sulphuric  
Acid Concentration.

Solution of  $\sim 10^{-3}M$  ferrous sulphate.

Curve A. Aerated Solution irradiated with  
an external source.

Curve B. Airfree solution irradiated with  
internal source.

FIGURE 34.



Dewhurst<sup>75</sup> found that no reduction of ferric ion could be detected in an  $\gamma$ -irradiated ferric ammonium sulphate solution, unless the solution was analysed immediately after the irradiation. When a ferrous sulphate solution in  $10^{-3}N$  acid was irradiated with  $\gamma$ -rays, Dewhurst<sup>38</sup> found that the addition of ferric ion lowered the ferrous ion oxidation yield.

To determine whether a back-reaction of this type took place in an  $\alpha$ -irradiated solution, the following experiment was made. A solution of approximately  $10^{-3}M$  ferrous sulphate,  $2.5 \times 10^{-4}M$  in ferric ammonium sulphate, and  $5 \times 10^{-4}M$  in sulphuric acid, was irradiated with the external source. No significant decrease in the ferrous ion oxidation yield, was observed.

(b) In airfree solution.

Irradiations were made on aerated and airfree solutions of approximately  $10^{-3}M$  ferrous sulphate in sulphuric acid of concentrations varying from  $0.01M$  to  $1M$ , using an internal source. As the polonium was supplied in a  $0.8N$  sulphuric acid solution, it was not possible, under the experimental conditions used, to irradiate with an internal

source, solutions of acid concentrations less than 0.01M. The values for  $G_{Fe}^{\alpha \cdots}$  obtained in airfree solutions at varying acid concentration, are given in Table 19. The value for  $G_{Fe}^{\alpha \cdots}$ , in airfree solution, was expressed as a function of the sulphuric acid concentration (Figure 34, Curve B).

Over the range studied, the value for  $G_{Fe}^{\alpha \cdots}$ , in airfree solution, appeared to be independent of the acid concentration.

The results obtained for the  $\alpha$ -induced oxidation of ferrous sulphate, in aerated and airfree solution, with varying acid concentration, cannot be explained on the basis of the reactions taking place in an X- or  $\gamma$ -irradiated solution. The value for  $G_{Fe}^{X \gamma}$  was found to decrease as the acid concentration was decreased below  $10^{-1}M$ , for an airfree solution and  $5 \times 10^{-2}M$ , for an aerated solution. 38

For the reasons stated previously, it was not possible to study the effects produced by  $\alpha$ -rays on ferrous sulphate solutions of acid concentration less than 0.01M. Only one point was obtained for aerated solutions irradiated at low acid concentration. On the basis of these studies, it is not possible to state definitely the effect of the acid concentration on the  $\alpha$ -induced oxidation of ferrous sulphate. The results did indicate, however, that

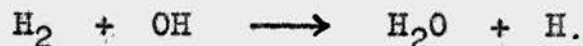


the value for  $G_{Fe}^{\alpha}$  was independent of the acid concentration in a region where the value for  $G_{Fe}^{\gamma}$  was acid-dependent. It would appear, therefore, that the reactions proposed<sup>29</sup> to account for the acid-dependence of the  $\gamma$ -induced oxidation of ferrous sulphate, do not apply to solutions irradiated with  $\alpha$ -rays. Since the  $\alpha$ -induced oxidation of the ferrous ion takes place along the tracks of the  $\alpha$ -particles, it is probably the acid concentration in the track, and not in the bulk of the solution, which is the determining factor. It has been stated<sup>72</sup> that the concentration of hydrogen at the instant immediately after the passage of the  $\alpha$ -particle ions in an  $\alpha$ -particle track may be about  $1N$ , and it is of interest that although the production of hydrogen peroxide in water irradiated with X-rays is dependent on pH, the production of hydrogen peroxide in  $\alpha$ -irradiated water is independent of the acid concentration.<sup>78(b)</sup>

- (iv) The effect of  $\alpha$ -rays on ferrous sulphate solutions saturated with hydrogen and with carbon dioxide.

According to the "molecular decomposition" theory of Allen<sup>5</sup>, when  $\alpha$ -particles pass through aqueous solutions hydrogen is formed. If this is the case, low ferrous ion oxidation yields may be

observed, due to the reaction of the hydrogen with the hydroxyl radicals



It has been shown<sup>29</sup> that the ferrous ion oxidation yield in a  $\gamma$ -irradiated airfree ferrous ion solution is lowered when the solution is saturated with hydrogen. Experiments were made to determine whether any reaction occurred between hydrogen and the hydroxyl radicals produced in an  $\alpha$ -irradiated solution of ferrous sulphate. Control experiments were made in which solutions saturated with carbon dioxide were irradiated. It was shown previously (III, 3(5)) that external sources were impractical for the irradiation of gas-saturated solutions. The irradiations were made, therefore, using internal sources. A vessel was constructed which was similar to that shown in Figure 4, except that a tube was sealed into the bulb so that gases could be passed continuously through the solution.

Solutions of approximately  $10^{-3}\text{M}$  ferrous sulphate in 0.8N sulphuric acid containing 0.1 mc/ml of polonium, were used. The course of the oxidation was followed first in aerated solution, then as the gas was bubbled continuously through the solution, and finally in re-aerated solution. A suitable

TABLE 20.

The effect of dissolved gases on the  $\alpha$ -induced ferrous ion oxidation yield.

Gas used	Ferrous ion oxidation yield $\mu\text{M}/\text{hour}$		Ratio of yield in aerated yield in gas saturated solution
	Aerated solution	Gas saturated solution	
Commercial carbon dioxide	4.44	2.90	1.53
"	4.99	3.16	1.58
Commercial hydrogen	5.69	3.55	1.60
"	5.59	3.31	1.69
Purified hydrogen	5.60	3.45	1.63
"	4.71	2.68	1.76
"	5.71	2.65	2.16
"	5.05	2.28	2.21

correction was applied for the decrease in the volume of the solution due to evaporation. The gases used were commercial quality carbon dioxide and hydrogen. The ferrous ion oxidation yields in the re-aerated solutions were the same as in the aerated solutions. This indicated that no impurity had been introduced as a result of the gas passed through the solution. Irradiations were also made on solutions saturated with hydrogen which had been passed over heated platinised asbestos. The results of these experiments are given in Table 20.

The effect produced by saturating the solution with hydrogen or carbon dioxide appeared to be chiefly one of de-aeration. From the results obtained with purified hydrogen, it is difficult to say whether any reaction occurred between the hydroxyl radicals and the hydrogen. To determine accurately, the effect of the hydrogen, it is essential to de-aerate the solution and to study the oxidation of the ferrous ions with a stream of specially purified hydrogen bubbling through the solution. This has not yet been successfully accomplished. It would appear, however, that if any reaction does occur between hydrogen and hydroxyl radicals in an  $\alpha$ -irradiated solution, it is small.

(3) Discussion.

The most significant point arising from the present work is that the chemical effects produced in aqueous solutions by  $\alpha$ -rays occur as a result of the formation of free radicals and not as a result of the "molecular decomposition" of water. The formation of free hydrogen atoms and free hydroxyl radicals in an  $\alpha$ -irradiated solution explains many of the anomalies which have been observed in irradiated water and aqueous solutions.

In addition to the free radicals produced in an irradiated solution, it has been postulated<sup>5</sup> that "molecular decomposition" occurs and that the yield of hydrogen evolved is independent of the solute. Although hydrogen is evolved from an air-free solution of ferrous sulphate irradiated with  $\alpha$ -rays, there is considerable evidence that <sup>in any appreciable quantity</sup> hydrogen is not evolved from an aerated solution. When aerated ferrous sulphate solutions are irradiated with X- or  $\gamma$ -rays, the oxidation proceeds linearly until the dissolved oxygen has been used up in producing  $\text{HO}_2$  radicals. At this point, the ferrous ion oxidation yield decreases by a factor of two, the oxidation taking place in an effectively airfree solution.<sup>22</sup> Wright<sup>76</sup> showed that when an

aerated ferrous sulphate solution was irradiated with mixed  $\alpha$ - and  $\gamma$ -rays, in the core of a nuclear reactor, the break in the ferrous ion oxidation, due to the oxygen being used up, the same amount of ferric ion had been produced occurred when approximately  $\frac{1}{2}$  as in an irradiation where  $\gamma$ -rays alone, were used. Had any hydrogen been evolved from the solution irradiated with  $\alpha$ - and  $\gamma$ -rays, the "oxygen break" would not have occurred until the solution had been irradiated for a longer period. Additional evidence that hydrogen was not evolved from an  $\alpha$ -irradiated aerated ferrous sulphate solution, was provided by the present work. Had hydrogen been evolved, the oxidation of ferrous ions by the radical  $\text{HO}_2$  would have been low and the effect of deaerating an  $\alpha$ -irradiated solution would not have been so pronounced as that observed experimentally (Section (2)(ii)). The studies made using hydrogen saturated solutions showed that little, if any, dissolved hydrogen reacts with the hydroxyl radicals present in solution. It appeared, therefore, that the hydrogen atoms produced along the track of an  $\alpha$ -particle, react principally with the oxygen dissolved in the solution.

The fact that no hydrogen is evolved from an

aerated ferrous sulphate solution, and that the oxidation of the ferrous ions is due to free radicals, contradicts the "molecular decomposition" theory. The formation of hydrogen peroxide and hydrogen in  $\alpha$ -irradiated water can be explained by the equations (4) to (7), given previously in Section (1). These reactions also explain the evolution of oxygen from  $\alpha$ -irradiated water<sup>77</sup> and the fact that the yield of hydrogen peroxide produced in water is independent of the presence of dissolved oxygen<sup>78(a)</sup>. These effects have been observed when  $\alpha$ -sources were used which were sufficiently weak that no decomposition of hydrogen peroxide occurred. Had hydrogen peroxide been produced solely by the combination of two hydroxyl radicals, the presence of dissolved oxygen would have increased the yield, due to the reactions (6) and (7).

One of the more striking results of the quantitative study of the chemical effects produced by  $\alpha$ -particles, is the low value for  $G_{Fe}^{\alpha}$  compared with  $G_{Fe}^{\gamma}$ . The experiments described earlier in this section, showed that the chemical effects produced by  $\alpha$ -rays could be explained by the mechanisms which apply to  $\gamma$ -induced reactions.



The experiments provided convincing evidence that the chemical effects produced by  $\alpha$ -rays are due to the formation of free radicals. It has been shown<sup>47</sup> that only a small percentage of the total ionisation produced by an  $\alpha$ -particle takes place outside the  $\alpha$ -track. The reaction of the ferrous ions with the hydroxyl and  $\text{HO}_2$  radicals, and the reaction of the hydrogen atoms with oxygen, must take place along the  $\alpha$ -track. The high ion density along an  $\alpha$ -track results in a high concentration of free radicals, many of which will recombine to give water before they are able to react with the solutes, or with each other.



The extent to which recombination of radicals occurs along the track of an ionising particle depends on the energy of the particle. For  $\gamma$ -rays and hard X-rays, the ion clusters are widely spaced along the tracks of the secondary electrons, and little recombination occurs; the value for  $G_{\text{Fe}}^{\text{x},\gamma}$  is consequently high. For soft X-rays and low energy  $\beta$ -particles, more recombination takes place and the values for  $G_{\text{Fe}}^{\text{e},\text{x}}$  are lower (Table I). For densely ionising radiation, such as  $\alpha$ -particles, a



large amount of recombination takes place and the value for  $G_{Fe}^{\alpha}$  is consequently only one third of that for  $G_{Fe}^{\gamma}$ .

According to the "radical segregation" theory of Lea<sup>49</sup>, high ion density along the track of an ionising particle would favour the formation of hydrogen peroxide by the combination of two hydroxyl radicals. Since ferrous ions are oxidised equally well by hydrogen peroxide and two hydroxyl radicals, the value for  $G_{Fe}^{\alpha}$  should, on this theory, be higher than that obtained by experiment.

It is clear, therefore that the "radical segregation" and the "molecular decomposition" theories do not explain adequately the observed results, and the molecular products in irradiated water are not produced by the combination of like radicals, but by a more complicated free radical mechanism.

#### IV. THE CHEMICAL EFFECTS OF $\gamma$ -RAYS ON AQUEOUS SOLUTIONS.

##### 1. The Benzene System.

###### (1) Introduction.

In a series of publications,<sup>21</sup> the benzene system has been proposed as a chemical dosimeter for X- and  $\gamma$ -rays and  $\beta$ -particles. A saturated solution of benzene in pure, aerated water, or a 0.5% aqueous solution of benzoic acid, or sodium benzoate was irradiated, and the resulting phenolic products were estimated. The chemical change produced in the irradiated solution was found to be linear with dose and only small changes of yield were observed when the initial concentration of the reactant or the pH of the solution was varied. These factors, together with the ease of preparation and stability of the solutions, supported the use of the benzene system as a chemical dosimeter.

In the original publication, the phenolic substances produced in the irradiated solution were estimated colorimetrically using the Folin-Ciocalteu reagent. Carr<sup>80</sup> suggested that the phenol produced in irradiated aqueous benzene solution could be estimated spectrophotometrically at a wave-length of

270 m $\mu$ .

The object of the work described in this section was to investigate more fully the spectrophotometric determination of the phenols produced in the irradiated benzene system, and to compare the utility of the benzene and ferrous systems as chemical dosimeters.

## (2) Spectrophotometric Studies.

### (a) Benzene-Phenol solutions.

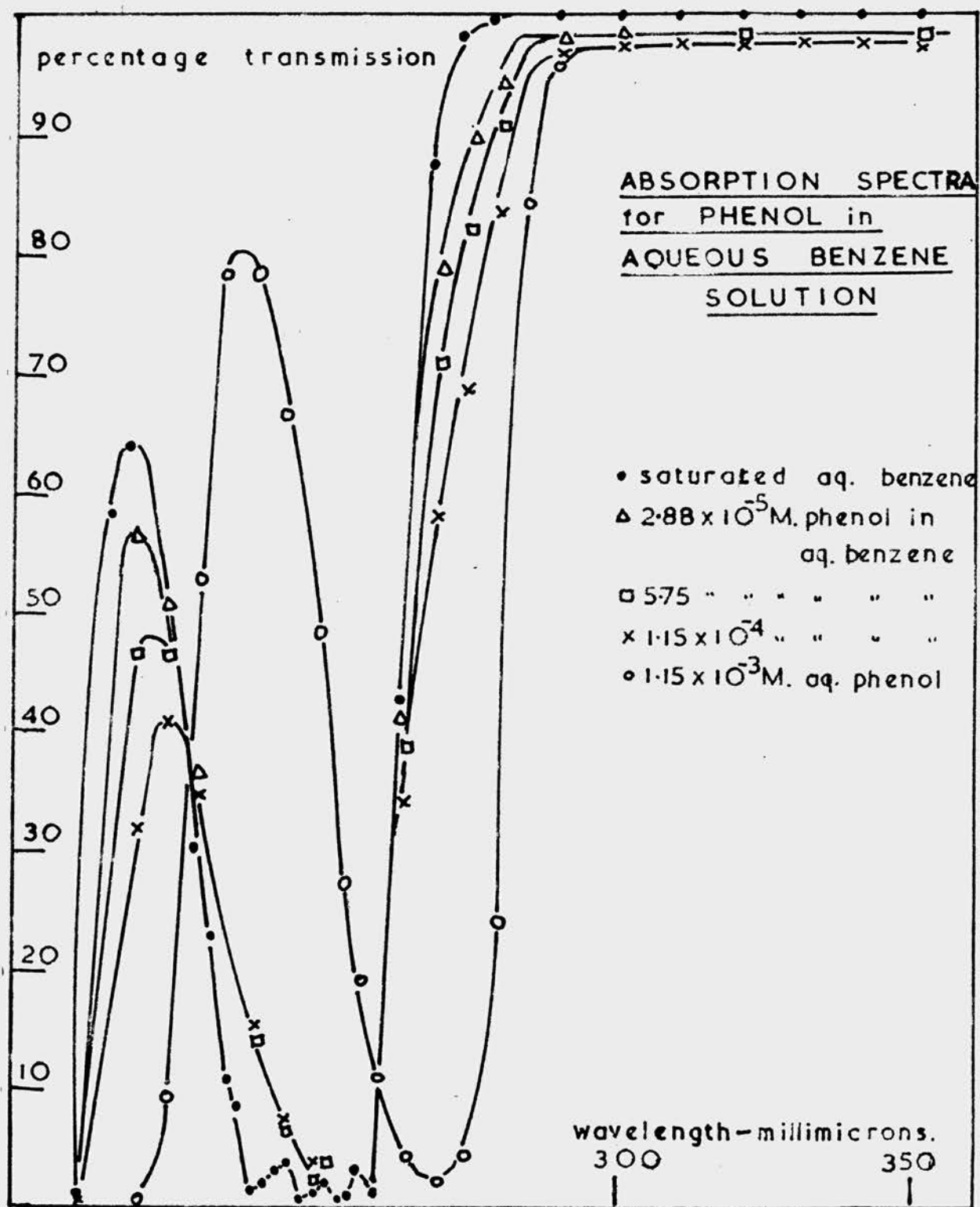
A saturated solution of benzene was prepared by shaking A.R. benzene with specially distilled water; after an hour, the excess benzene was removed, leaving an aqueous solution of benzene.

A solution of  $1.15 \times 10^{-3}M$  phenol was prepared by dissolving a weighed amount of A.R. phenol in the requisite volume of specially distilled water. Solutions of  $1.15 \times 10^{-4}M$ ,  $5.75 \times 10^{-5}M$  and  $2.875 \times 10^{-5}M$  phenol in aqueous benzene were prepared by diluting aliquots of the  $1.15 \times 10^{-3}M$  aqueous phenol solution with the requisite volumes of saturated aqueous benzene solution. The composition of these solutions corresponded approximately to the composition of aqueous benzene solutions which had received radiation doses 40,000, 20,000 and 10,000 roentgens, respectively (calculated on a basis of  $G_{\text{Phenol}}^{\times \gamma} \approx 2.3 \text{ molecules/100 ev.}^{21(b)}$ )

Spectrophotometric measurements were made on the aqueous benzene, the aqueous phenol, and the three phenol in aqueous benzene solutions. The percentage transmission of each solution, was expressed as a function of wave-length between  $\lambda = 200 \text{ m}\mu$  and  $\lambda = 350 \text{ m}\mu$  (Figure 35). Pure water was used as the blank and 1 cm of spectrophotometric cells were used.

Carr<sup>80</sup> suggested that the phenol produced in an irradiated solution of aqueous benzene could be estimated spectrophotometrically at a wave-length of  $270 \text{ m}\mu$ , the absorption peak for phenol in aqueous solution. The curves in Figure 35 showed that at a wave-length of  $270 \text{ m}\mu$ , the absorption peak for phenol in aqueous solution was, for solutions of phenol in aqueous benzene, replaced by points of inflection on steeply sloping curves. The spectrophotometric estimation of phenol under conditions where the phenol absorption peak is completely masked by the presence of benzene, can hardly be considered an accurate method. The spectrophotometric method is, however, considerably more rapid than that in which the Folin-Ciocalteau Reagent is used. A curve, in which the concentration of phenol in each aqueous

FIGURE 35.



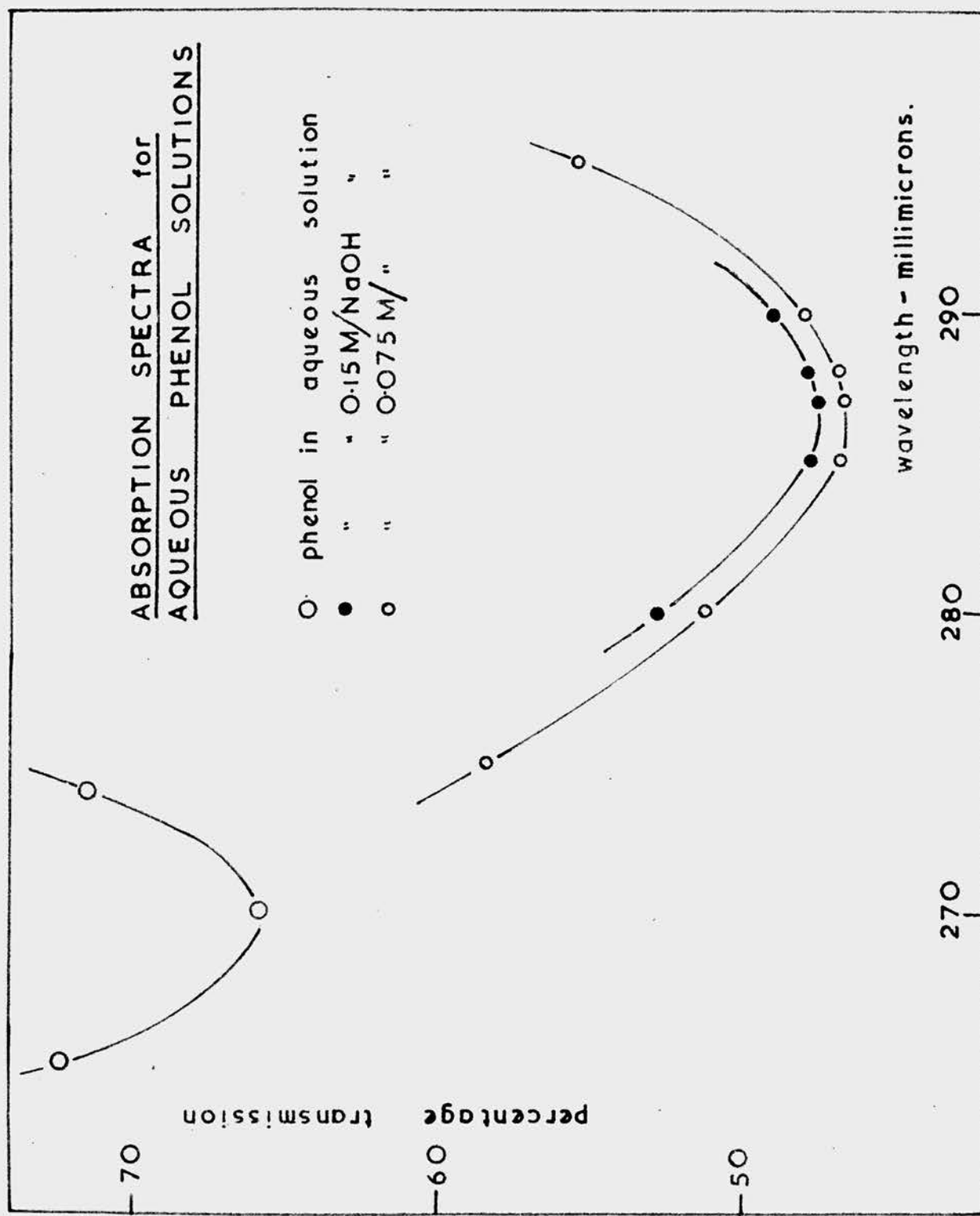
benzene solution was expressed as a function of the optical density observed at  $270\text{ m}\mu$  (obtained from Figure 35), showed approximate linearity. This indicated that the method could be used to provide a rapid, but approximate estimation of phenol in aqueous benzene.

A suggestion by Sworski<sup>81</sup> that the phenol absorption peak at  $270\text{ m}\mu$  could be changed to around  $290\text{ m}\mu$  by carrying out the estimation in a solution of sodium hydroxide, was investigated. Measurements were made on solutions of  $1.15 \times 10^{-4}\text{M}$  phenol in water and in  $0.075\text{M}$  and  $0.15\text{M}$  sodium hydroxide. The absorption spectra of the solutions are shown in Figure 36 and the values of the molar extinction coefficients are given in Table 21. The effect of sodium hydroxide was to change the wave-length of the phenol absorption from  $270\text{ m}\mu$  to  $287\text{ m}\mu$ , the absorption peak for phenate ion. At this wave-length, the interference by benzene is probably reduced. The molar extinction coefficient of the phenate ion is approximately double that of phenol.

(b) Benzoic Acid.

The irradiation of aqueous solutions of sodium benzoate has been shown to produce a mixture of the

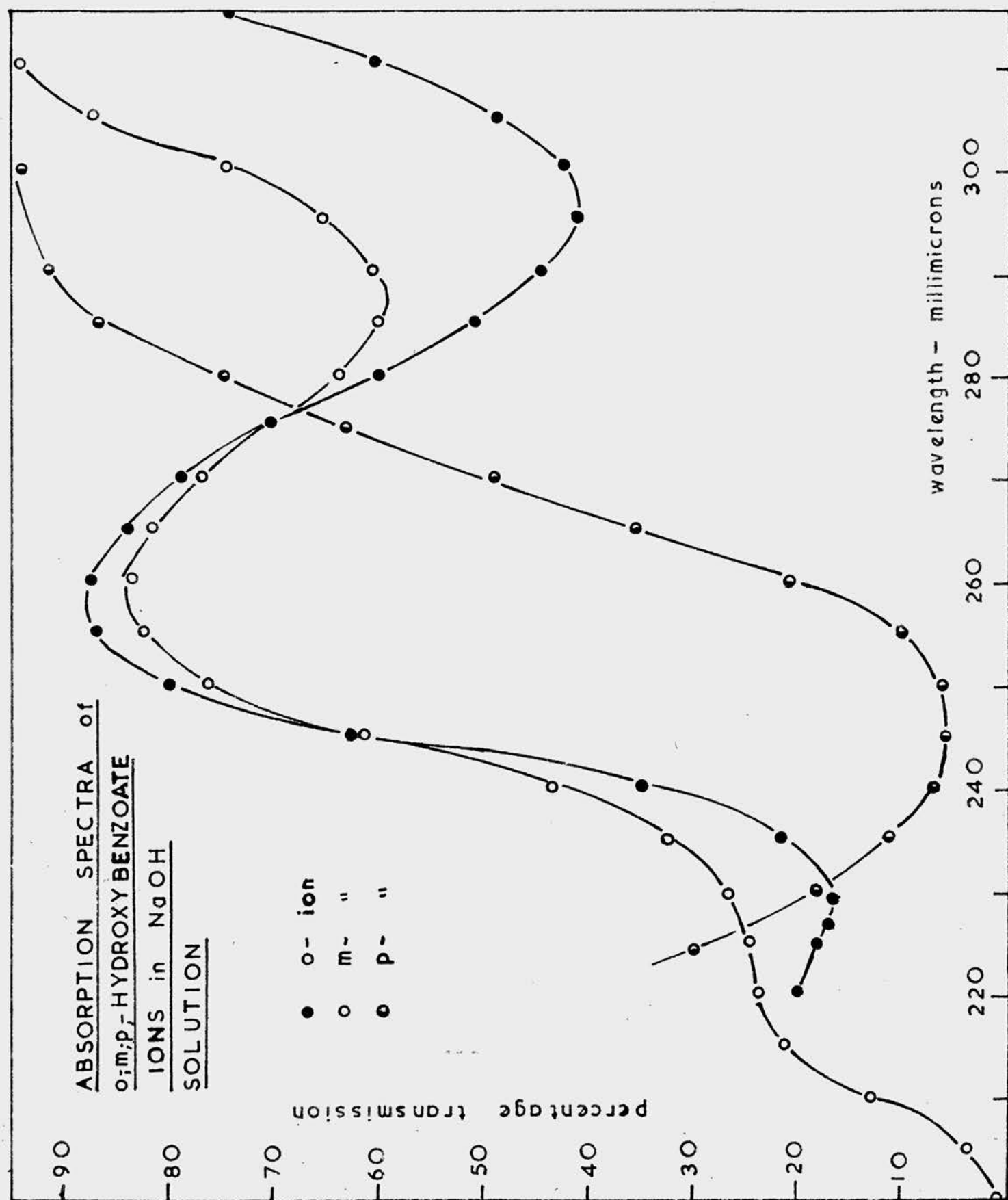
FIGURE 36.



isomeric hydroxy-benzoate ions.<sup>83</sup> The possibility of a spectrophotometric estimation of these ions, was investigated. Solutions of the three isomeric sodium hydroxybenzoates were prepared by weighing out the requisite amount of each acid into graduated flasks, neutralising with sodium hydroxide solution and diluting with distilled water. The solutions prepared were  $1.088 \times 10^{-3}M$  ortho-,  $10^{-3}M$  meta-, and  $1.035 \times 10^{-3}M$  para-hydroxybenzoates. The percentage transmission of each solution was expressed as a function of wave-length (Figure 37). Each hydroxybenzoate ion was found to absorb at a different wave-length. In the presence of sodium benzoate the absorption peaks at wave-lengths below  $260 m\mu$  would be obscured and only the minor absorption peaks of the o- and m-hydroxybenzoate ions could be used. The molar extinction coefficients are given in Table 21. Since the proportions of the isomeric hydroxybenzoates in an irradiated sodium benzoate solution are not known accurately, and their molar extinction coefficients are different, the direct spectrophotometric analysis of an irradiated solution is impracticable.



FIGURE 37.



(c) Estimation of Phenols using Folin-Ciocalteu Reagent.

The estimation of phenols using the Folin-Ciocalteu reagent depends upon the reduction of phospho-molybdtungstic acid, the resultant blue being known as "Tungsten Blue". The reagent was prepared according to the method described by Snell.<sup>82</sup> The method of analysis was as follows:- an aliquot of the phenol solution was placed in a 25 ml standard flask. 2 ml of Folin's reagent and 10 ml of hot 20% sodium carbonate solution were added. The solution was diluted to 25 ml with cold distilled water and the temperature of the resulting solution was approximately 40°C. The solution was allowed to stand for twenty minutes to allow the "Tungsten Blue" colour to develop. A variation of the method was to add 10 ml of cold 2% sodium hydroxide solution instead of the hot sodium carbonate solution. In this case, the "Tungsten Blue" colour was fully developed within two minutes. The absorption spectra of the "Tungsten Blue" developed in phenol, in sodium carbonate and in sodium hydroxide solutions are given in Figure 38. The molar extinction coefficients obtained for the Folin's reagent estimation of phenol and the three isomeric hydroxybenzoates, are given in Table 21.

FIGURE 38.

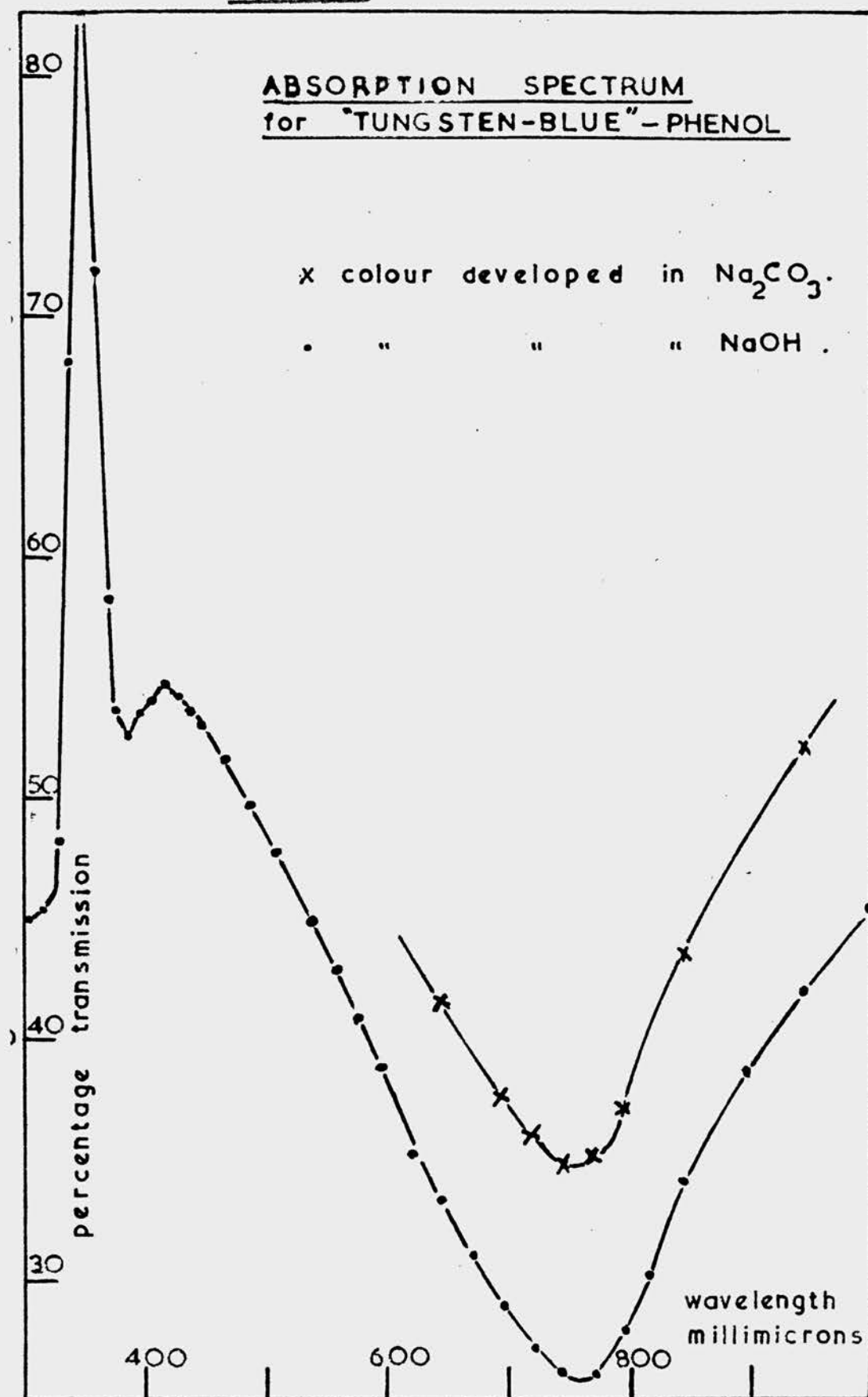


TABLE 21.

Spectrophotometric Data on the Benzene System.

System Used.	Wavelength of absorption peak $m\mu$	Molar Extinction Coefficient $E$
Phenol in aqueous solution	270	1477 1530
" " 0.075M sodium hydroxide	287	2890
" " 0.15M " "	"	2808
" " "tungsten blue" (sodium carbonate)	760	10050 9930
o-hydroxybenzoate ion	297	3480
m- " "	286	2220
o-hydroxybenzoate ion "tungsten blue" (sodium carbonate)	760	5500 5250
m- " " " " " "	"	9445 9315
p " " " " " "	"	9975 9470

It was found that certain phenolic substances such as phenol, sodium salicylate, and sodium o-hydroxybenzoate gave a greater intensity of "Tungsten Blue" colour in sodium hydroxide solution, whilst the m- and p-hydroxybenzoates gave a greater intensity of colour in sodium carbonate solution. It was found, however, that the colours developed in sodium hydroxide solution, unlike those in sodium carbonate solution, did not all have the same absorption peak. For this reason, the estimation of phenolic substances with Folin's Reagent was usually made in sodium carbonate solution, despite the slow development time of the "Tungsten Blue".

Since the extinction coefficients of the colours produced by the isomeric hydroxybenzoates were found to be different, the estimation of the chemical effects produced in an irradiated solution of sodium benzoate would be very difficult, unless the proportions of the isomeric hydroxybenzoates were known accurately. The molar extinction coefficients of the colours produced with Folin's reagent in phenol and in the isomeric hydroxybenzoates were considerably higher than those obtained in the direct spectrophotometric estimation.

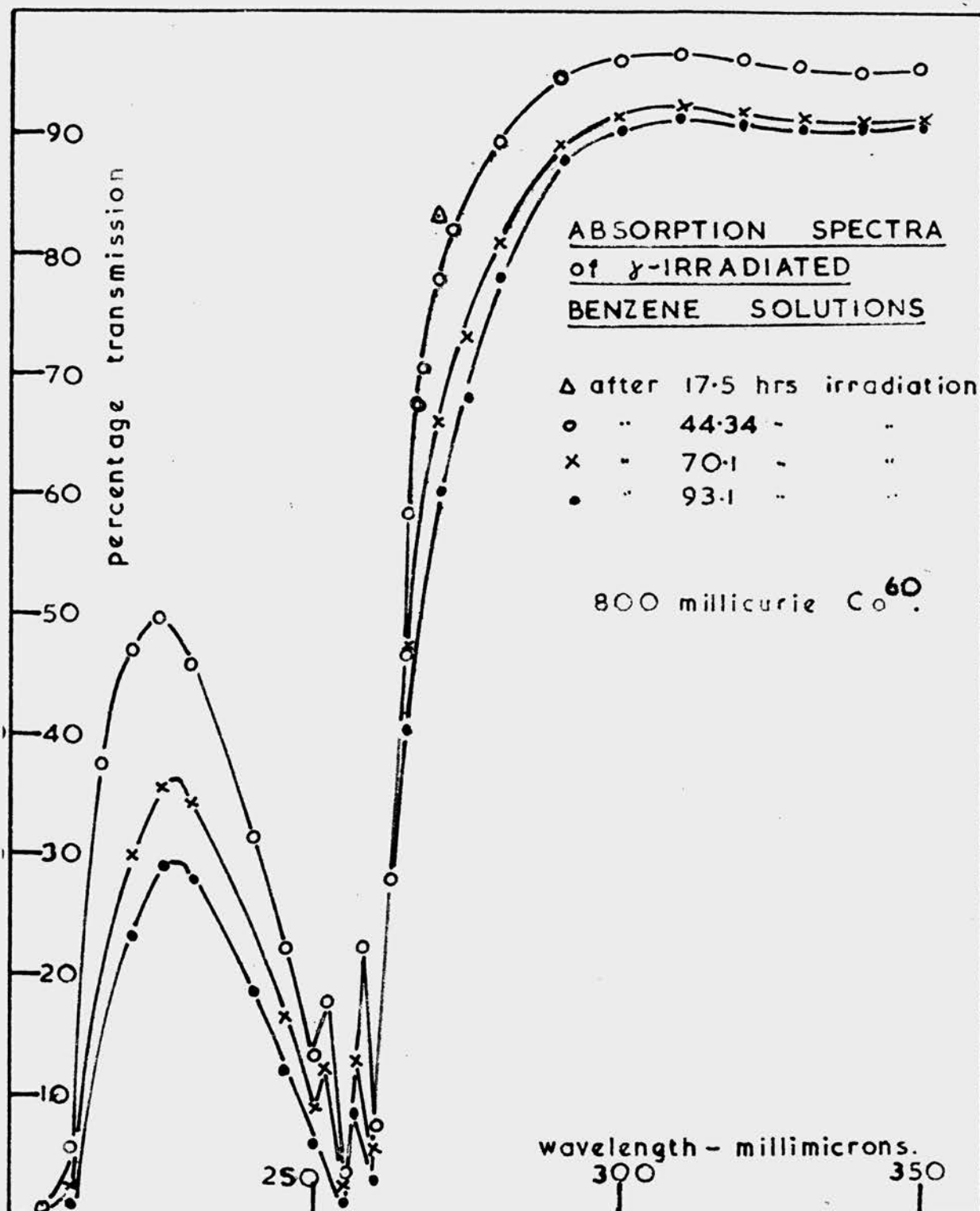
(d) The  $\gamma$ -irradiated benzene system.

5 ml portions of the saturated aqueous benzene solution were irradiated with  $\gamma$ -rays using the 800 mc cobalt source and the irradiation system described previously (Section II, 4(a)). The dose-rate was known from previous irradiations in which ferrous sulphate was used as a dosimeter. Pairs of tubes were removed from the irradiation block after periods of time which corresponded to doses of approximately 6,700, 16,800, 26,600 and 35,300 roentgens. The percentage transmission, of each solution, was expressed as a function of wave-length (Figure 39).

In contrast to the absorption spectra obtained for phenol in aqueous benzene, (Figure 35), the irradiated benzene solutions showed considerable absorption at wave-lengths  $> 300 \text{ m}\mu$ . The amount of absorption was greater in solutions which had been irradiated for longer periods. This was presumably due to the radiation-induced formation of substances other than phenol, possibly diphenyl and terphenyl, which have been isolated from the irradiation products of aqueous benzene. It is probable that the substances other than phenol which are produced in

$\gamma$ -irradiated aqueous benzene solutions, interfere with the spectrophotometric estimation of phenol both

FIGURE 39.



in the direct method and in the estimation using the Folin-Ciocalteu reagent.

(3) Conclusions.

The principal disadvantages of the benzene system, compared with the ferrous sulphate system, as a dosimeter, are as follows:-

- (a) The low value of the yield

$$\begin{aligned} G_{\text{Phenol}}^{\text{x}, \gamma} &\approx 2.3 \text{ molecules/100 ev.} \\ (G_{\text{Fe}^{++}}^{\text{x}, \gamma} &= 20 \text{ molecules/100 ev.}) \end{aligned}$$

- (b) The complex nature of the irradiation products.  
(c) The difficulty of estimating accurately the chemical changes produced in the irradiated solutions.

The only points of interest arising from the present work are as follows:-

- (a) The direct spectrophotometric determination of phenol in aqueous benzene was not found to be particularly accurate.  
(b) The spectrophotometric investigation of irradiated solutions of aqueous benzene revealed that substances other than phenol were present in the irradiation products.  
(c) The spectrophotometric study of the isomeric hydroxybenzoate ions indicated that the analysis



of the reaction products in an irradiated solution of sodium benzoate was likely to be complex.

## 2. The Nitrate-Nitrite System.

### (1) Introduction

In view of the recent interest taken in "redox" potentials<sup>4</sup>, the radiation-induced reaction



is important, being one of the few known radiation-chemical equilibria. The present investigation was undertaken with the object of determining the oxidation and reduction yields of the nitrite and nitrate ions, in a more quantitative manner than hitherto. However, on account of the low yields and the difficulty and labour of working with a system where irreproducible and anomalous results were often obtained, the investigation was abandoned, in favour of more profitable lines of research. Probably the most useful feature of this investigation has been the development of an improved spectrophotometric method for estimation of the nitrite ion.

The oxidation of the nitrite ion, with X-rays,

was first studied by Fricke and Hart<sup>7</sup>. An airfree, buffered, aqueous solution was used, and the course of the reaction was followed by determining the change in the nitrite ion concentration by an electrometric titration using potassium permanganate. The evolved gases were analysed, and hydrogen was found to be liberated in an amount equivalent to the amount of nitrite ion oxidised. The value of the oxidation yield, (recalculated on a basis of  $G_{Fe}^{X} = 20$  molecules/100 ev) for  $G_{NO_3}^{X} = 0.51$  molecules/100 ev, was independent of pH from pH 2 to pH 11. The reduction of the nitrate ion with X-rays was studied by Clarke and Pickett<sup>14</sup>. The value of the reduction yield (recalculated by Lea<sup>49</sup>) for  $G_{NO_2}^{X} \approx 0.25$  molecules/100 ev, was shown to be independent of dissolved oxygen and independent of the presence of the hydrogen peroxide which was formed in the airfree solution.

More recent studies<sup>8</sup> showed that a radiation-chemical equilibrium was set up at 60% nitrite ion oxidised and 40% nitrate ion reduced, for X-irradiations. Irradiation of a mixture of nitrate and nitrite ions in the equilibrium proportions, produced no chemical change. In airfree solutions irradiated with X-rays, hydrogen peroxide was found in the solutions of nitrate ion, and in the equilibrium

mixture, but not in the nitrite ion solution. For airfree solutions, the values quoted for the X-ray induced oxidation and reduction yields were

$G_{NO_3'} = 1.17$  molecules/100 ev. and  $G_{NO_2'} = 0.8$  molecules/100 ev., respectively.

The presence of dissolved oxygen in the irradiated solutions favoured oxidation, but the results obtained were found to be less reproducible.

## (2) The Spectrophotometric Estimation of the Nitrite Ion.

### (a) Introduction.

The estimation of the nitrite ion by a colorimetric method was first proposed by Ilosvay<sup>84</sup> and consisted of the formation of a red azo dye by the diazotisation of sulphanilic acid and coupling with

$\alpha$ -naphthylamine. The colour produced was somewhat unstable and was slow in developing. It was shown by Rider and Mellon<sup>85</sup>, that the development time was dependent on temperature. Germuth<sup>86</sup> used the dimethyl derivative of  $\alpha$ -naphthylamine and produced a dye which was allegedly more stable, and whose colour was more intense and could be fully developed in a shorter time than that produced by the original

$\alpha$ -naphthylamine. Bratton and Marshall<sup>87</sup> developed

a method for the analysis of small quantities of sulphanilamide in blood, in which N-(1-naphthyl) ethylene-diamine dihydrochloride was used as the coupling reagent. An intense and stable dye was produced. Shinn<sup>88</sup> developed a reliable analytical method using this coupling reagent and despite criticism by Kershaw and Chamberlain<sup>89</sup> that, in effect, Beer's law was not obeyed, the system was developed as a spectrophotometric method for the estimation of the nitrite ion. The absorption peak was given as 545 m $\mu$  and the molar extinction coefficient as  $4.7 \times 10^4$ .

The object of the present investigation was to confirm that the nitrite ion could be estimated accurately by Shinn's procedure and to study the effects of temperature, concentration of reagents, pH, etc., on the formation of the azo dye.

## (b) Experimental and Results

### (i) Shinn's Procedure.

The nitrite sample, in a solution of volume approximately 35 ml is placed in a 50 ml. graduated flask. 1 ml of 5N hydrochloric acid and 5 ml of 0.2% aqueous sulphanilamide are added, and the solution is allowed to stand for three minutes. 1 ml of 0.1% aqueous

N-(1-naphthyl) ethylene-diamine dihydrochloride is added and the solution is allowed to stand for 3 minutes, by which time the colour is fully developed.

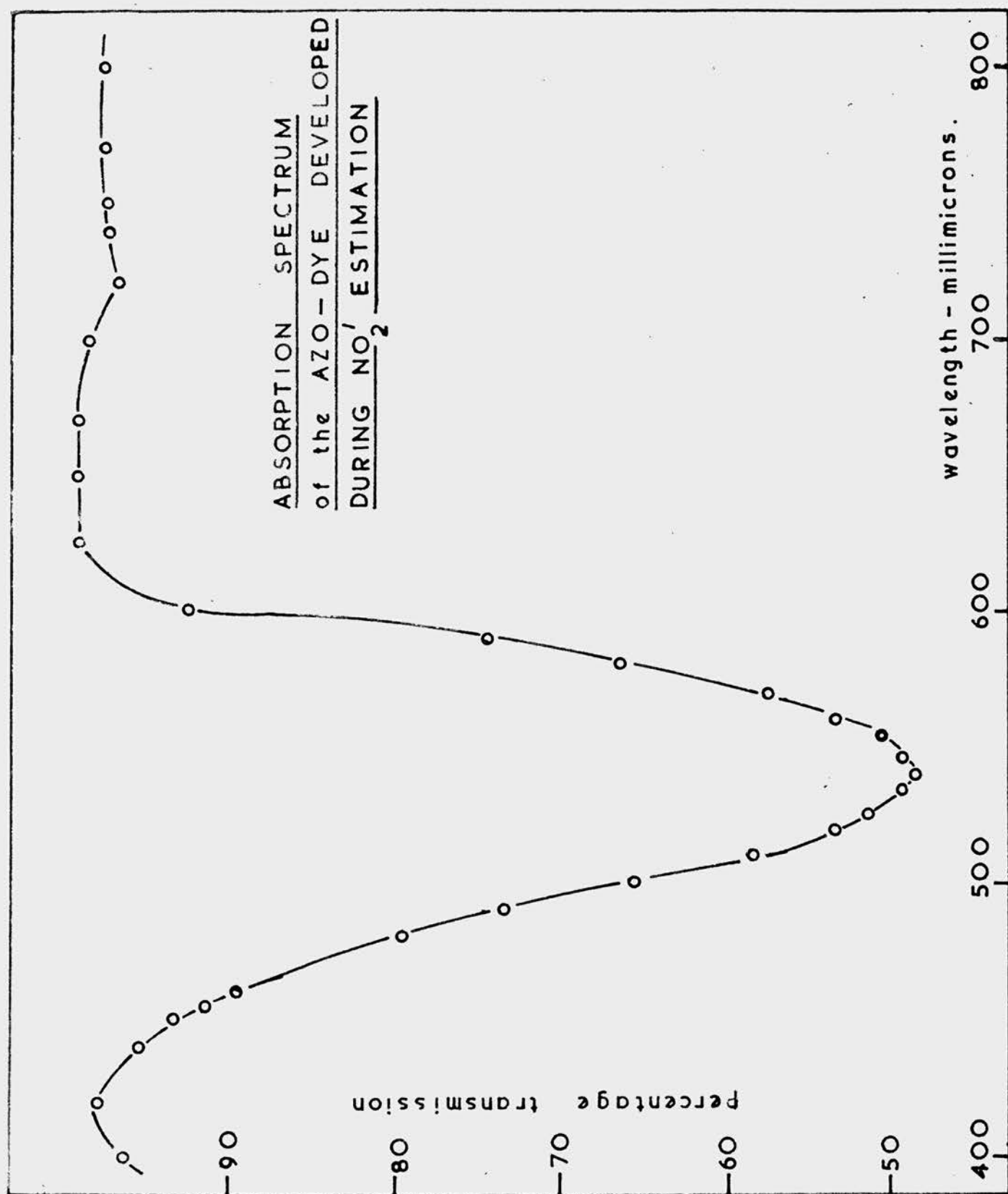
(ii) Spectrophotometric Procedure.

Shinn's procedure was modified so that spectrophotometric analysis could be made on the small volumes of dilute nitrite ion solutions used in irradiation experiments. 1 cm spectrophotometer cells were used throughout. An aliquot of the solution containing the nitrite ion, in volume less than 8 ml, was placed in a 10 ml. graduated flask. 0.2 ml of 5N HCl and 1 ml of 0.2% aqueous sulphanilamide were added. After allowing the solution to stand for 3 minutes, 0.2 ml of the coupling reagent was added and the colour was allowed to develop during a period of 3 minutes. The solution was diluted to 10 ml and was compared spectrophotometrically with distilled water containing the same amounts of added reagents.

The red azo dye was developed in an approximately  $10^{-4}M$  sodium nitrite solution. Using a 1 cm cell, the percentage transmission of the solution was expressed as a function of wave-length, between

$\lambda = 400 m\mu$  and  $\lambda = 800 m\mu$ , (Figure 40). A well defined absorption peak occurred at a wave-length of  $540 m\mu$  and all subsequent measurements were made

FIGURE 40.



at this wave-length.

(iii) Effect of Acid Concentration.

1 ml portions of an approximately  $10^{-4}M$  solution of sodium nitrite were pipetted into 10 ml graduated flasks. The effect of acid on the formation and stability of the azo dye was investigated in three ways:-

- (a) To the nitrite samples were added 1 ml portions of hydrochloric acid of varying concentration. The dye was developed and the solution was diluted to 10 ml with water, and estimated by the method described previously.
- (b) To each nitrite sample was added 1 ml of N hydrochloric acid. The dye was developed as before, and the solutions were diluted to 10 ml with hydrochloric acid of varying concentration.
- (c) To each nitrite sample was added 1 ml of 0.1N hydrochloric acid and after developing the dye, the solutions were diluted with acid of varying concentration and estimated as before.

The percentage transmission of each solution was determined at a wave-length of  $540\text{ m}\mu$ . The results obtained are given in Table 22.

TABLE 22.

The effect of acid concentration on the development and stability of the azo-dye.

Experiment	Concentration of Acid used.N	% Transmission
(a)	5	23.5
	1	23.2
	$5 \times 10^{-1}$	22.4
	$10^{-1}$	22.4
	$5 \times 10^{-2}$	28.5
	$5 \times 10^{-3}$	62.5
(b)	5	23.6
	1	23.8
	$5 \times 10^{-1}$	22.0
(c)	5	23.6
	1	23.4
	$10^{-1}$	23.8

The results of experiment (a) indicated that the intensity of the colour produced was independent of the concentration of the acid used to acidify the sodium nitrite, between 5N - 0.1N HCl. If more dilute acid was used, the intensity of the colour was



decreased.

Experiments (b) and (c) indicated that the azo dye was stable in hydrochloric acid solution.

(iv) Effect of Varying the Concentration of the Reagents.

1 ml portions of the approximately  $10^{-4}M$  sodium nitrite solution were pipetted into 10 ml graduated flasks and 1 ml of 0.5N HCl was added to each. Varying amounts of sulphanilamide and the coupling reagent (N-[1-naphthyl]ethylene-diamine dihydrochloride) were added, and the percentage transmission of each solution was determined. The results are given in Table 23.

TABLE 23.

The effect of varying the amounts of reagents added.

Volume of Sulphanilamide ml.	Volume of Coupling Reagent ml.	% Transmission.
0.1	0.02	38.3
0.5	0.1	23.4
1.0	0.2	22.4
3.0	1.0	22.3

TABLE 24.

The Effect of Temperature on Colour Development.

Temperature °C	20								
Time after addition of the coupling reagent (min.)	2	4	6	8	12	22	54		
% Transmission	22.1	21.4	21.6	21.6	21.6	21.9	21.6		
Temperature °C	53								
Time after addition of the coupling reagent (min.)	2	4	6	8	20	39			
% Transmission	22.0	21.9	21.9	21.8	21.9	21.9			

The results indicated that, within quite wide limits, the intensity of the colour produced was independent of the amounts of the reagents added.

(v) Effect of Temperature on Colour Development.

The percentage transmission of the azo dye was determined at intervals of time after the addition of the coupling reagent. The experiment was made with the solution first at a temperature of 20°C, then at 53°C. The results are given in Table 24.

The results indicated that the dye was fully developed within two minutes of adding the coupling reagent and that increase of temperature had no effect on the rate of development nor on the intensity of the colour produced.

(vi) The Effect of Dilution of a Nitrite Sample  
before Estimation.

Two 1 ml portions of an approximately  $5 \times 10^{-5}M$  solution of sodium nitrite were pipetted into 10 ml graduated flasks. One sample was diluted to 8 ml with distilled water. Reagents were added and the dye was developed in both samples. The percentage transmission of each solution was determined against a blank solution which was prepared in the same way. The results are given in Table 25.

TABLE 25.

The Effect of dilution on the intensity of the  
azo dye.

System of Analysis	% Transmission
1 ml nitrite sample/1 ml blank	50.2
8 ml " " /8 ml "	50.2
8 ml " " /1 ml "	49.8

The results showed that if the nitrite sample was estimated against the colour produced in a blank solution of the same volume, there was no change in the percentage transmission observed. The results also indicated that the water used to dilute the sodium nitrite sample contained a little nitrite ion.

Kershaw and Chamberlain<sup>89</sup> showed that when a sample of nitrite was diluted, a more intense colour was produced. This was probably due to the presence of nitrite ion in the water used for diluting the solution.

(vii) Effect of Varying the Temperature of the  
Diazotisation.

1 ml samples of approximately  $5 \times 10^{-5}$  M sodium nitrite solution were pipetted into 10 ml graduated flasks. 0.2 ml portions of 5N HCl and 1 ml portions of sulphanilamide were added to each. The diazotisation was allowed to take place for three minutes, first at a temperature of  $20^{\circ}\text{C}$ , then at  $50^{\circ}\text{C}$ . The coupling reagent was added and the percentage transmission of each solution was measured. The percentage transmission of both solutions was found to be the same.

Holbourn and Pattle<sup>90</sup> suggested that the diazotisation process was incomplete at  $20^{\circ}\text{C}$  unless a period of twenty minutes was allowed. It was found necessary to raise the diazotisation temperature to  $30^{\circ}\text{C}$  in order to produce the maximum intensity of colour, within the three minutes allowed for the diazotisation time. The present work showed that in the small volumes of solution used for the spectrophotometric estimation of the nitrite ion, varying the diazotisation temperature had no effect on the intensity of the colour produced.

(viii) The Effect of the Nitrate Ion.

Since small amounts of nitrite ion were to be detected in irradiated solutions of sodium nitrate,

it was important to determine whether the presence of the nitrate ion had any effect on the nitrite ion estimation.

Two 1 ml portions of approximately  $5 \times 10^{-5}M$  sodium nitrite were pipetted into 10 ml graduated flasks. To one, was added 1 ml of  $10^{-2}M$  sodium nitrate solution; to the other, 1 ml of water. The colours were developed and compared. It was found that the percentage transmission of both solutions was exactly the same. This indicated that the presence of the nitrate ion had no effect on the estimation of the nitrite ion.

(ix) Determination of the Molar Extinction Coefficient of the Nitrite Ion-Azo Dye.

All the volumetric apparatus used in this experiment had been calibrated previously. Three stock solutions, of concentration approximately  $10^{-1}M$ , were prepared from dry, A.R. sodium nitrite. The solutions were standardised<sup>91</sup> by adding an excess of standard potassium permanganate solution to a known volume of the sodium nitrite solution. The excess permanganate was determined using sodium oxalate.

From the three stock solutions of sodium nitrite, solutions of concentrations ranging from

$6.07 \times 10^{-6} \text{M}$  to  $1.785 \times 10^{-4} \text{M}$  were prepared, by suitable dilutions. The optical density of the colour produced in a 1 ml portion of each solution in a 10 ml flask was determined spectrophotometrically using a 1 cm cell. Optical density was expressed as a function of the nitrite ion concentration (Figure 41). The straight line obtained showed that Beer's Law was obeyed. The value of the molar extinction coefficient of the sodium nitrite-azo dye, obtained from the slope of the curve, was  $E = 51,200$ ;

(x) Conclusions.

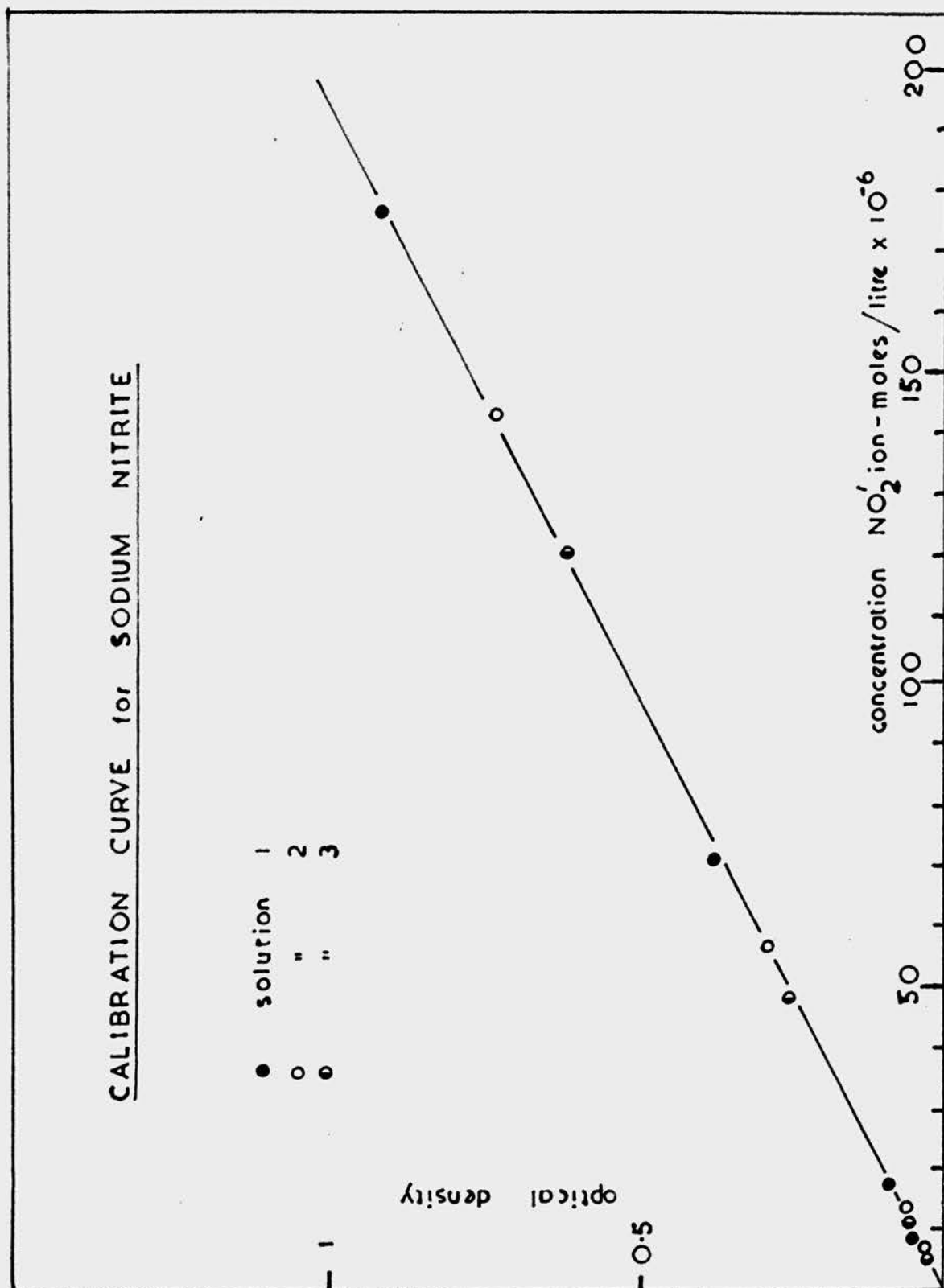
The spectrophotometric analysis of the nitrite ion, by the method described in the previous section, was rapid, and accurate to approximately 1%. The method was not found to be influenced by variations in pH, temperature, concentration of reagents nor by the presence of the nitrate ion.

(3) Studies in  $\gamma$ -irradiated solutions.

(a) Reduction of the nitrate ion in aerated solution.

The 800 mc. cobalt source and the irradiation system described in section II (4)(a) were used. Tubes containing 5 ml portions of aerated solutions, prepared from A.R. sodium nitrate and specially distilled water, were irradiated. Pairs of tubes were

FIGURE 41.

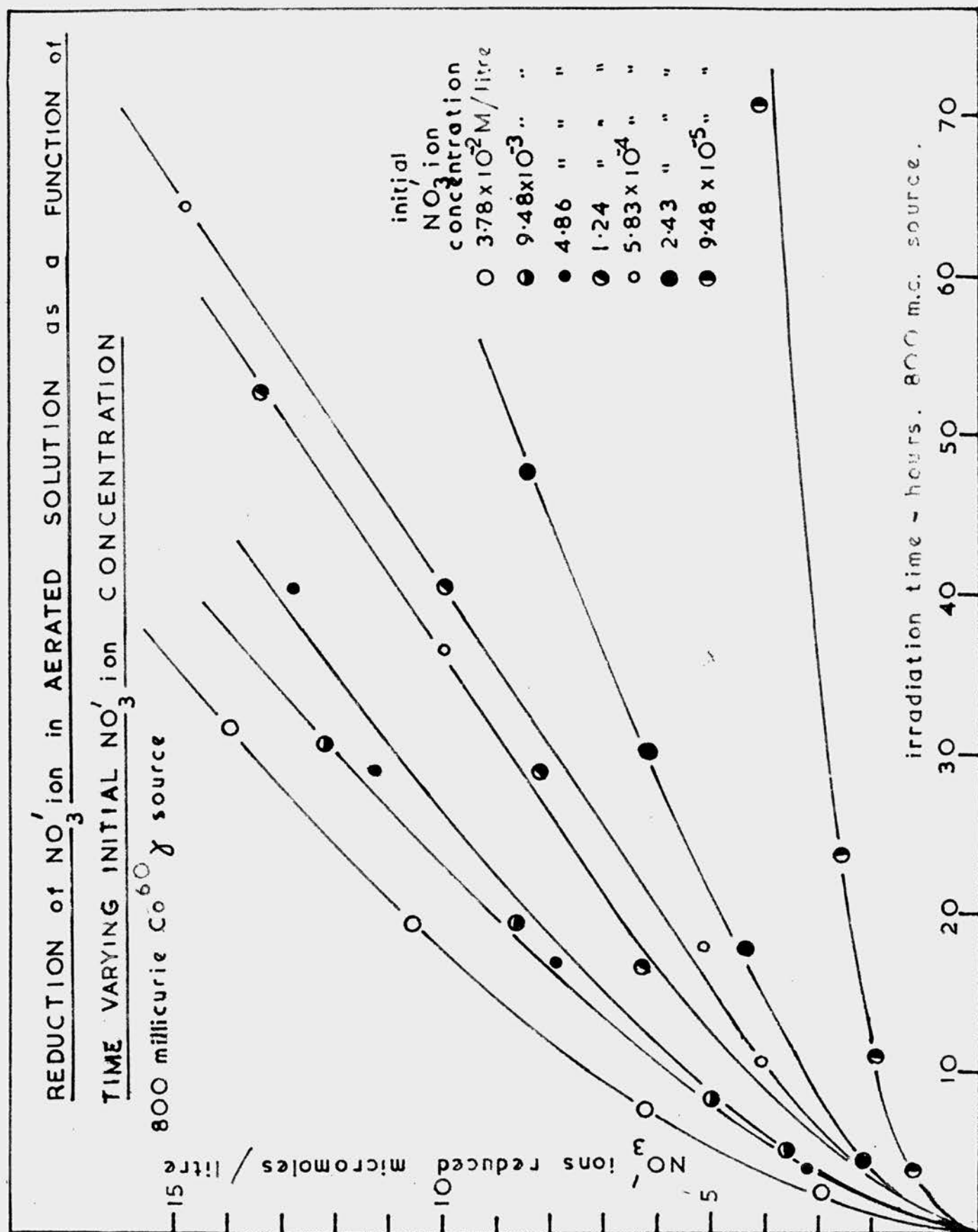




removed at intervals and the amounts of nitrite ion produced, were estimated spectrophotometrically. The amount of nitrite ion produced was expressed as a function of irradiation time. The curves obtained for solutions whose initial nitrate ion concentrations varied from  $3.8 \times 10^{-2} \text{M}$  to  $9.5 \times 10^{-5} \text{M}$ , are given in Figure 42. The rate at which the nitrate ion was reduced, decreased after a short irradiation time. This indicated the presence of a back reaction. The initial slopes of the nitrate ion reduction/irradiation time curves gave the initial nitrate ion reduction yields. Since the dose received (approximately 370r/hour) by the solutions was known from previous irradiations of ferrous sulphate solutions (using a value for  $G_{\text{Fe}^{2+}}^{\gamma} = 20 \text{ molecules/100 e.v.}$ ) it was possible to calculate the values for  $G_{\text{NO}_2}^{\gamma}$ . The value for  $G_{\text{NO}_2}^{\gamma}$ , the initial nitrate ion reduction yield obtained at each concentration, was expressed as a function of the initial nitrate ion concentration, (Figure 44). The value for  $G_{\text{NO}_2}^{\gamma}$  appeared to increase linearly, as the initial concentration of the irradiated nitrate ion solution was increased.

Since the initial yield for nitrate ion reduction  $G_{\text{NO}_2}^{\gamma}$ , is entirely dependent on the initial

FIGURE 42.



concentration of the nitrate ion in the solution irradiated, any value quoted for  $G_{NO_2}^{\gamma}$  is meaningless unless the concentration of the nitrate ion is also stipulated.

(b) Reduction of the nitrate ion in Airfree Solution.

Solutions of sodium nitrate were deaerated by the method described previously (Section II, 5(b)). 5 ml portions of the solutions were irradiated and analysed, as in the aerated solution experiments. The nitrate ion reduction/irradiation time curves obtained on irradiation of airfree solutions of varying initial nitrate ion concentration, are given in Figure 43. The value for  $G_{NO_2}^{\gamma}$ , calculated from the initial slope of the curve obtained at each nitrate ion concentration, was expressed as a function of the initial nitrate ion concentration (Figure 44).

As in the aerated solution, the value for  $G_{NO_2}^{\gamma}$  in the airfree solution was dependent on the initial concentration of the nitrate ion. At any given concentration, the value for  $G_{NO_2}^{\gamma}$  appeared to be lower in the airfree solution than in the aerated solution.

FIGURE 43.

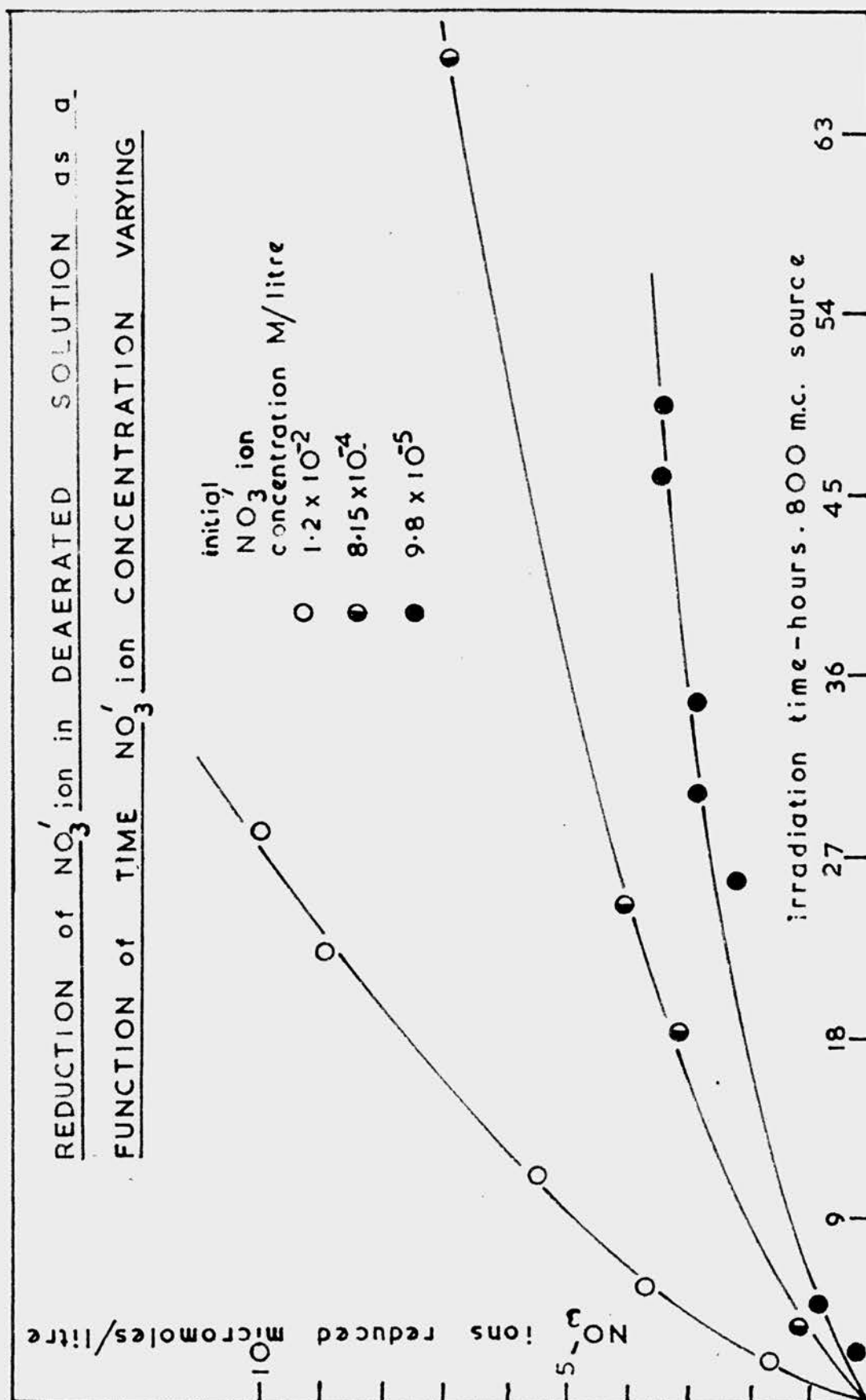
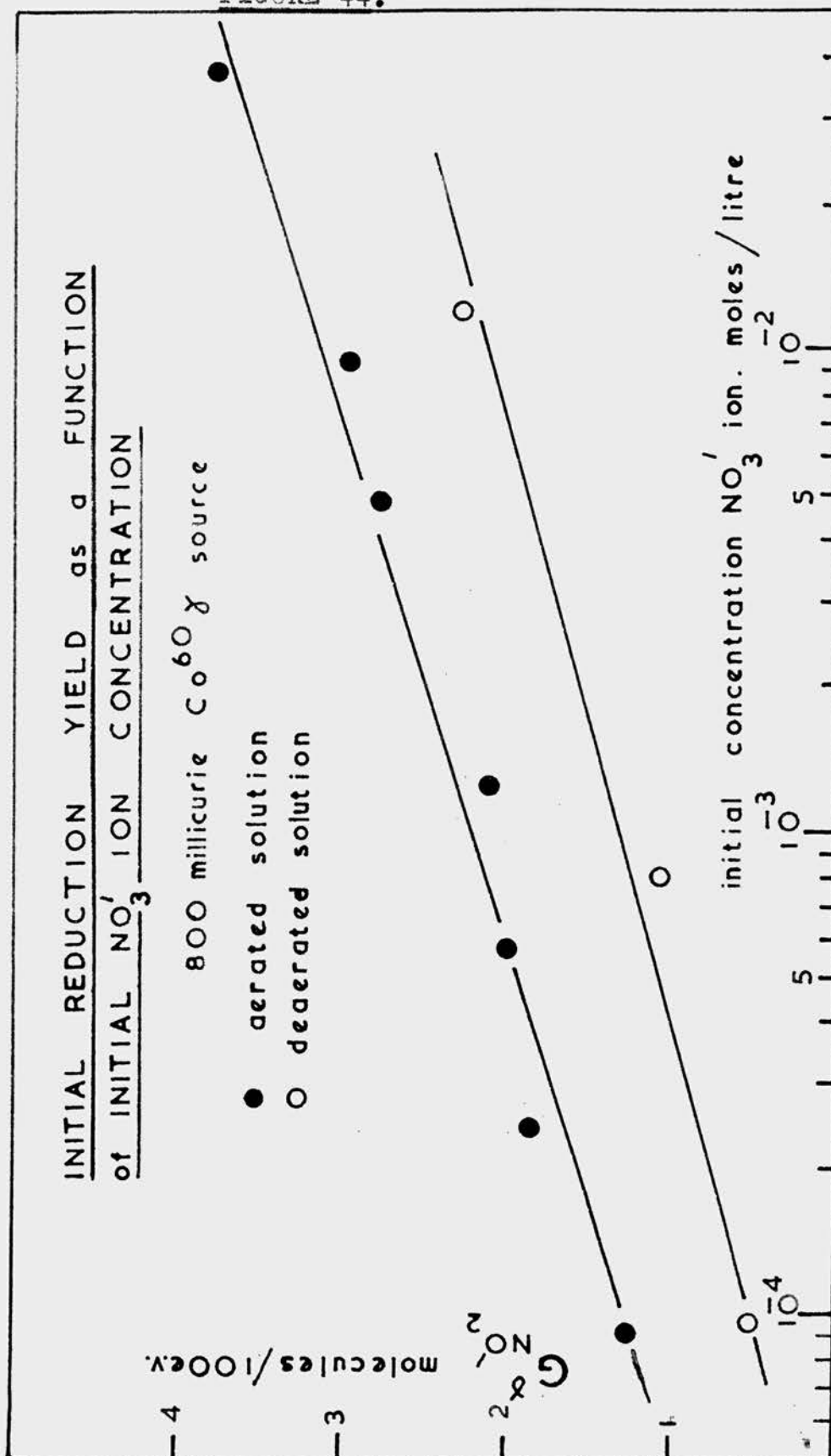


FIGURE 44.



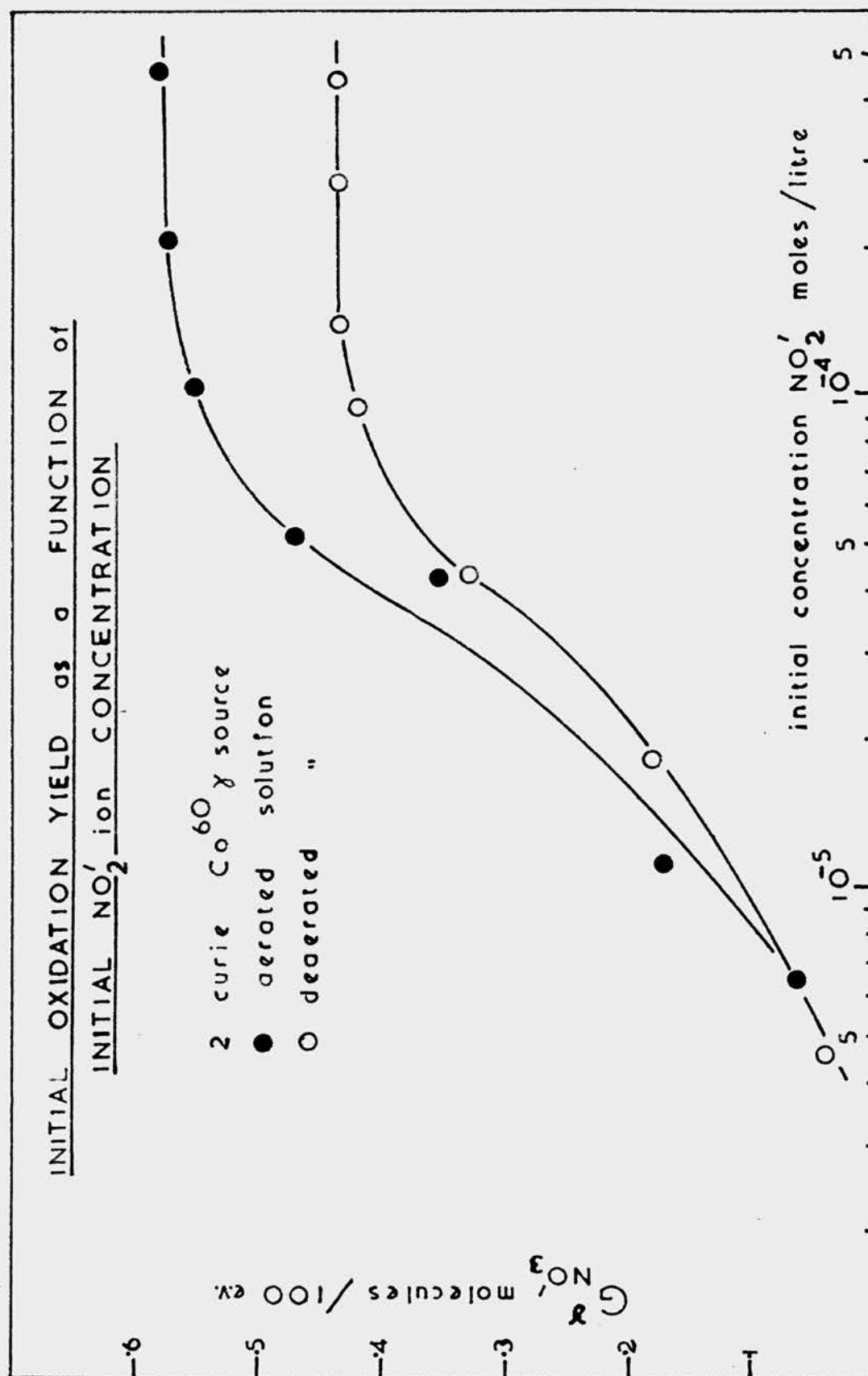
(c) Oxidation of the nitrite ion in aerated and airfree solution.

The procedure for irradiation and analysis of aerated and airfree solutions of sodium nitrite was the same as that described for sodium nitrate. Owing to the low yield for nitrite ion oxidation, the solutions were irradiated with the 2 curie cobalt source (dose rate, approximately 1860r/hour).

The nitrite ion oxidation/irradiation time curves obtained at varying nitrite ion concentration were approximately linear, even to more than 80% oxidation, in some cases. From the slopes of the lines, the values of the initial nitrite ion oxidation yields were calculated. The value for  $G_{NO_2}^8$  was expressed as a function of the initial nitrite ion concentration. The curves obtained for aerated and airfree solutions are given in Figure 45.

In confirmation of the experiments of Fricke and Hart<sup>7</sup> the value for the nitrite ion oxidation yield was found to be independent of the initial concentration of the nitrite ion in the irradiated solution, above approximately  $10^{-4}M$ . The values for the oxidation yields in aerated and airfree solutions of sodium nitrite, the concentrations of which were greater than  $10^{-4}M$ , were calculated:-

FIGURE 45.



Aerated	$G_{NO_3}^{\gamma} = 0.58$ molecules/100 ev.
Airfree	$G_{NO_3}^{\gamma} = 0.43$ molecules/100 ev.

The errors in the determination were considerable on account of the long irradiation times required and the low values of the oxidation yields. The results obtained are, however, in fair agreement with the value for  $G_{NO_3}^X = 0.51$  molecules/100 ev. obtained by Fricke and Hart, for an airfree solution.

- (d)  $\gamma$ -irradiation of an equilibrium mixture of nitrite and nitrate ions, in aerated solution.

Lefort<sup>8</sup> irradiated an airfree solution which contained nitrite and nitrate ions in the proportions 40% nitrite ion and 60% nitrate ion. No change was observed in the concentration of the nitrite and nitrate ions, although hydrogen peroxide was detected in solution.

An aerated solution,  $4.073 \times 10^{-4}M$  in sodium nitrate and  $2.72 \times 10^{-4}M$  in sodium nitrite (60%  $NO_3^-$  : 40%  $NO_2^-$ ) was irradiated using the two curie source. No change in the composition of the solution was observed, even after irradiations of 60 hours duration.

This experiment confirmed Lefort's value for the composition of the equilibrium mixture.



(e) Discussion of the results.

In view of the small amount of experimental evidence available it is difficult to put forward any mechanism for the radiation induced nitrite-nitrate equilibrium. This is especially so in the present work where some of the results are contradictory. The irradiation of a solution containing sodium nitrite and sodium nitrate confirmed Lefort's (8(b)) value for the composition of the equilibrium mixture. The irradiation of solutions of sodium nitrate showed that the nitrate ion reduction yield decreased as the irradiation proceeded, presumably because of the back reaction in which the nitrite ion was oxidised. The sources available were not sufficiently powerful to observe reduction of the nitrate ion up to the equilibrium concentration, but it is probable that equilibrium would have been reached at 40% reduction. It is difficult to explain, however, the anomalous behaviour of the irradiated nitrite ion solutions where the nitrite ion oxidation/irradiation time curves obtained were all linear and oxidations to more than 80% were recorded. The nitrite ion oxidation yield was found to be greater in aerated than in airfree solution. The results obtained in aerated and airfree nitrate ion solutions appeared to suggest the converse.

In view of these anomalies, and the fact that many of the results obtained could not be repeated accurately, it was not considered profitable to embark on the large experimental programme required to elucidate the mechanism of the nitrite-nitrate system. This would involve studies of the gas evolution from airfree and aerated solutions, the effect of pH, and the determination of possible changes in pH as a result of irradiating unbuffered solutions.

### SUMMARY.

1. Using a new type of polonium source, a quantitative study has been made of the chemical effects produced in an aqueous solution of ferrous sulphate by  $\alpha$ -particles.
2. A region exists where the ferrous ion oxidation yield is independent of the initial concentration of ferrous ions in the irradiated solution.
3. By comparing the ferrous ion oxidation yield with the saturation current produced in an ionisation chamber under the same conditions, an absolute value for the yield has been obtained.

$$G_{\text{Fe}^{2+}}^{\alpha} = 6.37 \text{ molecules/100 ev.}$$

4. A technique has been developed for producing solutions free from dissolved gases.
5. Preliminary studies of the  $\alpha$ -induced oxidation of ferrous sulphate in airfree solution, and in solutions containing ethanol, have shown that the chemical effects produced by  $\alpha$ -particles are due to the formation of free radicals along the tracks.
6. A spectrophotometric study of irradiated aqueous

benzene has shown that the products are complex, and that as an integral dosimeter for X- and  $\gamma$ -radiation, the benzene system compares unfavourably with ferrous sulphate.

7. An improved spectrophotometric method for the estimation of the nitrite ion has been developed. Studies of the effects produced by  $\gamma$ -rays in aqueous solutions of sodium nitrite and sodium nitrate have shown that a large experimental programme is required in order to elucidate the mechanism of the radiation-induced nitrite-nitrate equilibrium.

## REFERENCES

1. S.C. Lind, "Chemical Effects of Alpha Particles and Electrons." Chemical Catalog Co., Inc., 1928.
2. Dainton (a) Ann. Repts. on Progress of Chemistry (Chem. Soc. Lond.), 45, 5-33, 1948.  
(b) J. Phys. Coll. Chem., 52, 490, 1948.
3. Burton (a) Ann. Rev. Phys. Chem., 1, 113-32, 1950.  
(b) J. Phys. Coll. Chem., 51, 611, 1947.  
(c) J. of Chem. Education, 28, 404, 1951.
4. Dainton and Collinson, Ann. Rev. Phys. Chem., 2, 99-120, 1951.
5. Allen, (a) J. Phys. Coll. Chem., 52, 479, 1948.  
(b) Discussion of Faraday Soc. Leeds, April 1952, (in the press).
6. Weiss, Nature, 153, 748, 1944.
7. Fricke and Hart, J. Chem. Phys., 3, 365, 1935.
8. Haissinsky and Lefort (a) Compt. Rend., 228, 313, 1949.  
(b) J. Chim. Phys., 47, 782, 1950.
9. Fricke and Hart, J. Chem. Phys., 3, 596, 1935.
10. Clarke and Coe, J. Chem. Phys., 5, 97, 1937.
11. Hardwick, Can. J. Chem., 30, 23, 1952.
12. Fricke and Washburn (a) Phys. Rev., 40, 1033, 1932.  
Fricke and Brownscombe (b) J.A.C.S., 55, 2358, 1933.

### REFERENCES (Contd.)

13. Hopwood, Brit. J. Radiol., 13, 221, 1940.
14. Clarke and Pickett, J.A.C.S., 52, 465, 1930.
15. Dale, Meredith and Tweedie, Nature, 151, 280, 1948.
16. Fricke, Hart and Smith, J. Chem. Phys., 6, 229, 1938.
17. Collinson and Dainton. Discussion of the Faraday  
Soc., Leeds, April 1952 (in the press).
18. Hochanadel, J. Phys. Chem., 56, 587, 1952.
19. Day and Stein, Nucleonics, 8(2), 34, 1951.
20. Miller and Wilkinson, Discussion of the Faraday  
Soc. Leeds, April 1952 (in the press).
21. Stein and Weiss (a) Nature, 161, 650, 1948.  
(b) J.C.S., 681, 3245-3252, 1949.  
Day and Stein (c) Nature, 164, 672, 1949.
22. Miller, J. Chem. Phys., 18, 79, 1950.
23. Fricke and Morse (a) Amer. J. Roent. and Rad.  
Ther., 18, 426, 430, 1927.  
(b) Phys. Rev., 31, 1117, 1928.  
(c) Phil. Mag., 7, 129, 1929.
24. Fricke and Hart, J. Chem. Phys., 3, 60, 1935.
25. Nurnberger, J. Phys. Chem., 38, 47, 1934.
26. Liechti, Minder and Wegmuller, (a) Radiol. Clin.,  
14, 167, 1945.  
Minder and Liechti (b) Experientia,  
2, 410, 1946.
27. Hardwick, Can. J. Chem., 30, 17, 1952.

REFERENCES (Contd.)

28. Tod and Whitcher, A.E.C.D. - 458 (U.S. Atomic Energy Commission.)
29. Rigg, Stein and Weiss, Proc. Roy. Soc., 211A, 375, 1952.
30. Hardwick, Can. J. Chem., 30, 39, 1952.
31. Hardwick, Private communication to Dr. N. Miller, December, 1951.
32. Hart, A.E.C.U. - 1534 (U.S. Atomic Energy Commission).
33. Hardwick, Discussion of the Faraday Soc. Leeds, April 1952 (in the press).
34. Hart, J.A.C.S., 73, 1891, 1951.
35. Krenz and Dewhurst, J. Chem. Phys., 17, 1337, 1949.
36. Haber and Weiss, Proc. Roy. Soc., 147A, 332, 1930.
37. Shishacow, Phil. Mag., 14, 198, 1932.
38. Dewhurst, Trans. Farad. Soc., 1952 (in the press).
39. Weiss, Nature, 165, 728, 1950.
40. Amphlett (a) Nature, 165, 977, 1950.  
(b) Discussion of the Farad. Soc. Leeds, April 1952 (in the press).
41. Dewhurst, J. Chem. Phys., 19, 1329, 1951.
42. Brandt and Smith, Anal. Chem., 21, 313, 1949.
43. Wild, Discussion of Farad. Soc. Leeds, April 1952 (in the press).

REFERENCES (Contd.)

44. Miller, Unpublished Results.
45. Harker, Nature, 133, 378, 1934.
46. Lefort, J. Chim. Phys., 47, 624, 1950.
47. Dale, Gray and Meredith, Phil. Trans. Roy. Soc.,  
242A, 33, 1949.
48. Bonet-Maury and Lefort, Compt. Rend. 226, 173, 1948.
49. Lea, "Action of Radiations on Living Cells."  
Cambridge Univ. Press, 1946, P.26.
50. Dee and Richards, Nature, 168, 736, 1951.
51. Miller, Discussion of the Faraday Soc. Leeds,  
April 1952 (in the press).
52. Lind and Bardwell, J.A.C.S., 51, 2751, 1929.
53. Weininger and Adler, Acta Phys. Aust., 4, 81, 1950.
54. Lind and Bardwell, J.A.C.S., 47, 2696, 1925.
55. Garrison, Morrison, Hamilton, Benson and  
Calvin, (a) Science, 114, 416, 1951.  
Garrison and Rollefson (b) Discussion of the  
Faraday Soc. Leeds,  
April 1952 (in the press).
56. Gray, Proc. Camb. Phil. Soc., 40, 72, 1944.
57. Stetter, Z. Phys., 120, 639, 1943.
58. Gerbes, Ann. Phys., 23, 648, 1935.
59. Alder, Huber and Metzger, Helv. Phys. Acta,  
20, 234, 1947.



REFERENCES (Contd).

60. Schmieder, Ann. Phys., 35, 445, 1939.
61. Livingstone, MDDC 1517, 1945 (U.S. Atomic Energy Commission).
62. Valentine, Private communication, 1952.
63. McNally, Private communication, 1952.
64. Gurney (a) Proc. Roy. Soc., 107A, 332, 1925.  
(b) Proc. Roy. Soc., 107A, 340, 1925.
65. Hart, Private communication to Miller 1950.
66. Jesse, ANL 4778, 1952 (U.S. Atomic Energy Commission).
67. Weiss, Trans. Farad. Soc., 31, 668, 1935.
68. Hart, Private communication to Miller, 1952.
69. Haissinsky, Private communication to Miller, 1952.
70. Wright (a) } Discussion of the Faraday Soc. Leeds  
Lefort (b) } April, 1952 (in the press).
71. Bonet-Maury, Discussion of the Faraday Soc. Leeds,  
April, 1952 (in the press).
72. Gray, J. Chim. Phys., 48, 172, 1951.
73. Weiss, Trans. Farad. Soc., 36, 856, 1940.
74. Spicer, Trans. Farad. Soc., 31, 1706, 1935.
75. Dewhurst, Private communication, 1952.
76. Wright, Private Communication to Miller, 1952.
77. Bergwitz, Phys. Z., 11, 273, 1910.
78. Bonet-Maury and Lefort (a) Compt. Rend., 226,  
1363, 1445, 1948.  
(b) J. Chim. Phys., 47, 179,  
1950.

REFERENCES (CONTD).

79. Lanning and Lind (a) J. Phys. Chem., 42, 1229, 1938.  
Duane and Scheuer (b) Le radium, 10, 33, 1913.  
Lefort (c) J. Chim. Phys., 47, 624, 1950.
80. Carr, Nature, 167, 363, 1951.
81. Sworski, Private communication to Miller 1951.
82. Snell, "Colorimetric Methods of Analysis", Vol. 2,  
D. van Nostrand and Co., N.Y. 1937.
83. Loeb, Stein and Weiss, J.C.S., 405, 1951.
84. Ilosvay, Bull. Soc. Chim., 49, 388, 1889.
85. Rider and Mellon, J. Ind. Eng. Chem. Anal. Edit.,  
18, 96, 1946.
86. Germuth, J. Ind. Eng. Chem. Anal. Edit., 1, 28, 1929.
87. Bratton and Marshall, J. Biol. Chem., 128, 537, 1939.
88. Shinn, J. Ind. Eng. Chem. Anal. Edit., 13, 33, 1941.
89. Kershaw and Chamberlain, J. Ind. Eng. Chem. Anal.  
Edit., 14, 312, 1942.
90. Holbourn and Pattle, J. Lab. Clin. Med., 28,  
1028, 1943.
91. U.S. Pharmacopoeia, 11, 344, 1936.